# Determination of Burning Velocity and Pressure Record of Homogeneous, Non-Turbulent, Stoichiometric Acetylene--Air Mixtures In A Rigid Spherical Bomb with Central Ignition.

A
THESIS SUBMITTED IN PARTIAL
FULFILMENT OF REQUIREMENTS FOR THE DEGREE
OF

**Master of Engineering**

IN

**Applied Thermodynamics**
**(Power Engineering, Steam & I. C. Engines)**

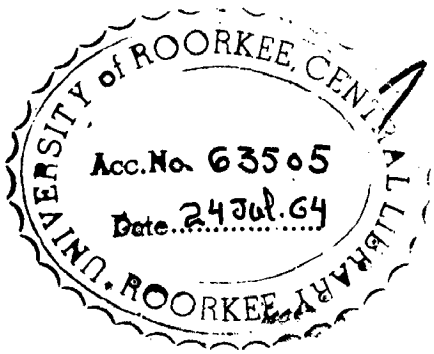




BY

S. P. SHARMA

DEPARTMENT OF MECHANICAL ENGINEERING
UNIVERSITY OF ROORKEE
ROORKEE (U.P.) INDIA

JUNE, 1964

## CERTIFICATE

Certified that the thesis entitled "DETERMINATION OF BURNING VELOCITY AND PRESSURE RECORD OF HOMOGENEOUS, NON-TURBULENT, STOICHIOMETRIC ACETYLENE-AIR MIXTURES IN A RIGID SPHERICAL BOMB WITH CENTRAL IGNITION", which is being submitted by Shri Shiv Prasad Sharma in partial fulfilment for the award of Degree of MASTER OF ENGINEERING in APPLIED THERMODYNAMICS (Power Engineering, Steam and I.C. Engines) of University of Roorkee, is a record of student's own work carried out by him under my supervision and guidance. The results embodied in this thesis have not been submitted for the award of any other degree or diploma.

This is further to certify that he has worked for a period of about 10½ (Ten & a half) months from 5th August, 1963 to 22nd June, 1964 for preparing thesis for Master of Engineering Degree at this University.

Thornton W. Price

(THORNTON W. PRICE)
USAID Guest Professor,
Department of Mechanical Engineering
University of Roorkee,
ROORKEE (U.P.) INDIA

ROORKEE
Dated 25th June, 1964.

## ACKNOWLEDGEMENT

I wish to express my sincere gratitude and appreciation to Dr. T.W.Price, USAID Guest Professor, Mechanical Engineering Department, University of Roorkee for esteemed guidance, unstinted assistance and excellent encouragement given throughout the period of preparation of this thesis, and for allowing access to his personal library. In fact, but for him, this will not be in the form it is today. It is virtually impossible to thank him for all the help he rendered.

I am highly grateful to Professor M.V.Kamlani, Head of Mechanical Engineering Department, University of Roorkee for perpetual encouragement and keen interest in progress and for extending all facilities for carrying out this work.

I also wish to thank Dr. W.U.Malik, Head of Chemistry Department, University of Roorkee, for soaring a number of spherical glass bombs during the course of testing. Thanks are also due to Sri Suresh Chandra, the then Reader in Mechanical Engineering Department, now Experimental Engineer, Automobile Division, TELCO, Jamshedpur and Sri A.B.L.Agarwal, Reader in Mechanical Engineering Department, University of Roorkee, for their valuable help and suggestions.

Last but not least, I want to express my thanks to the staff of Mechanical Engineering Workshops, I.C.Engine, Heat Transfer and Applied Instrumentation Laboratories for the co-operation during fabrication of the parts and setting up the experimental Apparatus.

UNIVERSITY OF ROORKEE
ROORKEE (U.P.)

June 22, 1964.

SHIV PRASAD SHARMA

CONTENTS


| | | |
|---|---|---|
| | CERTIFICATE | 1 |
| | ACKNOWLEDGEMENT | 2 |
| | LIST OF ILLUSTRATIONS | 4 |
| | LIST OF TABLES | 6 |
| | LIST OF PRINCIPAL SYMBOLS | 7 |
| | SYNOPSIS | 9 |
| | INTRODUCTION | 10 |
| I. | REVIEW OF LITERATURE | 12 |
| II. | THEORETICAL BACKGROUND | 16 |
| III. | DESCRIPTION OF APPARATUS | 37 |
| IV. | EXPERIMENTAL TECHNIQUE | 54 |
| V. | RESULTS AND DISCUSSION | 60 |
| | REFERENCES | 69 |
| | TABLES | 75 |
| | ILLUSTRATIONS | 82 |
| | APPENDIX A | 126 |
| | APPENDIX B | 128 |
| | APPENDIX C | 132 |
| | APPENDIX D | 134 |

## LIST OF ILLUSTRATIONS


Figure 1 Positions of an arbitrary elementary layer at different times.

Figure 2 Time variations in temperature and radius of an elementary layer during explosions in a spherical bomb.

Figure 3 Initial, intermediate and final spatial variations in pressure and temperature during explosion in a spherical bomb.

Figure 4 Spherical Bomb

Figure 5 Aluminium Plug

Figure 6 Prespex Split Ring

Figure 7 Aluminium Ring

Figure 8 Spherical Bomb Assembly

Figure 9 Diagram of a simple Drum Camera

Figure 10 Aluminium Drum

Figure 11 Light-Light Box

Figure 12 Line and Load connections to the variac Auto-Transformer.

Figure 13 Stroboscopic Principle

Figure 14 Ignition system

Figure 15 Kistler Pressure Transducer and cooling Adapter

Figure 16 Panel layout of Model 566 charge Amplifier

Figure 17 Cathode ray tube

Figure 18 Front Panel of Dual Beam Oscilloscope

Figure 19 Optical system of Type 300 Camera

Figure 20 Diagrammatic Sketch of experimental apparatus

Figure 21 A view of General arrangement of the experimental setup

Figure 22 A view of Oscillograph record Camera

Figure 23 A view of spherical Bomb and Drum Camera

Figure 24 A view showing calibration of pressure transducer.

Figure 25 A view showing calibration of variac motor speed control.

Figure 26 A view showing adjustments on oscilloscope.

Figure 27 A view showing loading of the film on Drum Camera.

Figure 28 Flame Record for $P_i$ = 6" Hg.Abs., $T_i$ = 303° K

Figure 29 Pressure Record for $P_i$ = 6" Hg.Abs., $T_i$ = 303°K

Figure 30 Flame Record for $P_i$ = 10" Hg.Abs., $T_i$ = 306°K

Figure 31 Pressure Record for $P_i$ = 10" Hg.Abs., $T_i$ = 306° K

Figure 32 Flame Record for $P_i$ = 15" Hg.Abs., $T_i$ = 306° K

Figure 33 Pressure Record for $P_i$ = 15" Hg.Abs., $T_i$ = 306° K

Figure 34 Flame Record for $P_i$ = 20" Hg.Abs., $T_i$ = 303° K

Figure 35 Pressure Record for $P_i$ = 20" Hg.Abs., $T_i$ = 303° K

Figure 36 Pressure and temperature relationship for adiabatic compression of a burned mixture.

Figure 37 Calibration curves of pressure transducer

Figure 38 Calibration curves of Variac Motor Speed Control.

Figure 39 Flame radius and pressure record for $P_i$ = 6" Hg.Abs., $T_i$ = 303° K

Figure 40 Plot of Flame radius and pressure record for $P_i$ = 10" Hg.Abs., $T_i$ = 306° K

Figure 41 Plot of Flame radius and pressure record for $P_i$ = 15" Hg.Abs., $T_i$ = 306° K

Figure 42 Plot of Flame radius and pressure record for $P_i$ = 20" Hg.Abs., $T_i$ = 308° K

Figure 43 Variation of Burning Velocity with temperatures at constant pressure

Figure 44 Variation of Burning velocity with pressure at constant temperature.

## LIST OF TABLES

Table 1 Partial pressures of Acetylene and Air for various initial pressures of mixture.

Table 2 Pressure and temperature relationship for adiabatic compression of unburned mixture

Table 3 Calibration Data of Pressure Transducer.

Table 4 Calibration Data of Variac Motor Speed Control

Table 5 Calculated and observed Data for $P_i$ = 6" Hg.Abs., $T_i$ = 303° K

Table 6 Calculated and observed Data for $P_i$ = 10" Hg.Abs., $T_i$ = 306° K

Table 7 Calculated and observed Data for $P_i$ = 15" Hg.Abs., $T_i$ = 306° K

Table 8 Calculated and observed Data for $P_i$ = 20" Hg.Abs., $T_i$ = 308° K

## LIST OF PRINCIPAL SYMBOLS

| | |
|---|---|
| $C_p$, $C_v$ | Specific heat at constant pressure and volume respectively |
| $C_{pu}$, $C_{vu}$ | Molar specific heats of the unburned gas at constant pressure and volume respectively. |
| $C_{pb}$, $C_{vb}$ | Molar specific heats of the burned gas at constant pressure and volume respectively. |
| E | Expansion Ratio |
| h | Enthalpy of chemical species in calories/g-mole. |
| $h_{RP}$ | Enthalpy of combustion at 25° C, Cal./g-mole. |
| K | A constant governing energy relations between burned and unburned gas in closed vessels. |
| $K_c$ | Equilibrium constant |
| $n_1$, $n_2$ | Number of moles present before and after combustion. |
| n | Burned fraction of contents of closed vessel |
| $\Sigma n_i$ | Number of moles of products per g-mole of fuel with dissociation. |
| $\Sigma n_i$ | Number of moles of products per g-mole of fuel without dissociation. |
| P, p | Pressure |
| $P_e$ | Pressure at end of combustion in closed vessel |
| $P_e'$ | Pressure at the end of explosion in closed vessel for equalised temperature $T_e'$. |
| $P_i$ | Pressure in closed vessel before ignition. |
| Q | Amount of heat added to the system during the process (per g-mole of Fuel) |
| R | Gas constant |
| R | Radius of spherical Bomb. |
| r | Flame Radius |
| $r_b$ | Radius of combustion wave in spherical vessel with central ignition. |
| $r_i$ | Preignition radius of spherical volume of unburned gas in spherical vessel with central ignition. |

| | |
|---|---|
| $S_f$ | Flame velocity relative to burned gases. |
| $S_u$ | Burning velocity |
| T | Temperature |
| $T_b$ | Temperature of Burned gas |
| $T_u$ | Temperature of unburned gas. |
| $T_i$ | Initial Temperature of system |
| $T_c$ | Temperature at any point in a closed vessel at the end of explosion. |
| $T_e$ | Equalized temperature in closed vessel at the end of explosion. |
| t | Time |
| V | Molal Gas Volume |
| V | Total volume of vessel |
| $V_b$, $V_u$ | Volume of the burned and unburned gas. |
| $x_i$ | Mole fraction |
| $\gamma$ | Ratio of specific heats at constant pressure and volume |
| $\gamma_u$, $\gamma_b$ | Ratios of specific heats at constant pressure and volume for unburned and burned gas respectively. |
| $\rho$ | Density |
| $\rho_b$ | Density of burned gas |
| $\rho_u$ | Density of unburned gas. |

## SYNOPSIS

A spherical, constant-volume bomb method was used to determine Laminar burning velocities of stoichiometric acetylene-air mixtures. The mixture was centrally ignited by means of an electric spark. Photographs of the growing sphere of flame and continuous pressure records were obtained simultaneously. The photographic recording of the luminous flame front was accomplished by the use of a rotating drum camera in which an image of the horizontal diameter of the growing spherical flame was continuously recorded on a film moving in a vertical direction at a known speed. The pressure-time behaviour during explosion was photographed by using a pressure-transducer-oscilloscope instrumentation equipped with an oscillograph record camera.

The burning velocities were calculated by two methods from the independently observed records of pressure and flame growth. The burning velocity data in the pressure range 30 to 150 Cm.Hg. and temperature range 300 to 450° K are reported. The effect of parameters such as pressure and temperature on burning velocity was examined. A correlation was deduced to predict the burning velocities in the range of pressures and temperatures mentioned above.

The results of this investigation are qualitatively in agreement with those of other investigators using the spherical bomb method. The lack of agreement of pressure-dependence of burning velocity measured by the spherical bomb method and by other methods is also discussed.

# INTRODUCTION

To a combustion Engineer, the study of flames and the mechanism of their propagation are the centre of interest. With a knowledge of progressive flames and the chemical kinetics of flame reactions, problems of combustion chamber design and engine performance can be approached with greater confidence. The studies of combustion processes are usually conducted in terms of Laminar burning velocity, flammability limits and quenching distance etc.

The purpose of the present inyestigation was to examine the use of the spherical Bomb method for determining the burning velocity of non-turbulent, stoichiometric Acetylene-Air mixtures at various pressures and temperatures. This method was originally devised by Flock (Ref. 14) and has been extended more recently by Lewis and Von Elbe (Ref. 17). This method, though believed to be an accurate method of determining burning velocity, has not be tested over a wider range of substances.

A review of the spherical bomb method including a set of data for stoichiometric mixtures of air with ethylene, methane and propane has been given by Manton, Von Elbe and Lewis (Ref. 16). An analysis of Ozone explosion in a spherical bomb and set of data for burning velocity of $CO-O_2$ mixtures with water vapour content is reported in Ref. 17.

In reference 21, (p. 158), Dugger, Simon and Gerstein have pointed out that the maximum flame velocities of all hydrocarbons with air at $25^{\circ}$ C and 1 atmosphere fall in the rango

30 to 80 cm./sec., with the exception of acetylene at 142 cm./sec

In the present investigation, the constant volume bomb method was employed. Stoichiometric acetylene-air mixtures were contained in a spherical-Glass-Bomb at sub-atmospheric pressures and ignited at the centre. Photographs of the growing sphere of flame and continuous pressure records were obtained by using a retating drum camera and pressure transducer-oscilloscope instrumentation equipped with an oscillograph record camera. Burning velocities at various pressures and temperatures are reported. The experimental advantages of this method are that it allows good control over the initial pressure and requires only small amount of gases.

A single explosion yields information on flame velocities in an explosive mixture at a series of pressures and temperatures connected by an isentropic path.

# I. REVIEW OF LITERATURE

Laminar Burning Velocity is a fundamental property of combustible mixtures. Due to an increased interest in the characteristics of flames and mechanism of their propagation, the accurate determination of burning velocities in non-turbulent gas mixtures has become important. The first attempt to measure the burning velocity was made by Bunsen (Ref. 1).

At the present time several methods are in use for the determination of burning velocity. The methods that have been used may be summarised under the following headings:

i) The Egerton-Powling Flat Flame Method (Ref. 2 & 3)

ii) The constant Pressure-Bomb Method (The Soap Bubble Technique) (Refs. 5 thru 13)

iii) The constant volume-Bomb Method (Refs. 14 thru 17)

iv) The Cylindrical Tube Method (Refs. 18 thru 20)

v) The Burner Methods (Refs. 21 thru 23)

The above methods are listed in order of increasing complexity of the flame shape from flat in (i) through Spherical in (ii) and (iii) to complex conical in (v).

The Egerton-Powling Flat flame method (Ref. 2 & 3) is only applicable to mixtures having burning velocities less than 15 or 20 cm. per sec. It is difficult to obtain flat flames with any mixture having a higher burning velocity. Therefore, this method is of little interest for studying flame structure and the method may be useful in defining lean flammability limits.

In Reference 4, Linnett pointed out that the Soap Bubble method can be used satisfactorily to measure burning velocities for those mixtures for which the soap film is satisfactory to enclose the gas. The soap-bubble method originally devised by Stevens (Ref. 5), used by Fiock and Roeder (Refs. 6, 7 & 8) and recently improved by Pickering and Linnett (Ref. 9) and Strehlow (Ref. 10) is essentially a constant-pressure bomb method. With the view to overcome the inherent disadvantages of the soap bubble method and at the same time retaining the advantages of the constant pressure bomb method, T.W.Price and J.H.Potter (Ref. 11) employed a spherical, transparent Rubber baloon in their investigation. Dorothy M. Simon and Edgar L. Wond (Ref. 12 & 13) have re-examined the use of the Soap-Bubble Technique for fast burning flames and to compare burning velocities measured by this method with those of other methods reported in the literature.

The constant volume bomb method is probably most satisfactory but it has not been sufficiently tested. This method was developed initially by Fiock (Ref. 14), improved further by Fiock, Marvin, Caldwell and Roeder (Ref. 15) and has been extended more recently by Manton, Von Elbe and Lewis (Ref. 16 & 17).

The cylindrical tube method can be used with fast flames but with slow moving flames, cooling by walls causes the values to be slightly low. This method was introduced by Coward and Hartwell (Ref. 18), examined by Hoare and Linnett (Ref. 19) and modified by Gerstein, Levine and Wong (Ref. 20).

The Bunsen Burner method (Refs. 21, 22 & 23) is most difficult to use accurately, and it can lead to very erroneous results. The reason for this lies in the complicated shape of the

flame surface.

In a recent review of the methods of measuring burning velocity (Ref. 24), Gordon L. Dugger, Dorothy M. Simon, and Melvin Gerstein have pointed out that there are large differences in flame velocities reported by various investigators for the same fuel oxidant mixtures at the same conditions. However, from the data reported in References 4, 12 & 24, it appears that the measured Laminar burning velocities for hydrocarbons in air are in better agreement among the various methods than for hydrocarbons in Oxygen.

In case of faster burning flames, the variation of measured burning velocities reported in the Literature is much greater, for example, for Methane-Oxygen flames, a burner method (total cone height) gives 330 cms./sec. (Ref. 17 p. 465), another burner method (frustum) gives 445 cms./sec. (Ref. 17 p. 467) while the soap bubble method measurement was 620 cms./sec. (Ref. 5).

Of the various methods of measuring burning velocity the constant volume bomb method (using the pressure record only) may prove to be most precise ( $\approx 1\%$). The numerical calculations of Manton, Von Elbe & Lewis (Ref. 16) have shown that a remarkably good agreement exists for the values obtained by the two methods of calculation. Their results are self consistent. A comparison with data obtained by the soap bubble Technique (Ref. 12) and the Slot-Burner method (Ref. 25) for Stoichiometric Ethylene-Air mixtures (6.51% Ethylene) corroborates the above conclusion.

COMPARISON OF BURNING VELOCITIES FOR STOICHIOMETRIC ETHYLENE AIR FLAMES BY DIFFERENT METHODS

| Ethylene percent | Burning Velocity cm. per Sec. | Method | Reference |
|---|---|---|---|
| 6.51% | 63.0 | Spherical Bomp Method | 16 |
| 6.51% | 62.3 | Soap Bubble Method | 12 |
| 6.51% | 64.0 | Slot Burner Method | 25 |

# II. THEORETICAL BACK GROUND

## 2.1 GENERAL

Our interest here is directed to the propagation of an explosion of a combustible mixture centrally ignited in a spherical bomb by means of an electric spark. Before we gain an insight into the mechanism underlying flame propagation in such a container, it is worthwhile to consider few definitions:

Combustible Mixture: A combusitible mixture is defined as one capable of propagating flame indefinitely away from, and in the absence of a source of ignition within certain limits of Fuel-Air Ratio, Known as Lean and rich limits (Ref. 26).

Flame: A flame is a thermal wave accompanied by exothermic chemical reactions which travels with Subsonic velocities. (Ref.27) Luminosity in a flame is not essential, but it is almost always present. The flame propagation at subsonic speeds is termed a Deflagration Wave while that travelling at supersonic speeds is termed a Detonation wave. A detonation wave is a steady state wave in which an exothermic chemical reaction supplies the energy to maintain the stationary conditions.

The velocity of Detonation is determined by the equations of conservation of mass, momentum and energy (alongwith the Chapman-Jouguet conditions) where as the velocity of flame propagation depends upon the detailed chemical kinetics and the coefficients of diffusion and thermal conductivity. The velocity of propagation of these waves ranges from about 20 cms./sec. to 10,000 times this velocity.

Flame Quenching: In a burning gas, any heat which is lost by conduction from hot gases is compensated by gain of fuel and Oxygen by diffusion. Solid boundaries on the other hand cause heat to be absorbed from the gas without giving the gas any fresh reactants in return. (Ref. 28). Therefore, if a flame is forced to propagate through some constriction, it will be extinguished, although the mixture may be well within the flammable range. This is due to the fact that the walls act as a sink for the chain carriers and exert repressive influence on the flame. The effect of walls on the flame propagation is termed quenching. And the minimum diameter or rectangular opening through which a flame will propagate is known as the Quenching Distance (Ref. 26).

## 2.2 BURNING VELOCITY

An explosion introduced into a sufficiently large section of an explosive mixture propagates in the unburned mixture at a definite velocity. It is, therefore, essential to understand the meaning of the term "Burning Velocity".

For an infinite plane flame the burning velocity is defined as the Linear Velocity of the flame front normal to itself and relative to unburnt gas. More generally, Flame Velocity is defined as the volume of the unburnt gas consumed per unit time divided by the area of the flame front in which that volume is consumed (Ref. 18, p. 2676 & Ref. 29).

Symbolically: $$S_u = \frac{dL}{dt} = \frac{\frac{dV}{dt}}{A} \qquad \ldots (2.1)$$

Applying the general definition to the case of a flame propagating radially with spherical symmetry about the ignition point, we have:

$$S_b = \frac{dV}{Adt} \qquad \text{... (2.2)}$$

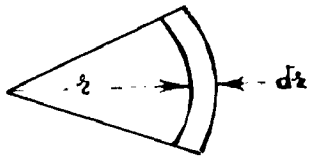


where $S_b$ = Flame Velocity relative to burned gases.

$dV$ = Volume burned in time dt

$$= \frac{4}{3}\pi\left[(r + dr)^3 - r^3\right] \cong 4\pi r^2.dr.$$

$A$ = Area of Flame Surface = $4\pi r^2$

$dr$ = Distance travelled in time dt

$$\therefore \quad \boxed{S_b = \frac{dr}{dt}} \qquad \text{... (2.3)}$$

This equation was originally derived by R.J.Dery.

From continuity Equation:

$$S_b \cdot \rho_b = S_u \cdot \rho_u \qquad \text{... (2.4)}$$

combining Equations (2.3) & (2.4), we get:

$$\boxed{S_u = \frac{\rho_b}{\rho_u} \cdot \frac{dr}{dt}} \qquad \text{... (2.5)}$$

For example, in view of the above equation, Burning velocity, as measured by the Soap Bubble Technique, may be calculated from the following equation:

$$S_u = \frac{S_b}{E} \qquad \text{... (2.6)}$$

where $S_b$ = Spatial velocity, or change in Flame sphere radius with time.

$E$ = Expansion Ratio

= Ratio of volumes of Burned gas to unburned gas.

Thus $$E = \frac{V_b}{V_u} = \frac{\rho_u}{\rho_b} = \left(\frac{r_i}{r_b}\right)^3$$

Since $\rho_b$ and $\rho_u$ are in inverse relation to the corresponding volumes and the latter according to the third power of

the radii of the sphere.

Hence $$S_u = S_b \left( \frac{r_b}{r_i} \right)^3 \qquad \ldots (2.7)$$

This is the situation, in a "Constant Pressure Bomb" but of variable volume which has been experimentally realised for purposes of measurements by enclosing the explosive mixture in a soap bubble (Refs. 5, 10 & 12) or a spherical, transparent Rubber Baloon (Ref. 11) and igniting it in the centre by a spark.

In the case of a solid container, the pressure must rise and the progress of the explosion is complicated by the compression of the fresh charge by means of combustion gases. The mechanism of flame propagation and the correlation of the rate of pressure rise with the Burning velocity in a constant volume Bomb will be discussed in some detail according to Lewis and Von Elbe (Ref. 16 & 17), in sections 2.3.1 & 2.3.2.

In reference 4, Linnett has mentioned that it is almost impossible to give a precise definition for Burning velocity which will be equally applicable to plane and spherical flames so that exactly the same value may be expected for the burning velocity from experiments on both systems. However, if a suitable flame area is divided into a volume flow rate, the same value, within the inevitable experimental error will be obtained for the burning velocity using both plane and spherical flames.

Other systems, such as a cylindrical flame, may be considered in the same way. Systems like the Bunsen flame are even more complicated.

In general, it has been experimentally observed that to reduce the difference between the "Burning Velocities" measured in different systems and to ensure that the values are close to the true burning velocity for a plane flame, it is important to divide the volume of the unburnt gas by an area measured as near the low temperature side of the flame as possible.

## 2.3 THEORY OF THE SPHERICAL BOMB METHOD

The flame propagation in closed chambers is complicated by the fact that there is change of pressure during combustion which brings into play not merely one value for the Burning Velocity but rather a multiplicity of Burning velocities at various pressures and temperatures. The phenomenon is of considerable importance for its practical application and merits explanation in some detail.

The method was developed initially by Fiock (Ref. 14) and has been extended more recently by Lewis and Von Elbe (Ref. 17). The combustible mixture is contained in a spherical bomb and is centrally ignited by an electric spark. Thermal conduction and diffusion of chain carriers initiate chemical reaction in adjacent layers of gas mixture and the flame tends to spread through the whole mass of the combustible mixture. The unburned fresh charge is adiabatically compressed by the expanding burning gases and thus heated. The compression of the fresh charge by the expanding burning gases and the compression of the charge burned at first by the gas burning later also causes the temperature of the gas burned at first (the inside of spherical bomb) to be higher (at complete combustion) than the part burned last by several hundreds of degrees (upto 900° C) (Ref. 17 & 30). As a result of this

temperature gradient, the maximum pressure during an explosion in a spherical bomb is little lower than that theoretically possible at an evenly distributed temperature. Moreover, there is re-illumination of the gas around the point of ignition which is also known as "After Burning" because it was at first considered that another reaction took place (Ref. 1. p. 137).

According to Lewis and Von Elbe, the qualitative explanation for this temperature gradient may be understood as follows:

The combustion of every thin layer of gas can be regarded as taking place at practically constant pressure i.e. the prevailing pressure at which the layer of gas expands from an initial volume to a terminal volume. That is to say, a volume of gas at the point of ignition will burn under the initial pressure and the volume in the immediate proximity to the wall will burn under the terminal pressure $P_e$. The volume in the centre performs work on the surrounding gas mass during its expansion at pressure $P_i$. Thereafter, it is re-compressed to approximately its initial volume by a pressure rise from $P_i$ to $P_e$ , as a result of combustion of the rest of the charge in the vessel.

Thus, for the first portion of charge, the later work of compression is greater than the former work of expansion. As a result, the volume element gives off less energy to the remaining gas mass than it later takes up again. It must, therefore, be hotter at the end than the average temperature of the entire gas mass.

Conversely, a volume element near the edge is compressed

at pressures between $P_i$ and $P_e$ , but it expands again at the highest pressure $P_e$. Thus, for the last portion of charge, the latter work of expansion is greater than the former work of compression. As a result, it gives off more energy at expansion than it has taken up during compression. It will, therefore, be colder at the conclusion than its average temperature.

In short, we may say that the gas that burns last loses some of its energy while the gas that burns first gains energy in excess of the chemical energy released within it. The result is the establishment of a temperature gradient which rises from the portion burned last to the portion burned first. Similar considerations apply to the volume of burned gas at any stage of the process when only a fraction of the contents has burned.

### 2.3.1 THEORY OF PRESSURE RISE AND TEMPERATURE GRADIENT IN BOMB EXPLOSIONS, ACCORDING TO FLAMM AND MACHE

A more exact theory of pressure rise and temperature distribution in bomb explosions according to Flamm and Mache (Ref. 31) and Lewis and Von Elbe (Ref. 17) is presented here.

The conditions of an elementary layer of gas mixture before and after the flame overtakes it, may conveniently be represented by means of figures (1 & 2). This gives us a qualitative picture at different time intervals. The figures are self-explanatory. In them are shown the variations of temperature and radius of a thin layer of gas mixture as a function of time as the wave progresses from centre to the wall. The same analysis would be true for every other layer, but the initial conditions may be different. Further, there is graphed the position of the flame front at different time intervals.

At any given instant of time, the pressure is constant over the entire chamber. In the unburned mixture the temperature is spatially constant but increases with time. In the burned portion, there is a moderate negative temperature gradient, where as in the burning zone this gradient is very steep. Figure 3 shows the variations in pressure and temperature during explosion in a spherical bomb (Schematic).

We must consider the changes in condition that appear in the combustion of a thin layer of gas (Spherical shell) in the unburned as well as in the burned mixtures. The combustion of a very thin spherical layer can be regarded as taking place at constant pressure, P.

Due to the expansion of the burning layer, both the fresh gas and the burned gas are adiabatically compressed. Thus, the state of the unburned gas at any time, is determined by its initial state and its rise in pressure, when compression is assumed isentropic.

The situation is somewhat more complicated in the burned gas. Here each succeeding elementary layer is burned at a higher initial temperature ($T_u$) and pressure P due to its adiabatic compression by the previously burning gases. A more detailed consideration is, therefore, required in determining the condition of the burned gases.

In the bomb volume $V = \frac{4}{3}\pi R^3$, let $m_i$ moles of initial mixture be present. Let the initial pressure and temperature be $P_i$ and $T_i$. Let the maximum pressure reached at complete combustion be $P_e$. The pressure and temperature of unburned gas

will be designated by P and $T_u$ which, of course, are different from $P_i$ and $T_i$ except for the time t = 0.

If a layer of gas burns at constant pressure, P, $T_u$ rises to a value $T_b$. $T_b$ depends on $T_u$ and P, thus making it different for each layer. In each burned layer of gas, pressure and temperature continue to rise until the end of the combustion to the terminal value $P_e$ independent of the place and to a terminal $T_e$ which like $T_u$, varies from layer to layer.

Since the condition P, $T_u$ of the fresh gas arises by means of adiabatic compression from the condition $P_i$, $T_i$, the following is valid if $v_u$ and $v_i$ are the corresponding volumes.

$$P_i \, v_i^{\gamma_u} = P \, v_u^{\gamma_u}$$

$$\text{or} \quad P_i^{\frac{1-\gamma_u}{\gamma_u}} RT_i = P^{\frac{1-\gamma_u}{\gamma_u}} RT_u = F_u \qquad \ldots (2.8)$$

where $F_u$ is an abbreviation for the expression (2.8).

Applied to the burned gas, an analogous adiabatic relation is obtained.

$$\frac{m_e}{m_i} P^{\frac{1-\gamma_b}{\gamma_b}} RT_{bp} = \Phi (r) \qquad \ldots (2.9)$$

In this, the ratio $\frac{m_e}{m_i}$ appears at the left because the mole-number in this relation has been changed. We can apply no general expression here as explained above since the initial condition is different from layer to layer. For that reason, the expression on the left side of Equation (2.9) is not a constant but changes from layer to layer i.e. $\Phi (r)$ is a function of r.

The temperature in the elemental layer after it has burned is denoted by $T_b$. As the element is subsequently further compressed adiabatically, $T_b$ rises to some temperature $T_{bp}$ corresponding to the subsequent pressure.

For an exact calculation, we should take into account the fact that the reaction does not generally take a complete course and that the reaction products are partly dissociated. Further the specific heats and thus also $\gamma = \frac{c_p}{c_v}$) are not independent of the temperature. In order to avoid complicating the derivations too much, we shall first disregard dissociation. Secondly, we shall assume for the fresh gas and for the burned gas in the temperature interval considered a constant average value for $C_p$ and $C_v$. By the choice of suitable average values, an error introduced in this manner could be kept quite small.

We must now seek a further relation for the burned gases that permits us to determine $\Phi$ in the equation (2.9).

If $C_{v(u)}$ is the average specific heat per mole of unburned gas, then the adiabatic compression work done on $m_i$ g-moles of reactants is:

$$m_i \, C_{v(u)}(T_u - T_i) \qquad \ldots (2.10)$$

The central volume element (at the point of ignition) burns to the lowest possible combustion temperature $T_{bi}$. Every other gas layer that has been precompressed burns to a higher temperature $T_b$ (At the wave surface $T_{bp}$ equals $T_b$) If $C_{v(b)}$ is the average specific heat (per g-mole of the burned gas) then the excess energy referred to the volume element in the centre, is:

$$m_e \, C_{v(b)} \, (T_b - T_{bi}) \qquad \ldots (2.11)$$

Now the excess energy that the second volume element, with the initial temperature $T_u$, has over the first volume element, is determined by the adiabatic work done conducted to it before, in other words:

$$\frac{m_e}{m_i} C_{v(b)} (T_b - T_{bi}) = C_{v(u)} (T_u - T_i) \qquad \ldots (2.12)$$

To repeat once more: In this equation $T_u$ and $T_b$ are the temperatures varying from concentric layer to layer; immediately before and after combustion. $T_i$ and $T_{bi}$ have fixed values. The first is the initial temperature, the second the combustion temperature of the very first layer to be computed from the initial temperature and heat of combustion. If equation (2.12) is changed around in such a way that only these fixed values appear on one side, the resulting expression for given initial conditions must be a constant whose value can be given as:

$$\frac{m_e}{m_i} C_{v(b)} \, T_{bi} - C_{v(u)} \, T_i = \frac{m_e}{m_i} C_{v(b)} \, T_b - C_{v(u)} \, T_u = K \qquad \ldots (2.13)$$

Since no great error can occur if $C_p$ is substituted for $C_v$ in equation (2.12) (Ref. 1. p. 151), we shall continue to use the substitution. Instead, therefore, of starting from equation (2.13), we shall use the analogous from equation (2.13′) which uses $C_p$. It will be found that the succeeding expressions will be more easily integrated.

Thus:
$$\frac{m_e}{m_i} C_{p(b)} \, T_{bi} - C_{p(u)} \, T_i = \frac{m_e}{m_i} C_{p(b)} \, T_b - C_{p(u)} T_u \qquad \ldots (2.13')$$

This equation is to be regarded as an approximation. By means of this relation, we shall now obtain the function from equation (2.9). By inserting equations (2.8) and (2.9) into equation (2.13), we obtain:

$$\frac{m_e}{m_i} C_{P(b)} \frac{\Phi}{\frac{m_e}{m_i} P^{\frac{1-\gamma_b}{\gamma_b}} R} - C_{P(u)} \frac{T_i}{P^{\frac{1-\gamma_u}{\gamma_u}} R} = K \qquad \ldots (2.14)$$

Since $$\frac{C_p}{R} = \frac{C_p}{C_p - C_v} = \frac{\gamma}{\gamma - 1}$$

this becomes

$$\frac{\gamma_b}{\gamma_b - 1} \Phi P^{\frac{\gamma_b - 1}{\gamma_b}} - \frac{\gamma_u}{\gamma_u - 1} F_u P^{\frac{\gamma_u - 1}{\gamma_u}} = K \qquad \ldots (2.15)$$

and from this

$$\Phi(z) = \left[ K + \frac{\gamma_u}{\gamma_u - 1} P^{\frac{\gamma_u - 1}{\gamma_u}} F_u \right] \frac{\gamma_b - 1}{\gamma_b} P^{\frac{1-\gamma_b}{\gamma_b}} \qquad \ldots (2.16)$$

We are now interested in the condition of the burned gas at radius r or for a volume element that is burned after a known fraction of the total volume has been converted. So far this element is characterized only by the pressure P that prevailed at combustion. We shall obtain a relation between 'P' and 'n' if we impose the condition that the total volume must remain constantly equal to the volume of the bomb even though the volumes of the fresh gas and the burned gases change. To begin with, we can apply the equation of ideal gases for the total volume of the Bomb:

$$V = \frac{m_i R T_i}{P_i} \qquad \ldots (2.17)$$

If the portion'n'of the total gas is burned and if $T_u$ is the temperature of the fresh gas at the pressure P, then the

If we insert the value of $\Phi$ from equation (2.16), we have a differential equation for the degree of conversion 'n' as a function of the momentary pressure P:

$$K(\gamma_b-1) = \frac{\gamma_u-\gamma_b}{\gamma_u-1} F_u P^{\frac{\gamma_u-1}{\gamma_u}} + \left[ \frac{RT_i}{P_i} - \frac{\gamma_u-\gamma_b}{\gamma_u} F_u P^{-\frac{1}{\gamma_u}} (1-n) \right] \frac{dP}{dn} \quad \ldots (2.24)$$

Since $$\frac{\gamma_u-\gamma_b}{\gamma_u} P^{-\frac{1}{\gamma_u}} \frac{dP}{dn} = \frac{d}{dn}\left( \frac{\gamma_u-\gamma_b}{\gamma_u-1} P^{\frac{\gamma_u-1}{\gamma_u}} \right)$$

Equation (2.24) can be converted into:

$$K(\gamma_b-1) = \frac{RT_i}{P_i} \cdot \frac{dP}{dn} - \frac{d}{dn}\left[ (1-n) \frac{\gamma_u-\gamma_b}{\gamma_u-1} F_u \cdot P^{\frac{\gamma_u-1}{\gamma_u}} \right] \quad \ldots (2.24')$$

which can be integrated without difficulty.

If we integrate between the limits 'n' and 1 for 'n', we obtain (taking into consideration that for n = 1, the pressure becomes $P = P_e$)

$$K(\gamma_b-1)(1-n) = \frac{RT_i}{P_i}(P_e-P) + \frac{\gamma_u-\gamma_b}{\gamma_u-1} F_u (1-n) P^{\frac{\gamma_u-1}{\gamma_u}} \quad \ldots (2.25)$$

This equation represents with the above assumptions the exact relation between momentary pressure 'P' and degree of conversion 'n':

Solved according to (1-n), we get:

$$(1-n) = RT_i \frac{P_e-P}{P_i} \cdot \frac{1}{K(\gamma_b-1) - \frac{\gamma_u-\gamma_b}{\gamma_u-1} RT_u} \quad \ldots (2.26)$$

in which according to equation (2.8), $F_u P^{\frac{\gamma_u-1}{\gamma_u}}$ is replaced by $R\,T_u$. If we introduce numerical values, it is clear that $\frac{\gamma_u-\gamma_b}{\gamma_u-1} R\,T$ is always small in relation to $K(\gamma_b - 1)$. We, therefore, make no great error in substituting $T_i$ for $T_u$ ;

equation (2.17) is valid for the volume of the fresh gas $V_{(1-n)}$:

$$V_{(1-n)} = \frac{m_i\,(1-n)\,R\,T_u}{P} \qquad \ldots (2.18)$$

For a small fraction 'dn' of the burned gas, the gas equation is like wise valid:

$$dV = \frac{m_e \cdot dn \cdot R\,T_{bp}}{P} \qquad \ldots (2.19)$$

Since $T_{bp}$ changes from element to element, the entire volume of the burned gases can be obtained only by integration over the ranges of variable temperature:

$$V_n = m_e \cdot \frac{R}{P} \int_0^n T_{bp} \cdot dn \qquad \ldots (2.20)$$

and the condition for the constancy of the total volume:

$$V_{(1-n)} + V_n = V$$

becomes

$$\frac{m_i\,R\,T_i}{P_i} = \frac{R}{P}\left[ m_e \int_0^n T_{bp} \cdot dn + m_i\,T_u\,(1-n) \right] \qquad \ldots (2.21)$$

Since we donot have at our command an explicit relation between $T_{bp}$ and n, this expression is not very convenient. The temperatures $T_u$ and $T_{bp}$ in equation (2.21) can be expressed by equations (2.8) and (2.9) and we obtain:

$$\int_0^n \Phi \cdot dn = \frac{RT_i}{P_i} \cdot P^{\frac{1}{\gamma_b}} - F_u\,P^{\frac{1}{\gamma_b}-\frac{1}{\gamma_u}} \cdot (1-n) \qquad \ldots (2.22)$$

From this equation, we obtain by differentiation for 'n'

$$\Phi = F_u\,P^{\frac{1}{\gamma_b}-\frac{1}{\gamma_u}} + \left[ \frac{RT_i}{P_i} \cdot \frac{1}{\gamma_b} \cdot P^{\frac{1-\gamma_b}{\gamma_b}} - F_u \left(\frac{1}{\gamma_b}-\frac{1}{\gamma_u}\right) P^{\frac{1}{\gamma_b}-\frac{1}{\gamma_u}-1} (1-n) \right] \frac{dP}{dn} \qquad \ldots (2.23)$$

If we insert the value of $\Phi$ from equation (2.16), we have a differential equation for the degree of conversion 'n' as a function of the momentary pressure P:

$$K(\gamma_b - 1) = \frac{\gamma_u - \gamma_b}{\gamma_u - 1} F_u P^{\frac{\gamma_u - 1}{\gamma_u}} + \left[ \frac{RT_i}{P_i} - \frac{\gamma_u - \gamma_b}{\gamma_u} F_u P^{-\frac{1}{\gamma_u}} (1-n) \right] \frac{dP}{dn} \quad \ldots (2.24)$$

Since $$\frac{\gamma_u - \gamma_b}{\gamma_u} P^{-\frac{1}{\gamma_u}} \frac{dP}{dn} = \frac{d}{dn} \left( \frac{\gamma_u - \gamma_b}{\gamma_u - 1} P^{\frac{\gamma_u - 1}{\gamma_u}} \right)$$

Equation (2.24) can be converted into:

$$K(\gamma_b - 1) = \frac{RT_i}{P_i} \cdot \frac{dP}{dn} - \frac{d}{dn} \left[ (1-n) \frac{\gamma_u - \gamma_b}{\gamma_u - 1} F_u \cdot P^{\frac{\gamma_u - 1}{\gamma_u}} \right] \quad \ldots (2.24')$$

which can be integrated without difficulty.

If we integrate between the limits 'n' and 1 for 'n', we obtain (taking into consideration that for $n = 1$, the pressure becomes $P = P_e$)

$$K(\gamma_b - 1)(1-n) = \frac{RT_i}{P_i} (P_e - P) + \frac{\gamma_u - \gamma_b}{\gamma_u - 1} F_u (1-n) P^{\frac{\gamma_u - 1}{\gamma_u}} \quad \ldots (2.25)$$

This equation represents with the above assumptions the exact relation between momentary pressure 'P' and degree of conversion 'n':

Solved according to (1-n), we get:

$$(1-n) = RT_i \frac{P_e - P}{P_i} \frac{1}{K(\gamma_b - 1) - \frac{\gamma_u - \gamma_b}{\gamma_u - 1} RT_u} \quad \ldots (2.26)$$

in which according to equation (2.8), $F_u P^{\frac{\gamma_u - 1}{\gamma_u}}$ is replaced by $R\,T_u$. If we introduce numerical values, it is clear that $\frac{\gamma_u - \gamma_b}{\gamma_u - 1} R\,T$ is always small in relation to $K(\gamma_b - 1)$. We, therefore, make no great error in substituting $T_i$ for $T_u$ ;

Otherwise equation (2.26) yields, for n = 0

$$K(\gamma_b - 1) - \frac{\gamma_u - \gamma_b}{\gamma_u - 1} RT_i = RT_i \frac{P_e - P_i}{P_i} \qquad \ldots (2.27)$$

If we substitute $T_i$ for $T_u$ in equation (2.26) and make use of equation (2.27) we obtain the approximation equation:

$$1 - n \cong \frac{P_e - P}{P_e - P_i} \text{ or } \boxed{n \cong \frac{P - P_i}{P_e - P_i}} \qquad \ldots (2.28)$$

which states that the fraction of gas burned is equal to the fraction of the total pressure rise.

($P = P_e$ when $n = 1$ and $P = P_i$ when $n = 0$)

The equation (2.28) is sufficiently accurate for an analysis of the combustion process in Bombs. It is strictly valid for small pressure rise in the early stages of the process. The value of the pressure $P_e$ is not taken as the true maximum pressure of the explosion but is calculated thermodynamically under the assumption that the heat capacities and dissociation equilibria of the burned gas in the early stages remain unchanged during the course of the combustion process.

The temperature in any given mass element rises by adiabatic compression from $T_i$ to $T_u$ which is the temperature just prior to arrival of the combustion wave. As the wave passes over the mass element the temperature rises to $T_b$ which is calculable from thermechemical data, and later to $T_e$, owing to further adiabatic compression.

In reference 16, Manton, Von Elbe and Lewis have indicated the way to calculate the "Fiticious" temperature $T_e$ corresponding to $P_e$ from the following enthalpy relation:

$$C_{v(b)}\ T_e + \frac{m_i}{m_b} R\ T_i = C_{p(b)} \cdot T_b. \qquad \ldots (2.29)$$

Where $T_b$ = is flame temperature computed for combustion at constant pressure $P_i$ with due regard to the values of specific heats and dissociation equilibria applicable to the explosive gas.

$m_b$ = is number of moles formed by combustion of $m_i$ moles of explosive gas.

$C_{v(b)}$ and $C_{pb} = C_{v(b)} + R$ = are the molar specific heats of the burned gas at constant volume and pressure

& $R$ = is the gas constant.

$C_{v(b)}$ may with sufficient accuracy be identified with:

$$C_{v(b)} = \sum f\ C_v \qquad \ldots (2.30)$$

where $f$ = denotes the mole fraction and $C_v$ the molar specific heat of any constituent present in the burned gas at thermodynamic equilibrium corresponding to $T_b$ and $P_i$.

The pressure $P_e$ is found from the equation:

$$\boxed{P_e = P_i \frac{m_b}{m_i} \cdot \frac{T_e}{T_i}} \qquad \ldots (2.31)$$

The use of Thermodynamically calculated pressure $P_e$ can be made in determining the burning velocity from pressure record along. The expression for burning velocity using pressure record alone will also be indicated in the succeeding paragraphs.

## 2.3.2. CORRELATION OF RATE OF PRESSURE RISE WITH BURNING VELOCITY

As a result of ignition by spark at the centre of a combustible mixture in a spherical Bomb, a combustion wave propagates spherically from centre to the wall. The area of the burning surface increases as the explosion proceeds. Hence a pressure-time curve of a Bomb explosion may take the course as shown in the following figure.

In order to find the actual burning velocity, we must compute the position of the burning surface using the pressure, the fraction of gas burned 'n', and the known dimension of the Bomb (Radius R). For this purpose we proceed in the following manner, according to Lewis and Von Elbe (Refs. 16, 17 & 32) and Fiock and Marvin (Ref. 33).

The fraction 'n' of the gas which, on burning, gives rise to a pressure P, occupies, before ignition, a sphere of radius ' $r_i$ ' so that

$$n = \left(\frac{r_i}{R}\right)^3 = \frac{P - P_i}{P_e - P_i} \qquad \ldots (2.32)$$

$$\therefore \quad \frac{r_i}{R} = \left(\frac{P - P_i}{P_e - P_i}\right)^{1/3} \qquad \ldots (2.33)$$

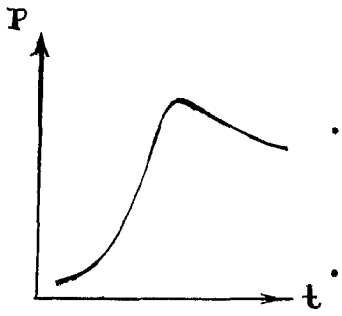


R, being the radius of the Bomb.

The volume occupied by the fraction 'n' when burned is a sphere of radius '$r_b$'. The relation between '$r_b$' and 'n' is obtained from the equation for the volume of the residual unburned gas:

$$v_b = V - m_i (1 - n) \frac{R T_u}{P} \qquad \ldots (2.34)$$

where $V$ = volume of the Bomb = $\frac{m_i R T_i}{P_i}$

$T_u$ = Temperature of the unburned gas when adiabatically compressed from temperature $T_i$ and pressure $P_i$

$$= T_i \left(\frac{P}{P_i}\right)^{\frac{\gamma_u - 1}{\gamma_u}}$$

Whence $$\left(\frac{v_b}{V}\right)^{1/3} = \frac{r_b}{R} = \left(1 - \frac{P_i}{P}\cdot\frac{T_u}{T_i}\cdot\frac{P_e - P}{P_e - P_i}\right)^{1/3} \qquad \ldots (2.35)$$

To obtain Burning velocities it is necessary to plot values of $r_i$ corresponding to any given pressure on the pressure time record as a function of time and determine the slopes $\frac{dr_i}{dt}$. If during the travel of the flame through the vessel, the burned gas had not expanded, then an element $dr_i$ on this curve would represent the thickness of a shell at the temperature $T_i$ and the pressure $P_i$ about to be traversed by the wave in the time element dt. Its volume would have been:

$$4\pi r_i^2 . dr_i \qquad \ldots (2.36)$$

However, as a result of the thermal expansion of the burned gas, the pressure in the vessel is increased from $P_i$ to P and the unburned gas is adiabatically compressed so that its temperature is increased from $T_i$ to $T_u$. Hence the volume of the shell corresponding to the actual state of the unburned gas is:

$$4\pi r_i^2 \cdot dr_i \left(\frac{T_u}{T_i}\cdot\frac{P_i}{P}\right) \qquad \ldots (2.37)$$

Since the thickness of the shell is equal to $s_u$ . dt, its volume is also equal to:

$$4\pi r_b^2 \cdot S_u \cdot dt \qquad \ldots (2.38)$$

By equating the terms of equations (2.37) and (2.38) and substituting the value of $\frac{T_u}{T_i}$, we obtain the expression for the

Burning Velocity:

$$S_u = \frac{dr_i}{dt} \cdot \left(\frac{r_i}{r_b}\right)^2 \cdot \left(\frac{P_i}{P}\right)^{1/\gamma_u} \qquad \ldots (2.39)$$

Using equation (2.32) viz. $\left[ n = \frac{r_i^3}{R^3} \right]$, equation (2.39) may be written as:

$$S_u = \frac{1}{3} \cdot \frac{dn}{dt} \cdot \frac{R^3}{r_b^2} \cdot \left(\frac{P_i}{P}\right)^{1/\gamma_u} \qquad \ldots (2.40)$$

Equation (2.35) may be re-written as:

$$\left(\frac{r_b}{R}\right)^3 = 1 - \left(\frac{P_i}{P}\right)^{1/\gamma_u} \cdot (1-n) \qquad \ldots (2.40a)$$

or $$n = 1 - \left(\frac{P}{P_i}\right)^{\frac{1}{\gamma_u}} \cdot \left(1 - \frac{r_b^3}{R^3}\right) \qquad \ldots (2.41)$$

By differentiating equation (2.41), we obtain:

$$\frac{dn}{dt} = 3\left(\frac{P}{P_i}\right)^{\frac{1}{\gamma_u}} \cdot \frac{r_b^2}{R^3} \cdot \frac{dr_b}{dt} - \frac{1}{\gamma_u}\left(\frac{P}{P_i}\right)^{\frac{1}{\gamma_u}-1} \left(1 - \frac{r_b^3}{R^3}\right) \frac{1}{P_i} \cdot \frac{dP}{dt} \qquad \ldots (2.42)$$

Combination of equations (2.40) and (2.42) yields:

$$S_u = \frac{dr_b}{dt} - \frac{R^3 - r_b^3}{3P\gamma_u r_b^2} \cdot \frac{dP}{dt} \qquad \ldots (2.43)$$

or $$S_u = \left(1 - \frac{R^3 - r_b^3}{3P\gamma_u r_b^2} \cdot \frac{dP}{dr_b}\right) \frac{dr_b}{dt} \qquad \ldots (2.44)$$

The above expression for Burning velocity has also been derived by Fiock, Marvin, Caldwell and Roeder (Ref. 15) from the differential form of the equation of adiabatic compression of the unburned gas:

$$\frac{dP}{P} = -\gamma_u \cdot \frac{dv_u}{v_u}$$

where $dv_u$ = differential volume change due to adiabatic compression

$$= 4\pi r_b^2 \left(dr_b - S_u\, dt\right)$$

$$v_u = \frac{4}{3}\pi \left(R^3 - r_b^3\right)$$

In either procedure, $S_u$ is obtained as a difference of two quantities.

If Synchronous experimental records of the pressure rise and flame growth are taken, the quantities $\frac{dr_b}{dt}$, $\frac{dP}{dt}$, $r_b$ and P are the measured data. The value of $\gamma_u$ can usually be determined with high accuracy from available information on specific heats, so it is possible to calculate $S_u$ from equation (2.44).

Close to the centre, $\frac{dr_b}{dt} = S_b$, and since $\frac{Su}{S_b}$ is the density ratio $\frac{\rho_b}{\rho_u}$, the bracketted term is small composed to unity. Equation 2.44 yields $S_u$ as a difference of two terms of comparable magnitude except in the late stage of the process where the combustion wave approaches the wall of the Bomb. So any error in the differential quotients and the other data would be greatly magnified and the results may be expected to scatter widely.

Lewis and Von Elbe, (Ref. 16 & 17) recommend the method of utilizing simultaneous records of $r_b$ and P together with the thermodynamically calculated value of $P_e$. Fraction n ( $= \frac{P - P_i}{P_e - P_i}$) can be computed with precision from pressure P by means of Thermodynamic relations, assuming that thermodynamic equilibrium is established in the flame. This appears to be an excellent assumption which can be verified by computing $r_b$ from equation (2.40a) (using the thermodynamically calculated value of 'n') and comparing the calculated value of $r_b$ with the experimental value. From the experimental curve (P, t) the curve n, t) can obtained permitting the determination of the burning velocity by means of equation (2.40) from the pressure record alone.

To obtain an equation for $S_u$ in which the flam

## III. DESCRIPTION OF APPARATUS

The general arrangement of the set up (including instrumentation) is shown in figure 20 and the photographic view in figure 21. The equipment consisted of:

1. A Spherical Bomb
2. A Rotating Drum Camera
3. A Mixture Proportioning System
4. An Ignition System, and
5. A Pressure Recording System

The detailed description of the systems mentioned above follow:

### 3.1. THE SPHERICAL BOMB

The spherical bomb shown with dimensions in Figure 4 was a pyrex glass round bottom, wide mouth and short neck flask of 1 litre capacity. The inside diameter of the bomb was 12.7 cms. and the thickness of the wall 2.38 mm. Keeping in view the safety of the bomb, it was tested with compressed air to a pressure of 100 psig. The actual final combustion pressures realised during the explosions were not generally very much over this limit.

Since the explosive gas mixture chosen for burning velocity measurements was Acetylene-Air in which the rate of pressure rise due to combustion was very rapid, it was decided to keep the initial pressures of the mixture sub-atmospheric.

In order to give a complete spherical shape to the flask, to maintain vacuum inside and to incorporate the pipe-fittings, pressure transducer and steel electrodes the connections shown in Figures 5, 6 & 7 were designed and fabricated. The assembled view of the spherical bomb with its neck connections is shown in Fig. 8.

In either procedure, $S_u$ is obtained as a difference of two quantities.

If Synchronous experimental records of the pressure rise and flame growth are taken, the quantities $\frac{dr_b}{dt}$, $\frac{dP}{dt}$, $r_b$ and P are the measured data. The value of $\gamma_u$ can usually be determined with high accuracy from available information on specific heats, so it is possible to calculate $S_u$ from equation (2.44).

Close to the centre, $\frac{dr_b}{dt} = S_b$, and since $\frac{Su}{S_b}$ is the density ratio $\frac{\rho_b}{\rho_u}$, the bracketted term is small composed to unity. Equation 2.44 yields $S_u$ as a difference of two terms of comparable magnitude except in the late stage of the process where the combustion wave approaches the wall of the Bomb. So any error in the differential quotients and the other data would be greatly magnified and the results may be expected to scatter widely.

Lewis and Von Elbe, (Ref. 16 & 17) recommend the method of utilizing simultaneous records of $r_b$ and P together with the thermodynamically calculated value of $P_e$. Fraction n ( $= \frac{P - P_i}{P_e - P_i}$) can be computed with precision from pressure P by means of Thermodynamic relations, assuming that thermodynamic equilibrium is established in the flame. This appears to be an excellent assumption which can be verified by computing $r_b$ from equation (2.40a) (using the thermodynamically calculated value of 'n') and comparing the calculated value of $r_b$ with the experimental value. From the experimental curve (P, t) the curve n, t) can be obtained permitting the determination of the burning velocity $S_u$ by means of equation (2.40) from the pressure record alone.

To obtain an equation for $S_u$ in which the flame trace

$\frac{dr_b}{dt}$ is the only time derivative, the term $\frac{dP}{dt}$ in equation (2.42) is replaced by $(P_e - P)$. $\frac{dn}{dt}$ (since $n = \frac{P-P_i}{P_e-P_i}$), the equation is solved for $\frac{dn}{dt}$ and the solution is substituted in equation (2.40). By introducing n from Equation (2.41) into the last term of equation (2.42) and eliminating n by means of equation (2.28), we obtain finally:

$$S_u = \frac{\frac{dr_b}{dt}}{1+\left(\frac{P_e}{P}-1\right)/\gamma_u} \qquad \ldots (2.45)$$

This equation may be used as a further test of the self consistency of the Bomb method by utilizing the experimental flame trace for the determination of burning velocity.

## III. DESCRIPTION OF APPARATUS

The general arrangement of the set up (including instrumentation) is shown in figure 20 and the photographic view in figure 21. The equipment consisted of:

1. A Spherical Bomb
2. A Rotating Drum Camera
3. A Mixture Proportioning System
4. An Ignition System, and
5. A Pressure Recording System

The detailed description of the systems mentioned above follow:

### 3.1. THE SPHERICAL BOMB

The spherical bomb shown with dimensions in Figure 4 was a pyrex glass round bottom, wide mouth and short neck flask of 1 litre capacity. The inside diameter of the bomb was 12.7 cms. and the thickness of the wall 2.38 mm. Keeping in view the safety of the bomb, it was tested with compressed air to a pressure of 100 psig. The actual final combustion pressures realised during the explosions were not generally very much over this limit.

Since the explosive gas mixture chosen for burning velocity measurements was Acetylene-Air in which the rate of pressure rise due to combustion was very rapid, it was decided to keep the initial pressures of the mixture sub-atmospheric.

In order to give a complete spherical shape to the flask, to maintain vacuum inside and to incorporate the pipe-fittings, pressure transducer and steel electrodes the connections shown in Figures 5, 6 & 7 were designed and fabricated. The assembled view of the spherical bomb with its neck connections is shown in Fig. 8

To assemble the components of the spherical bomb: First the aluminium ring (Figure 7) was screwed over the lower half of the Prespex-Ring (Figure 6) which embraced the neck of the bomb. Then the Aluminium-plug (Figure 5) with a Rubber-O-Ring in the groove of its flange as shown was screwed on the other half of the prespex ring. The O-Ring fitted tightly on the top of the neck and was mainly responsible to make the bomb air-tight. The curved-surface on the bottom of the plug gave complete spherical shape to the vessel.

As shown in Figure 5, a vertical hole of 1/8" dia. was drilled centrally and 14 mm. x 1.25 mm. pitch spark plug threads cut up to a depth of 3/4" in the aluminium casting for mounting the pressure transducer. The diaphragm of the pressure transducer was in communication with the spherical bomb through 1/8" dia. hole. The combustible mixture was introduced through a second hole (1/8" dia.) with 1/4" Threads (18 T.P.I.; 0.540" O.D.) in the casting for an adopter for the pipe fittings. Since the bomb was to be centrally ignited, the spark gap (about 2 mm.) formed by 2.54 mm. (the largest dia.) mild steel electrodes was accurately arranged in the centre. The electrodes were pointed like needles at the spark gap. One of the electrodes was electrically insulated from the aluminium plug by passing it through a pyrex glass tube (3/16" O.D.) which itself passed through a third hole in the casting inclined at an angle of $8^{\circ}$ with the vertical. The axis of the hole was intersecting the centre of the bomb. An adhesive (suchas Araldite) was used to fix the electrode and the tube and the tube to the aluminium plug at places shown in the figure. The other electrode was mounted in the plug it self as shown. A good

electrical contact between the plug and the second electrode was obtained by providing a force fit between the two. During combustion, the wall of the glass bomb was likely to get heated up momentarily due to high combustion temperatures. Hence to avoid any direct contact between metal and glass wall, a little quantity of Freezer Tape was wraped round the aluminium plug.

The spherical bomb was fitted inside the Light-tight box by means of screws.

### 3.2. THE DRUM CAMERA

The principle of working of a Drum Camera may be explained with the help of Figure 9. An image of the line AB is formed on the film at CD. As the drum rotates, any bright object which moves along the line AB will trace out a diagonal the inclination of which is determined by the rate of movement of the phenomenon along the line AB.

Based upon this simple principle, a drum camera was developed in which the image of a horizontal diameter of the growing spherical flame was continuously recorded on a moving film. The Figure 20 shows the sectional plan-view of the drum camera including the spherical bomb and Figure 23 gives the pictorial view.

Figure 10 shows the sectional view of a hollow Aluminium Drum 3" O.D., wall thickness 3/8" and 3" length directly driven by a 1/15 H.P. D.C. Motor with speed regulating device. The motor was mounted in a light tight box (Figure 11) and covered from outside by a cylindrical cover of thin metallic sheet and properly sealed by the plastic black tape.

The light tight box (Figure 11) was a 28" x 8" x 8" wooden chamber with wall thickness 3/4". The top of the box could opened like any ordinary box; but it had a wooden strip 3/4" x 1/2" on all the four sides of the top cover which made the box light tight. In order to permit the operator to load and unload the film, two holes nearly elliptical in size (4½" x 3¾") were cut in the top and side of the box as shown. Two rings of sheet metal of nearly the same size as holes were screwed outside these holes and carried black sleeves with rubber bands. The sleeves were perfectly light proof and were interjoined so as to permit the operator to move his hand from one to the other to transfer the film into the developing tank. The film storage can was also placed in one of the sleeves.

The spherical bomb was screwed to an ebonite plate ½" thick, as shown in Figure 20. An aluminium plate 1/16" thick which holds the camera lens was fitted in a groove cut in the wooden box. A horizontal slit of width 1/16" was formed close to the film surface. It was important to centre the image of the spark gap in the slit. In order to protect the camera lens, a clean glass 1/4" thick was interposed between the spherical bomb and the lens.

The motor rotating the Aluminium Drum was equipped with a Variac Motor Speed control and a variac autotransformer. A Strobometer was used to measure the speed of the drum. A brief description of each of these instruments follows:

3.2.1. VARIAC MOTOR SPEED CONTROL

The motor used to drive the Aluminium Drum was a 1/15 H.P. D-C Shunt Motor equipped with a Variac Speed Control Type

1701-AK and a 220/110 V, 0.5 KVA, 50 Transformer Type 1 DW.

Variac Motor Speed control provides adjustable constant-speed operation of the D.C. Motor from A.C. Lines. The range of control is wide and the speed can be adjusted smoothly from the rated value down to zero with constant torque over the entire range.

Variac Motor speed control has selenium rectifiers which supply the field and armature power (Ref. 36). A variac adjustable transformer, ahead of the armature rectifier, makes it possible to vary the armature voltage from the rated value down to zero smoothly and with good regulation. The superior performance of armature-voltage control is thus provided with particularly simple and reliable equipment. Outstanding characteristics are wide speed range at constant output torque, ability to start and stop heavy loads quickly, very low torque pulsation and long life with minimum maintenance.

Since no electronic tubes are employed, the motor can be started instantly without any warmup time. This characteristic of the variac speed control was very valuable for the present work where the motor was used intermittently and was not left turned on throughout the time.

Provision is made for operating the motor with weakened field to raise the maximum motor speed above its base speed. The permissible increase in speed in the Type 1701-AK control, rated 1/15 H.P. is 100%. Thus there are two speed ranges 0-1725 RPM, and 0-3450 RPM. On the high speed range, (Viz. 0-3450 RPM)

field excitation is reduced with corresponding reduction in maximum torque. The armature current for a given load is doubled for this range. The horse power output is unchanged with reduced field, but the maximum torque is reduced in porportion to the increase in speed. The speed of the motor varies with variations in the line voltage. In the operating Instruction Book (Ref. 36) for the Variac Speed Control, it is reported that the change in speed is approximately the same in percentage as the change in Line voltage. During the time of experiment, it was essential that the motor speed should remain constant. For this purpose, a Variac Autotransformer, Type: W20H described in section 3.2.2 was included in the circuit to supply a constant voltage by regulating the pointer-setting of the autotransformer.

The divisions marked on the dial of the variac speed control were calibrated in terms of the shaft speed of the motor by means of a storobometer described in Section 3.2.3 so that no time was actually lost in finding out the speed at the time of experiment.

3.2.2. See p-53.

3.2.3. STROBOMETER

In order to measure the speed of the rotating drum, a Strobometer was used. The usual speedometer would not give correct results because as soon as it is pushed on to the shaft end, the speed of the shaft drops down depending upon the pressure exerted.

The working principle of the Strobometer, type E 102 (India Make) may be explained as follows (Figure 13).

When a flash light of adjustable frequency is thrown on

a rotating object with one distinguishing mark, the mark appears to be stationary when the rotational speed of the object is the same as the frequency of the flash light. A light source developing the flashes at variable frequencies which can be measured is called a Strobotac and this principle is known as Stroboscopic principle. The reading of the rate of flashing which can be read on the Strobometer gives the speed of the rotating object.

When the flashing rate is a whole multiple of the speed of the rotating object, multiple stand still marks will appear e.g. with a flashing light on frequency double the shaft speed there will appear two marks at 180° apart and so on.

The circuit of the Strobometer (Type E 102) consists of a multivibrator whose output is applied to a discharge lamp, causing a series of short duration flashes. The frequency of the multivibrator and therefore the flashing rate is controlled by the setting of a potentiometer. A printed scale covers three speed ranges corresponding to the three sets of coupling condensers selected by a rotary switch (Ref. 38).

The rotary selector switch (Lower Centre, front panel) selects easily the desired condition of operation. The first position 'Low' is for speeds 250 to 1125 r.p.m. The 'medium' covers range four times higher, 1000 to 4500 r.p.m. In the third position 'High' the range covered is four times the 'medium' range in from 4000 to 18000 r.p.m. In the fourth position 'Line or Trigger' the flash lamp is controlled by the frequency of the mains supply.

The illuminated scale is read through a window on the top of the instrument. To provide large and more easily readable figures, the scale readings have been divided by 100; thus the calibration 30 is 3000 rpm.

## 3.3. THE MIXTURE PROPORTIONING SYSTEM

The mixture selected for burning velocity measurements was Acetylene-Air in Stoichiometric quantities. To proportion the mixture inside the spherical bomb itself, a number of Brass-pipe-fittings and needle valves were used. Figure 23 gives the idea of the fittings and the valves' arrangement. An adopter (1/4" to 1/8") was used to connect the pipe fittings and the hole in the aluminium plug leading to the spherical bomb.

As already pointed out that the initial pressures of the acetylene-air mixture were kept subatmospheric. To achieve this a vacuum pump of the rotary type driven by an electric motor was used. Leading through the pipe fittings were three tube connections from the vacuum pump, 0-30" Hg vacuum gauge and the Acetylene cylinder. A separate inlet was provided for atmospheric air. Each of these tubes and the air inlet pipe was fitted with a needle valve.

From the well-known Dalton's Law of partial pressures we know that the total pressure of the mixture is the sum of the partial pressures of the individual gases. Also from the equation of state: $pv = nRT$, the partial pressure of each of the constituents is proportional to the no. of moles present. Making use of these two basic facts, Stoichiometric acetylene-air mixtures were prepared knowing the partial pressures of acetylene and air

in the mixture. The spherical bomb was an air-tight vessel and was initially completely evacuated. Then the calculated number of moles (proportional to the partial pressures) of acetylene and air were put in and total initial pressure of the mixture was read on the vacuum gauge.

### 3.4. THE IGNITION SYSTEM

Figure 14 shows the circuit diagram of the Ignition System which consisted of an Induction Coil, a 6 V Battery, a condenser and a Switch to make and break the circuit.

Closing the ignition switch causes the current to flow through the primary circuit which consisted of the battery, switch primary winding of the induction coil and condenser. A magnetic field is build up through and around the soft iron coil core.

The breaking of the primary circuit causes the magnetic field to start to collapse. The collapsing magnetic field induces current which continues to flow in the same direction in the primary circuit and charges the condenser plates. The condenser builds up a potential opposing flow and discharges very quickly back through the primary circuit. This causes a sudden collapse of the remaining magnetic field inducing a high voltage in the secondary winding of the induction coil (Ref. 31).

The secondary circuit of the ignition system consisted of the secondary coil winding, the high-tension lead and the electrodes. One of the electrodes was grounded through the Aluminium plug and the other was well insulated with a glass tube. The voltage attained in the secondary winding is high enough to cause the spark to jump across the gap formed by the electrodes.

The spark so produced ignited the combustible mixture in the spherical bomb.

### 3.5. THE PRESSURE RECORDING SYSTEM

As in the soap bubble Technique it is necessary to measure the expansion ratio to calculate the Burning Velocity from the flame speed, so also in the Bomb Method to convert the flame speed to Burning Velocity it is necessary to follow the pressure during the course of explosion. In the present work, the pressure recording system included:

1. A Pressure Transducer
2. An Electrostatic Charge Amplifier.
3. A Dual-Beam Oscilloscope and
4. An Oscilloscope Camera

The Pressure Transducer mounted in its adopter was screwed to the Aluminium Plug and was communicating with the spherical bomb through a 1/8" dia. hole. Due to the practical difficulty it was not possible to mount the pressure transducer such that its diaphragm was flush with the inside wall of the bomb. Therefore, a little pressure drop might take place, as the combustion gases would flow through the hole, before exerting pressure on the diaphragm of the pressure transducer. However, we ignored this insignificant pressure drop in our calculations.

Leading from the pressure transducer were the cable connections to the charge amplifier and the oscilloscope. Each of these instruments merits brief description here as regards its working principle and the operating procedure:

### 3.5.1. THE PRESSURE TRANSDUCER

The pressure transducer used in the set up was a Kistler Quartz Pressure Transducer, Model 401.

Pressure applied to the diaphragm of the transducer is converted to a force acting on the transducer crystals, which generate an electrical charge output proportional to the pressure input. The phenomenon is known as "Piezo-Electric Effect". The basic sensitivity of the instrument is "Unit Charge per unit Pressure" and is expressed as pico coulombs per psi (pCb/psi) (Ref. 32 & 33) (pCb = Micro-micro coulombs = $10^{-12}$ coulombs)

Quartz crystal pressure transducers are uniquely adopted to applications which require measurement of an extremely wide range of pressures in very high or very low temperature environments. They also permit display and measurement of small dynamic pressure variations, including transients. In this application, the component due to static pressure is removed from the output signal and the dynamic signal is displayed on an expanded scale.

Initial preload on the transducer elements is greater than the equivalent of one atmosphere, permitting measurement of negative pressures to absolute zero. Usually quartz crystal pressure transducers are restricted to dynamic measurements. But when these are used with Kistler electrostatic charge amplifiers, they are also capable of near-static response under favourable conditions. Static Calibration at working levels is readily accomplished and short-term static measurements are obtained without difficulty.

The pressure transducer was mounted in an adopter (Model 427) (Figure 15) to provide thermal protection to the transducer and to facilitate installation.

Calibration of the pressure transducer is the exact determination of the electric charge output of the instrument in response to a specific pressure input. The charge sensitivity is expressed as the ratio of output to input or pico coulombs per psi (pCb/psi.) The specific procedure for calibration will be described in the next chapter. The Kistler Quartz pressure transducer features high linearity and repeatability over an extremely wide range of pressures and uniform charge sensitivity from very low to very high temperatures. The high natural frequency which results from the use of rigid quartz transducer elements allows measurement of high frequency pressure variations and the fast rise-time components of explosion and internal combustion engine pressures.

### 3.5.2. THE ELECTROSTATIC CHARGE AMPLIFIER

An amplifier is required to convert the high impedance charge signal from the transducer to a low impedance voltage or current signal which can be displayed on a oscilloscope or recorder.

The amplifier employed in the set up for Burning velocity determination was a multi-range, line powered feed back amplifier, Model 566. This was a d.c. voltage amplifier with a capacitive feed back path from the Low-impedance output circuit to the high-impedance input circuit. The output voltage which results from a charge signal input is returned to the input circuit through

the feed back capacitor, in the direction to maintain the input circuit voltage at or near zero. The net charge from the input circuit is stored in the feed back capacitor, producing a potential difference across it equal to the value of the charge divided by the value of capacitance and this potential difference determines the relatinship of the output voltage to the input charge signal. (Ref. 33). The 'gain' of the amplifier is dependent only on the value of the feed back capacitor and is unaffected by time, temperature or line voltage variations.

Referring to the 'Panel Layout' (Figure 16) of the Model 566 Charge Amplifier, we see that the eleven ranges are calibrated in millivott output per picocoulomb input, when the output is multiplied by the sensitivity of the transducer (picocaulombs per psi, g or lb.) the product is the output sensitivity in millivotts per psi, g or lb. Any piezo-electric transducer can be used, the Operate-Calibrate switch permits selection of extremely high input resistance, for short-term static response when calibrating with quartz crystal transducers, or of low input resistance for drift-free dynamic operation with quartz crystal transducers. A pushbutton GND Switch quickly removes any residual signal from the measuring system and restores the output to zero.

### 3.5.3. THE DUAL BEAM OSCILLOSCOPE

The charge signal from the pressure transducer is converted to a voltage signal in the charge amplifier. The output signal from the amplifier is displayed on an oscilloscope and can be photographed by means of an oscilloscope camera. The charge amplifier or the oscilloscope have rather complex electronic circuits to understand; but it is not very difficult to use these instruments even without

understanding their complex circuits. However, some knowledge of the principles of working of these instruments is helpful in using them.

The Oscilloscope used in the present work was a Dual-Beam Oscilloscope, type 502. It is a high-sensitivity fast response voltmeter with visible display. This is a voltage-sensitive instrument and has inertia-less electron beam falling on the fluorescent screen (Ref. 34).

The main part of the oscilloscope is a Cathode-Ray Tube shown in Figure 17. This is a vacuum tube in which a stream of electrons is emitted from cathode, when it is heated and is focussed sharply on the fluorescent screen. The electron beam impringes on the screen and shows off as spot of light. Two horizontal and two vertical deflection plates control the direction of the electron beam and hence the position of the bright spot on the screen. If a voltage is applied to any of the deflection plates it will deflect the beam either in horizontal or vertical direction proportional to its magnitude.

Few controls in the operation of the cathode ray tube are: Intensity, Focus, Vertical Positioning and Horizontal Positioning.

The intensity control decreases or increases the bias on the grid, so that the number of electrons passing out of the grid is controlled. The focus control in an electrostatic cathode ray tube changes the voltage on the focussing electrode and thus changes the restricting force on the beam.

The horizontal and vertical positioning controls are variable resistors provided to move the beam to any desired position in horizontal or vertical direction.

A Dual Beam Oscilloscope has two sets of vertical deflection plates and hence two vertical channels. Upper Beam and Lower Beam Channel. Figure 18 shows the functions of controls on the front panel of the 502 Type: Dual-Beam Oscilloscope, Tektronix make. Since the scope is a Dual Beam Type there are two identical input panels for the two beams.

### 3.5.4. OSCILLOSCOPE CAMERA

The pressure variation in the spherical bomb explosion was displayed on the screen of the Dual Beam Oscilloscope and photographed simultaneously by an oscillograph-record camera.

The camera employed in the present work was the Du Mont Type 299 Camera equipped with a special f/1.9 Lens which enables recording of very high writing rates (upto 200 inches per microsecond with E.K. Super XX Film.) and uses a Graflex Roll film holder with number 120 film. (Ref. 35).

The Dumont Type 299 is a specially designed Oscillograph-record camera used for photographing Cathode-ray Tube phenomena where Single-frame recordings of stationary patterns or single transients are required. The camera consists of the following major components: Housing, Mounting Plate, Data-recording facility, Sliding adapters and film holders, and optical system. A rubber eye-shield is provided for binocular viewing. A photographic view of the camera with identification of components is shown in the Figure 22.

The housing is the basic piece of the camera assembly and houses the optical and data-record systems. The right side of the housing contains the Lens access door through which the Lens, irisdiaphragm and shutter may be adjusted. The housing is provided with an adopter clamp ring for attachment to the oscillograph. The mounting plate is grooved to accommodate the sliding adapter.

The Data recording facility contains two lamps, a push buttom switch, a data recording surface and a dry cell located at the top of the camera housing just above the eyeshield. A window in the data-recording assembly is fitted with a spring return door which is covered on the inner side with a white plastic surface. A ground-glass light diffusing plate covers the opening under the door.

The optical system of the Du Mont Type 299 Camera with Lenses and other components is shown in Fig. 19. All air-to-glass surfaces of the Lens elements are coated to minimize reflections.

The dichroic mirror is of the interference type which consists of a number of transparent dielectric films of precisely controlled thickness deposited on flat glass. When the films are properly arranged with regard to their number, thickness and reflactive index, a chromatic selection takes place in which a certain portion of the spectrum is reflected and the remainder is transmitted. (Thus the name "dichtoic" is given to this beam splitter.)

The dichroic beam splitter used is designed to reflect actinic light (Blue) and transmit yellow light when the rays are

incident at 45°. The optical system of the camera is designed only for a 45° incidence angle. By use of this mirror, simultaneous direct binocular viewing and recording is possible.

### 3.2.2. THE VARIAC AUTOTRANSFORMER

The speed of the motor which rotates the Aluminium Drum fluctuates due to variations in the line voltage. The film on the drum should move at a known speed for the analysis of the photographic records. Therefore, a variac autotransformer was included in the motor-speed regulating system to supply a constant voltage to the motor through the variac motor speed control. During the experiment, the supply voltage was maintained constant by operating the pointer setting of the autotransformer. This operation also permitted the correct calibration of the variac motor speed control.

The autotransformer used in the set up was a W20H Variac Autotransformer. The line and load connections to the variac autotransformer are shown in Figure (12).

# IV. EXPERIMENTAL TECHNIQUE

The diagrammatic sketch of the experimental apparatus is shown in Figure 20. The experimental procedure included:

1. The Calibration of Pressure Transducer
2. The calibration of Variac Motor Speed Control
3. The method of conducting tests:
   - i) Proportioning the combustible mixture
   - ii) Oscilloscope and Drum Camera Adjustments
   - iii) Firing the combustible mixture.

The operational procedures follow:

## 4.1. CALIBRATION OF PRESSURE TRANSDUCER

The measuring system consisted of: the piezo-electric quartz crystal transducer with adapter, the electrostatic charge amplifier, the oscilloscope and the dead weight gage tester; as shown in Figure 24. Calibration was readily accomplished by applying a known input to the transducer and observing the value of the output signal of the amplifier on the oscilloscope screen.

The transducer (and the adapter) was mounted on the dead-weight gage tester and connected to its amplifier. The output connector of the amplifier was connected to the input of oscilloscope. The system was operated for about 30 minutes before calibration. The Zero-setting of the amplifier was checked and the operate-Calibrate switch was set to Calibrate (Long). The required output sensitivity was determined and amplifier "range switch" was set accordingly. Since, here advantage was taken of the short-term static response of the system, the input selector knob of the oscilloscope was set on D.C. and the

terminal used for input A or B or (A-B). Then GND button of the amplifier was depressed and released. The calibrated weights were placed on the dead-weight gage tester and the oil pressure was applied on the diaphragm of the pressure transducer by moving the hand wheel gradually till the plunger of the gage tester just started floating. Then the output signal was promptly read on the oscilloscope corresponding to the pressure input. The test pressures applied with the gage tester produce output voltage signals from the amplifier. Various test pressures were applied and the output voltage signals were measured and correlated with the applied pressures. The data obtained are shown in Table ( 3 ) and the curves shown in figure (37 ) were plotted for ready reference.

Note: The quartz crystal transducers need calibration each time before use. It is because the insulation resistance of the transducer changes from time to time owing to permeation of moisture. The insulation resistance is extremely high, normally in the order of $10^{14}$ ohms which should be checked before use. If the insulation resistance decreases, then extremely low frequency response is attenuated and the static calibration capability of the measuring system is lost.

## 4.2. CALIBRATION OF VARIAC MOTOR SPEED CONTROL

It was essential to know the speed of the Drum Camera motor before igniting the combustible mixture. This speed would correspond to the speed of the film on the drum. With the view to save the time in actually finding out the drum speed at the time of experiment, the variac motor speed control was calibrated before hand by

means of a Strobometer. The following procedure was adopted:

The assembled measuring system consisted of a D.C.Motor with drum mounted on its shaft, a variac motor speed control, a 220V/110V single phase transformer, a variac autotransformer and a strobometer (Figure 25). The description of these instruments is given in the preceding chapter.

A distinguishing mark (chalk mark) was made on the end of the Aluminium Drum. The Strobometer was placed near the Light tight box such that the flash light from the Lamp would fall on the end of the aluminium drum through the side hole in the box. The lid of the box was kept open so that the number of marks appearing on the drum could be visualised. The motor was started and the pointer setting on the variac motor speed control was increased in succession from Lower division to higher division marks on the dial. Selector Switch was set to 'Low', 'Medium' or 'High' depending upon the rate of speed to be measured. The light from the lamp was directed upon the end of the rotating drum and the speed control was adjusted until a single stationary image of the moving part was seen. Then the frequency of flashes was doubled and the speed control adjusted until two stand still marks appeared on the end of the rotating drum. Then the speed of the rotating drum was half the frequency of flashes. This procedure was repeated to find the speed of the drum corresponding to each division marked on the dial of the variac speed control. During the time of caliboration the voltage supply was kept constant by operating the pointer setting of the Variac Autotransformer. The data recorded is shown in Table ( 4 ). A graph was plotted with Div. on Variac Speed Control as abscissa and the Drum Speed (RPM)

an ordinate. The calibration curve obtained for ready reference is shown in Figure (38 ). The check was done many times in the course of testing to ensure that the calibration remained correct at all times.

## 4.3. THE METHOD OF CONDUCTING TESTS

### 4.3.1 PROPORTIONING THE COMBUSTIBLE MIXTURE

The spherical bomb was first evacuated by means of the vacuum pump. When the pointer of the vacuum gauge indicated 30" Hg. vacuum, the needle valve connecting the passage between the spherical bomb and the vacuum pump was closed. Calculations were made before hand (Appendix A ) for partial pressures of acetylene and air in stoichiometric acetylene-air mixtures. Acetylene was drawn into the bomb from the Acetylene-Cylinder and its supply was turned off quickly after the desired amount of Acetylene had been introduced. Then atmospheric air was introduced by opening the air-inlet valve. When the vacuum gauge showed that the stoichiometric quantities of Acetylene and air had been introduced, the air supply was turned off. The total volumetric proportion of Acetylene was always 7.75 percent, the remaining 92.25 percent being air. Thus Acetylene and air were homogeneously mixed inside the spherical bomb itself.

### 4.3.2. OSCILLOSCOPE AND DRUM CAMERA ADJUSTMENTS

The pressure transducer, amplifer and oscilloscope were connected and the system was operated for some time for initial warm up. At first, it was essential to balance the amplifiers of the oscilloscope by means of the D.C. Balance Knob. The Sweep was triggered from the external source (the 6 V Battery in the present work). The battery was connected to the Trigger input terminal

and the trigger selector switch was set at "External". When the Trigger Level Knob was turned counter-clock wise, the beam disappeared from the screen. (But when the ignition-switch would be closed and the circuit again broken, the wave form would trigger or start its sweep. Simultaneously, the spark would also jump across the electrodes which would ignite the acetylene air mixture already introduced into the spherical bomb. This operation was reserved till all the adjustments on the oscilloscope and drum camera were made to record the pressure variations and flame growth simultaneously) The sensitivity of the oscilloscope and the sweep rate were adjusted so that the entire screen was utilized. For dynamic pressure variations the input selector knob was set at A.C. and the operate-Calibrate Switch of the charge amplifier was set at Operate (Short). The position Knob in the horizontal display panel was adjusted so that the sweep started exactly from the left end graduations of the screen. This served as a check in determining the time required for complete combustion.

Next the operations on the drum camera included loading the film on the drum, adjusting the r.p.m-speed by the variac motor speed control and the supply voltage by the variac autotransformer. The films used were cut-films (HP 3, Ilford, 400 A.S.A) of size 1" x 1". The film was attached to the camera drum by a transparent "Scotch Tape".

For recording the pressure variation in the bomb explosion, the oscilloscope camera was attached to the oscilloscope screen by tightening the screw of its adapter clamp ring. The roll film holder containing no. 120 Tri-X Pan Film, 400 ASA was placed on the sliding adapter. The Lens access door was open and the

shutter speed was set at B (Bulb) by rotating the Knurled ring. The 'f' number was set at f/8.0 by sliding pointer over iris diaphragm scale. Then the Lens access door was closed after making adjustments.

4.3.3. FIRING THE COMBUSTIBLE MIXTURE

As an illustration, the various adjustments on the Oscilloscope and drum camera are indicated on the Schematic Diagram of the experimental set up for one set of observations. Before the combustible mixture (Stoichiometric Acetylene - Air Mixture at initial pressure: say, 15" Hg Abs.) was ignited, the scope sensitivity was 5 mV/cm., sweep rate 1 m.sec./cm., externally triggered, amplifier sensitivity at 10 mV/pCb., time constant: Short; pointer setting of variac speed control at 7.0 (drum speed from calibration curve 1520 RPM), supply voltage: 200 V (kept constant by variac autotransformer).

Then the "Viewing Door" of the Oscilloscope camera was opened and the beam intensity was increased to obtain a good picture. The Trigger level knob was turned counter clockwise so that the beam disappeared from the screen. The viewing door was temporarily closed. The dark slide from the film holder was removed. The eyes were set on the eye-shield and viewing door was again opened. With one hand, the shutter release cable was pressed which allowed the exposure. And with the other hand the ignition switch was closed and then circuit broken again. This action ignited the mixture in the bomb and at the same time triggered the sweep. The shutter was closed by releasing the Shutter-Release Cable. Thus the pressure variation was recorded in the Oscilloscope camera and the flame growth in the drum camera simultaneously.

## V. RESULTS AND DISCUSSION

The purpose of the present investigation was to examine the use of the spherical bomb method for determining the burning velocity of Stoichiometric Acetylene-Air Mixtures and to deduce the dependence of burning velocity upon pressure and temperature.

In a given explosion the pressure varies with time from initial pressure $P_i$ to the final explosion pressure $P_e$. The temperature at the flame front varies in time as a result of compression of the unburned mixture. Consequently, since burning velocity may be dependent upon both pressure and temperature, a single measurement of flame and pressure record will not provide data to determine the variation of burning velocity with pressure at constant temperature or with temperature at constant pressure. Hence, a series of simultaneous flame record and pressure measurements were made for stoichiometric mixtures at several initial sub-atmospheric pressures.

From the data recorded, burning velocities at various pressures and temperatures were calculated according to Lewis and Von Elbe method. The calculations were made on the basis of the following assumptions:

ASSUMPTIONS:

1. The gases are ideal and the mixtures are ideal mixtures.
2. The heat capacities are independent of pressure and temperature.
3. The composition of burned gas is fixed.

4. The pressure is uniform at all times, and
5. No heat transfer takes place within the gas or from the gas to the wall.

Gaudry (Ref. 42) has analysed the probable error caused by the assumptions of constant composition of burned gas (no dissociation) and of no heat transfer within the burned gas. He concluded that, for an initial pressure of one atmosphere the error was sufficiently small and that the assumptions are valid if high precision is not demanded. At low pressures and high temperature reached during burning an assumption of ideal behaviour of the gases is admissible. However, at high pressure this assumption becomes questionable.

A set of Flame Records and Pressure-Time Curves for Stoichiometric Acetylene Air Mixtures (7.75% Acetylene) at initial pressures of 6", 10", 15" and 20" Hg.Abs., and the room temperature are shown in Figs. (22 thru 35). The calculated and the observed data are shown plotted in figures (36 thru 44). The method of analysing the Flame and Pressure records with sample calculations is given in Appendices A, B and C. The results are summarised in Tables (5 thru 8).

For determining the burning velocities both methods of calculations were used i.e. by using pressure record alone as well as the experimental flame trace $\frac{dr_b}{dt}$ in conjunction with the thermodynamically calculated value of $P_e$.

In determining the burning velocity from pressure record alone it was essential to check independently the validity of the thermodynamic data and the procedure for calculating $P_e$. For this

purpose, using the pressure record, values of $r_i$ and $r_b$ were were calculated from equations (2.33) and (2.35). Then the calculated radii $r_b$ were compared with the experimental radii. Discrepancies of 6-12% were observed in the calculated values of $r_b$ in comparison to those of experimental values. However, this suggests that within the inevitable experimental error, the two methods of calculating burning velocities are probably correct and the results are therefore self-consistent. Discrepancies may arise from several causes. In reference (43), Lewis has pointed out that since the calculation is based on the assumption that the combustion wave is a mathematical surface, there arises the problem of selecting an experimentally determinable reference surface in the actual combustion. Furthermore, the flame may not be an ideal sphere. A possible third cause may be a lag period in the establishment of thermodynamic equilibrium in the burned gas. The author concludes that at comparatively higher initial pressure, the discrepancies in the observed and calculated radii 'rb' are less possible because of short ignition lag at a higher initial pressure of the mixture. In the present work, the initial pressures were sub-atmospheric. There is some evidence of a large ignition delay at a lower initial pressure. This can be seen from the flame and pressure records.

## EFFECTS OF PRESSURE AND TEMPERATURE ON BURNING VELOCITY

The effects of physical variables such as pressure and temperature on burning velocity have also been examined. The data are plotted in figs. (43 and 44) to show the variation of burning velocity with temperature ($T_u$) of the unburned mixture at constant pressure and with pressure at constant temperature respectively.

The range of data, however, is limited. Therefore, the curves have been extrapolated to deduce a correlation which may enable to determine the burning velocity at various pressures and temperatures.

From the curves (Figs. 43 and 44) it appears that Burning velocity varies Linearly with pressure and temperature. It is also evident that the effect of temperature on burning velocity is more predominant than the effect of pressure. At room temperature (say, 300° K), the effect of pressure on burning velocity is hardly of any significance. It may, therefore, be concluded that burning velocity has small pressure dependence at room temperature; but increases with increase in pressure and temperature.

Contradictory data regarding pressure-dependence of burning velocity are reported in the Literature It is worthwhile to discuss the results of other investigators Bernard Lewis (Ref 44) has shown that flame velocities of Stoictiometric methane, propane, and ethane-air mixtures are independent of pressure whether measured by the constant-volume bomb method or the slot-burner method. Table XVII (Ref 24, p 145) indicates that flame velocities of Stoichiometric Acetylene-Air Mixtures (Pressure range 0.01-1.0 atm.) are independent of pressure. The flame velocities were measured by Wolfhard using Luminous-cone angle method. Experiments conducted by Pickering and Linnett (Ref. 45) using a Burner method showed pressure-dependence of burning velocity. The same investigators found the flame velocity to be independent of pressure by using the soap bubble method. Cullen (Ref. 46) has shown that flame velocities of, propane-air and ethane-air mixtures were inversely proportional to the

Logarithm of pressure in the range 1/3 to 1 atmosphere. Many other investigators also report pressure effects.

Therefore, the author is led to believe that probably there is effect of apparatus on the measurement of pressure-dependence of burning velocity. And this effect should be more clearly resolved before we can accept the finality of pressure dependence of burning velocity.

Recent studies for investigating the effect of pressure on burning velocity for a variety of hydrocarbon fuels in mixtures of Oxygen with inert gases such as Nitrogen, helium and argon, in the pressure range below atmospheric (Range 1/25 - 1 atm.) have been carried out by John Manton and Milliken (Ref. 47) using the spherical bomb method. Their results suggest a very remarkable trend whereby the pressure dependence is of variable order and primarily dependent upon the absolute value of the burning velocity. They found a decrease of burning velocity with increasing pressure for mixtures whose burning velocity at atmospheric pressure is below approximately 50 cm./sec. and an increase for mixtures whose burning velocity at atmospheric pressure is higher than 100 cm./sec. and in the range 50 to 100 cm./sec; a change of burning velocity with pressure is hardly detectable. Strauss and Edse (Ref. 48) have used both the Burner method and a modified version of Stevens' Soap Bubble method to determine burning velocities of various mixtures from one atmosphere upward to 100 atmospheres. They also found independently that burning velocity increases with decreasing pressure for the mixtures having burning velocities below approximately 50 cm./sec.

and an increase in the burning velocity with increasing press for the mixtures having burning velocities greater than 50 cm./sec. The results of these investigators appear to be more reasonable as they have shown that the pressure dependence of burning velocity is primarily dependent upon the absolute value of the burning velocity.

CORRELATION OF BURNING VELOCITY WITH PRESSURE & TEMPERATURE

Since with the aid of the spherical Bomb Method, consistent values of Burning Velocity using both pressure and Flame records have been obtained, the effect of parameters such as pressure and temperature on burning velocity has also been examined. Qualitatively, the results are comparable with those of other investigators like John Manton, and Milliken who have also employed spherical Bomb Method for Investigating the effect of pressure on burning velocity of various hydrocarbon fuel-air mixtures at sub-atmospheric pressures. The burning velocity of stoichiometric Acetylene-Air mixture at 300° K and 1 atmosphere is found to be 114 cm.per sec. Reference 21 (p.153) reports the maximum flame velocity of acetylene with air at 25° C and 1 atmosphere to be at 142 cm. per sec.

A correlation is deduced by which the burning velocity of Stoichiometric acetylene-air mixtures at various pressures and temperatures can be predicted with an average deviation of 2 percent. From the data reported here, Linear relationships were found between the burning velocity and temperature at constant pressure and between the burning velocity and pressure at constant temperature. The following correlation is obtained for the

pressure range 30 Cm.Hg. to 150 Cm.Hg. and the temperature range 300° K to 450° K. (See Appendix D).

$$S_u = \left(5.06 \times 10^{-3} T_u - 1.41\right) \cdot (P + 70) + 98$$

Where $S_u$ = Burning Velocity in Cm. per sec.

$T_u$ = Temperature of unburned mixture, °K.

$P$ = Pressure, Cm.Hg.

This correlation indicates that the temperature has an appreciable effect on flame velocity. For example, in Stoichiometric mixtures of acetylene and air at 1 atmosphere (76 cm.Hg.) when the temperature is increased from 300° K to 450° K, the burning velocity increases from 114 cm. per sec. to 225 cm. per sec.

On the other hand, the above correlation also suggests that at room temperature (say 300° K), the pressure dependence of burning velocity is hardly of any significance. For example, at 300° K, when the pressure is increased from 30 cm.Hg. to 150 cm.Hg. burning velocity increases from 109 cm.per sec. to 122 cm.per.sec. But at a temperature of 450° K, when the pressure is increased from 30 to 150 cm. Hg.; burning velocity increases from 185 cm./sec. to 290 cm. per sec.

Thus, we see that the above correlation can be satisfactorily used to predict the burning velocities in the range of data reported here. The author, however, does not claim that the correlation will predict burning velocities equally well in other pressure and temperature ranges.

## CONCLUSIONS

The results of this study of the spherical Bomb Method of Laminar Burning Velocity measurement for Stoichiometric Acetylene-Air mixtures at various pressures and temperatures are reported in this thesis. Over the range of pressures and temperatures reported, the following conclusions appear to be justified:-

(1) A single explosion using the spherical bomb method provides two sets of values of the burning velocity which are obtained independent of each other from the independently observed records of pressure and flame growth.

(2) The results show good agreement of observed and calculated flame diameters and of the burning velocities obtained from either the flame trace or the pressure record. The method is, therefore, self corroborating.

(3) For stoichiometric acetylene-air mixtures, the burning velocity rises nearly linearly with the increase of pressure and temperature.

(4) The measurement of pressure dependence of burning velocity is qualitatively in agreement with measurement by other investigators using the spherical bomb method for a variety of other hydrocarbon fuel air mixtures at subatmospheric pressures.

(5) The lack of agreement between the spherical bomb method and other methods (e.g. the burner method or the Soap bubble method) reported in the literature is probably due to the effect of apparatus on the measurement of pressure dependence of burning velocity.

## CONCLUSIONS

The results of this study of the spherical Bomb Method of Laminar Burning Velocity measurement for Stoichiometric Acetylene-Air mixtures at various pressures and temperatures are reported in this thesis. Over the range of pressures and temperatures reported, the following conclusions appear to be justified:-

(1) A single explosion using the spherical bomb method provides two sets of values of the burning velocity which are obtained independent of each other from the independently observed records of pressure and flame growth.

(2) The results show good agreement of observed and calculated flame diameters and of the burning velocities obtained from either the flame trace or the pressure record. The method is, therefore, self corroborating.

(3) For stoichiometric acetylene-air mixtures, the burning velocity rises nearly linearly with the increase of pressure and temperature.

(4) The measurement of pressure dependence of burning velocity is qualitatively in agreement with measurements by other investigators using the spherical bomb method for a variety of other hydrocarbon fuel air mixtures at subatmospheric pressures.

(5) The lack of agreement between the spherical bomb method and other methods (e.g. the burner method or the Soap bubble method) reported in the literature is probably due to the effect of apparatus on the measurement of pressure dependence of burning velocity.

(6) A correlation of burning velocity with pressure and temperature is deduced from the data reported in this thesis to predict the burning velocities with an average deviation of 2 percent, in the pressure range 30 to 150 cm.Hg. and the temperature range 300° K to 450° K. The following correlation is obtained:

$S_u = (5.06 \times 10^{-3} T_u - 1.41)(P + 70) + 98$ cm./sec.

where $T_u$ is in °K and P in Cm.Hg.

(7) The correlation indicates that the temperature has an appreciable effect on the burning velocity. It also suggests that the pressure dependence of burning velocity at room temperature is insignificant, but a marked pressure dependence is observed at higher temperatures.

(8) Since the experimental precision in this method is fairly high, it may be regarded as a precision method and at the same time a standard method against which the validity of the other methods may be tested.

It is hoped that the present limited experimental development will help toward a further study of burning velocity data by extending the pressure and temperature range; and will be of some small assistance in guiding future experiments.

## REFERENCES

1. Jost, Wilhelm: Explosion and combustion processes in Gases. McGraw Hill Book Co. Inc. 1946. p. 66.

2. Powling, J: A new Burner Method for the determination of Low Burning Velocities and Limits of inflammability Fuel, Vol. XXVIII, No. 2, 1949, pp. 25-28.

3. Egerton, Alfred and Sen, D.: Flame Propagation - The influence of pressure on the burning velocities of Flat flames. Fourth Symposium (International) on combustion. The Williams and Wilkins Co. (Baltimore), 1953, pp. 321-328.

4. Linnett, J.W.: Methods of measuring Burning velocities. Fourth Symposium (International) on combustion. The Williams and Wilkins Co. (Baltimore), 1953, pp. 20-30.

5. Stevens, F.W.: A constant pressure bomb. NACA Rep. 176, 1923 See also - The Gaseous Reaction - A study of the Kinetics of composite fuels. NACA Rep. 305, 1929.

6. Fiock, Ernest F., and King, H.Kendall: The effect of water Vapour on Flame velocity in equivalent CO-$O_2$ Mixtures. NACA Rep. 531, 1935.

7. Fiock, Ernest F., and Roeder, Carl H.: The Soap Bubble Method of studying the combustion of mixtures of

CO and $O_2$. NACA Rep. 532, 1935.

8. Fiock, Ernest F, and Roeder Carl H.: Some effects of Argon and Helium upon explosions of carbon Monoxide and Oxygen. NACA Rep. 553, 1936.

9. Pickering, H.S., and Linnett, J.W.: Burning velocity Determinations. Part IV - The use of Schlieren photography in determining velocities by the Soap Bubble Method. Trans. Faraday Soc. Vol.47 1951, pp. 989-992.

10. Strehlow, R.A., and Stuart, Joseph G.: An improved Soap bubble method of measuring Flame velocities. Rep. No. 835, Ballistic Res. Labs. Aberdeen Proving Ground (Maryland), Oct. 1952. (Proj. No. TB 3 - 0110V of Res. and Dev. Div. Ord. Corps.)

11. Price, T.W. and Potter, J.H.: Factors Affecting flame velocity in Stoichiometric Carbon monoxide Oxygen Mixtures. Fourth Symposium (International) on combustion. The Williams and Wilkins Co. (Baltimore) 1953, pp. 363-369.

12. Simon, Dorothy M. and Wong, Edgar L.: An Evaluation of the Soap Bubble method for Burning Velocity measurements using Ethylene-Oxygen-Nitrogen and Methane-Oxygen-Nitrogen Mixtures. N.A.C.A. Tech. Note 3106, 1954.

13. Simon, Dorothy M. and Wong, Edgar L.: Burning velocity measurement. Jour. Chem. Phys. Vol. 21, Nos. 5 936, May 1953.

14. Fiock, E.F., and King, H.K.: N.A.C.A. Repts. No. 531, 1935.

15. Fiock, E.F., Marvin, C.F., Caldwell, F.R., and Roeder, C.H. N.A.C.A. Repts. No. 682, (1940).

16. Manton, John, Von Elbe, Guenther and Lewis, Bernard,: Burning velocity measurements in a spherical vessel with central ignition. Fourth Symposium (International) on combustion. The Williams and Wilkins Co. (Baltimore) 1953, pp. 358-363.

17. Lewis, B. and Von Elbe, G.: Combustion, Flames and Explosions of Gases, New York, Academic Press (1951)

18. Coward, H.F., and Hartwell, F.J.: J.Chem. Soc. (London), pp. 1996, 2676 (1932)

19. Hoare, M.F., and Linnet, J.W.: Trans. Faraday Soc.

20. Gerstein, M., Levine, O., and Wong, E.L.: J.Am. Chem. Soc., 73, 418 (1951)

21. Lewis, B. & Von Elbe, G.: J.Chem. Phys., 11, 75 (1943)

22. Dery, R.J.: See Ref. 23 and Lewis and Von Elbe, Combustion Flames and Explosions of Gases; p. 464. New York, Academic Press (1951)

23. Harris, M.E., Grumer, J., Lewis, B., & Von Elbe, G. Third Symposium on Combustion, Flame and

Explosion Phenomena, p. 80. Baltimore, The Williams and Wilkins Co. (1949).

24. Dugger, Godon L., Simon, Dorothy M. & Gerstein, Melvin. Laminar Flame Propagation. Table X. p. 134. NACA Report 1300, 1959.

25. Singer, J.M.: Burning velocity measurements on slot Burners, Comparison with cylinderical burner determinations, pp. 357. Fourth Symposium (International) on combustion. The williams & Wilkins Co. (Baltimore) 1953.

26. Belles, F.E. and Swett, C.C.: Ignition & Flammability of Hydrocarbon Fuels. pp. 83-126, NACA. Rep. 1300, 1957.

27. Hirschfelder, Curtiss and Bird: Molecular Theory of Gases and Liquids. p. 756. John Wiley and Sons. Inc. New York.

28. Spalding, D.B.:Some Fundamentals of Combustion, p. 172 Butterworths Scientific Publications, London, 1955.

29. Lewis, B. and Von Elbe, G: Combustion, Flames and Explosions of Gases, pp. 226-241, New York, Academic Press (1951).

30. Lewis, B. and Von Elbe, G.: J.Chem. Phys., 2,659,665 (1934)

31. Flamm, L. and Mache, H.: Wien Ber. 126, 9(1917)

32. Lewis, B. and Von Elbe, G.: J.Chem. Phys., 2,283 (1934)

33. Fiock, E.F., and Marvin, C.F.: Chem. Rev., 21, 367 (1937)

34. Lichty, L.C.: Internal Combustion Engines (P. 338)
McGraw Hill Book Co. Inc., 1951.

35. Operating and Service Instructions Kistler Quartz Pressure Transducers, Model 401. Kistler Instrument Corporation, New York.

36. Operating and Service Instructions Electrostatic Charge Amplifier, Model 566 Multi-Range. Kistler Instrument Corporation; New York.

37. Instruction Manual for Dual Beam Oscilloscope Type 502 Tektronix, Inc., Beaverton, Oregon, 1961

38. Dumont: Oscilloscope Cameras Instruction Manual Allen B. DuMont Laboratories, Clifton, New Jersey, U.S.A.

39. Variac Motor Speed Controls: General Instructions General Radio Company, West Concord, Massachusetts,USA

40. W20 H Variac Autotransformers: Operating Instructions General Radio Company, West Concord, Massachusetts, USA

41. Strobometer Type E:102 Instruction Book. Toshniwal Instruments (Bombay)

42. Gaudry, H: Rev. inst. franc. petrole et Ann combustible liquids, 4,521 (1929)

43. Lewis, B.: Combustion Processes, High Speed Aerodynamics and Jet Propulsion. Volume II. p - 308. Princeton, New Jersey; Princeton University Press, 1956.

44. Lewis, B.: et al, Research of Flame and Ignition phenomena. Semi-Annual Prog. Rep. James Forrestal Res. Center, Princeton University, Apr. 1, 1953 pp. 81-91.

45. Pickering, H.S. and Linnett, J.W.: Burning velocity determinations VII - The burning velocities of some Ethylene + Oxygen + Nitrogen mixtures. Trans. faraday Soc., Vol. 47, pt. 10, Oct. 1951, pp. 1101-1103, discussion pp. 1104-1106.

46. Cullen, R.E.: A non-dimensional correlation of Flame Propagation at subatmospheric Pressures. Trans. ASME.Vol. 75, no. 1, Jan.1953, pp. 43-49.

47. Manton, J. and Milliken, B.B. : Proc. Gas dynamics Symposium on Aerothermochemistry Aug. 22-24, 1955, North Western University, Evanston, Illinois (Published 1956). of B.Lewis "Selected Combustion Problem" (Agard) p. 178 discussion remark. Butter worths London, 1954.

48. Strauss, W.A. and Edse, R.: WADC Technical Report 56-49 (1956) "Seventh Symposium on Combustion", p. 377 Butterworths, London, 1959.

TABLE 1

PARTIAL PRESSURES OF ACETYLENE & AIR
FOR
VARIOUS INITIAL PRESSURES OF MIXTURES

| Total initial pressure of mixture | | Partial Pressure of Acetylene | | Partial Pressure of Air | | Percent Acetylene in Stoichiometric $C_2H_2$ - Air Mixture |
|---|---|---|---|---|---|---|
| In. Hg. | Cm. Hg. | In. Hg. | Cm.Hg. | In.Hg. | Cm.Hg. | |
| 6 | 15.2 | 0.465 | 1.175 | 5.535 | 14.025 | 7.75% |
| 10 | 25.4 | 0.775 | 1.961 | 9.225 | 23.439 | " |
| 15 | 38 | 1.16 | 2.94 | 13.84 | 35.06 | " |
| 20 | 50.8 | 1.55 | 3.922 | 18.45 | 46.878 | " |

TABLE 2

PRESSURE AND TEMPERATURE RELATIONSHIP FOR ADIABATIC COMPRESSION OF UNBURNED MIXTURE

$$P^{\frac{1-\gamma_u}{\gamma_u}} T_u = P_i^{\frac{1-\gamma_u}{\gamma_u}} T_i \quad ; \quad \gamma_u = 1.4 \ ,$$

| $P_i$ (Cm. Hg.) | $T_i$ ($^oK$) | $P^{\frac{1-\gamma_u}{\gamma_u}} T_u = F_u$ (Const.) |
|---|---|---|
| 15.2 | 303 | 130 |
| 25.4 | 306 | 121 |
| 38.0 | 306 | 109 |
| 50.8 | 308 | 100 |

## TABLE 3

## CALIBRATION OF PRESSURE-TRANSDUCER

1. OSCILLOSCOPE INPUT SELECTOR KNOB SET ON D.C.
2. CHARGE AMPLIFIER TIME CONSTANT : LONG;

| Pressure Input (psi.) | OSCILLOSCOPE OUTPUT (Cms.) | | | |
|---|---|---|---|---|
| | Scopesensitivity 20 mV/Cm. Amplifier Sensitivity 10 mV/pcb. | Scope: 10 mV/Cm. Amplifier: 10mV/pcb. | Scope: 5 mV/Cm. Amplifier: 10 mV/pcb | Scope: 5 mV/Cm. Amplifier: 20 mV/pcb. |
| 25 | 1.2 | 2.4 | 4.8 | 9.6 |
| 50 | 2.4 | 4.8 | 9.6 | ... |
| 75 | 3.6 | 7.2 | ... | ... |
| 100 | 4.8 | 9.6 | ... | ... |

# TABLE 4

## CALIBRATION OF VARIAC MOTOR SPEED CONTROL

### SPEED: 0-1725 RPM; FORWARD

| Divisions on Variac Speed Control | Motor Speed (RPM) | | |
|---|---|---|---|
| | 180 Volts | 200 Volts | 220 Volts |
| 0 | 0 | 0 | 0 |
| 2.0 | 400 | 450 | 490 |
| 3.0 | 590 | 660 | 730 |
| 4.0 | 800 | 850 | 1000 |
| 5.0 | 1020 | 1050 | 1160 |
| 5.4 | 1070 | 1140 | 1260 |
| 5.8 | 1180 | 1230 | 1360 |
| 6.2 | 1270 | 1330 | 1480 |
| 6.6 | 1360 | 1430 | 1570 |
| 7.0 | 1450 | 1540 | 1690 |
| 7.4 | 1550 | 1620 | 1810 |
| 7.8 | 1640 | 1700 | 1910 |
| 8.2 | 1710 | 1780 | 2000 |
| 8.6 | 1790 | 1880 | 2110 |
| 9.0 | 1880 | 1980 | 2210 |

NOTE: (1) Strobometer Range: 250 to 18,000 RPM.

(2) Accuracy: When standardised in terms of a frequency controlled power line, ± 1% above 1000 r.p.m. & ± 2% below 1000 r.p.m. as reported in the Instruction-Book.

# TABLE 5

## CALCULATED AND OBSERVED DATA

### SET NO. 1

$P_i$ = 15.2 Cm.Hg. ( = 6" Hg.Abs.)

$T_i$ = 303° K

R = 6.35 Cms.

$\gamma_u$ = 1.40

$\frac{P_e}{P_i}$ = 10.75, $t_e$ = total time for combustion = 9.1 m.Sec.

Mixture Composition: Acetylene = 7.75%

Air = 92.25%

$$S_u = \frac{dr_i}{dt} \cdot \left(\frac{r_i}{r_b}\right)^2 \left(\frac{P_i}{P}\right)^{\frac{1}{\gamma_u}} \quad ; \qquad S_u' = \frac{dr_b/dt}{1+\left(\frac{P_e}{P}-1\right)/\gamma_u}$$

| P Cm.Hg. | Time m.Sec. | $r_i$ Cms. | $\frac{dr_i}{dt}$ Cm./Sec | $T_u$ K | $S_u$ Cm./Sec. | $r_b$ Calc. Cm. | $r_b$ Obs Cm. | Diff. % | $\frac{dr_b}{dt}$ Cm./Sec. | $S_u'$ Cm./Sec. |
|---|---|---|---|---|---|---|---|---|---|---|
| 16.37 | 4.55 | 1.262 | ... | 312 | ... | 2.34 | 3.2 | 26.8 | ... | ... |
| 20.0 | 5.91 | 2.02 | ... | 330 | ... | 3.74 | 4.5 | 16.9 | ... | ... |
| 25.4 | 6.87 | 2.60 | ... | 350 | ... | 4.40 | 5.25 | 16.2 | ... | ... |
| 30.0 | 7.37 | 2.94 | 645 | 370 | 147 | 4.85 | 5.55 | 12.6 | 625 | 149.5 |
| 40.0 | 8.20 | 3.50 | 770 | 405 | 169.5 | 5.28 | 6.0 | 12.0 | 555 | 173.2 |

TABLE 6

CALCULATED AND OBSERVED DATA

SET NO. 2

$P_i$ = 25.4 Cm.Hg.( = 10" Hg.Abs. )

$T_i$ = 306° K

R = 6.35 Cms.

$\gamma_u$ = 1.40

$\frac{P_e}{P_i}$ = 10.65,

$t_e$ = total time for combustion = 9.1 m.sec.

Mixture Composition: Acetylene = 7.75%

Air = 92.25%

$$S_u = \frac{dr_i}{dt} \cdot \left(\frac{r_i}{r_b}\right)^2 \cdot \left(\frac{P_i}{P}\right)^{1/\gamma_u} ; \qquad S_u' = \frac{dr_b/dt}{1+\left(\frac{P_e}{P}-1\right)/\gamma_u} ,$$

| P Cm.Hg. | Time m.Sec. | $r_i$ Cm. | $\frac{dr_i}{dt}$ Cm./Sec. | $T_u$ °K | $S_u$ Cm./Sec. | $r_b$ Cals. Cm. | $r_b$ Obs. Cm. | Difference % | $\frac{dr_b}{dt}$ Cm./Sec. | $S_u'$ Cm./Sec. |
|---|---|---|---|---|---|---|---|---|---|---|
| 30 | 4.40 | 1.69 | 530 | 330 | 124 | 3.3 | 3.75 | 12.0 | 820 | 122 |
| 40 | 6.10 | 2.48 | 570 | 350 | 135 | 4.33 | 4.85 | 10.70 | 685 | 134 |
| 50.8 | 6.95 | 2.99 | 660 | 372 | 150 | 4.90 | 5.35 | 8.4% | 620 | 156.5 |
| 60 | 7.45 | 3.32 | 770 | 395 | 173 | 5.15 | 5.60 | 8.05 | 620 | 176 |
| 76 | 7.95 | 3.76 | 920 | 420 | 200 | 5.45 | 5.85 | 6.85 | 575 | 203 |
| 86 | 8.19 | 3.99 | 1100 | 435 | 227 | 5.66 | 5.95 | 4.88 | 575 | 227 |

## TABLE 7

## CALCULATED AND OBSERVED DATA

### SET NO. 3

$P_i$ = 38 Cm.Hg.

$T_i$ = 306° K

R = 6.35 Cms.

$\gamma_u$ = 1.4

$\frac{P_e}{P_i}$ = 10.65;

$t_e$ = Total time for combustion = 8.2 m.Sec.

Mixture Composition: Acetylene = 7.75%

Air = 92.25%

$$S_u = \frac{dr_i}{dt} \cdot \left(\frac{r_i}{r_b}\right)^2 \cdot \left(\frac{P_i}{P}\right)^{1/\gamma_u} \quad ; \quad S'_u = \frac{dr_b/dt}{1+\left(\frac{P_e}{P}-1\right)/\gamma_u}$$

| P Cm. Hg. | Time m.Sec. | $r_i$ Cm. | $\frac{dr_i}{dt}$ Cm./Sec. | $T_u$ K | $S_u$ Cm./Sec. | $r_b$ Calc. Cm. | $r_b$ Obs. Cm. | Difference % | $\frac{dr_b}{dt}$ Cm./Sec. | $S'_u$ Cm./Sec. |
|---|---|---|---|---|---|---|---|---|---|---|
| 40 | 2.34 | 1.12 | 470 | 310 | 116 | 2.205 | 2.4 | 8.11 | 855 | 114 |
| 50.8 | 4.30 | 2.08 | 550 | 330 | 125.8 | 3.83 | 4.4 | 12.95 | 732 | 122.5 |
| 60 | 5.05 | 2.48 | 610 | 350 | 143.5 | 4.34 | 4.95 | 12.31 | 700 | 137.2 |
| 76 | 5.74 | 2.96 | 732 | 375 | 165.5 | 4.87 | 5.40 | 9.81 | 690 | 168 |
| 86 | 6.03 | 3.23 | 854 | 390 | 193 | 5.07 | 5.55 | 8.65 | 680 | 187 |
| 100 | 6.35 | 3.51 | 880 | 400 | 212 | 5.32 | 5.70 | 6.67 | 670 | 210 |
| 150 | 7.21 | 4.27 | 1340 | 450 | 277 | 5.75 | 6.05 | 4.95 | 610 | 275 |

## TABLE 8

## CALCULATED AND OBSERVED DATA

### SET NO. 4

$P_i$ = 50.8 Cm.Hg. (= 20" Hg.Abs.)

$T_i$ = 308° K

R = 6.35 Cms.

$\gamma_u$ = 1.40

$\frac{P_e}{P}$ = 10.60; $t_e$ = Total time for combustion = 8.2 m.Sec

Mixture Composition: Acetylene = 7.75%

Air = 92.25%

$$S_u = \frac{dr_i}{dt} \cdot \left(\frac{r_i}{r_b}\right)^2 \cdot \left(\frac{P_i}{P}\right)^{1/\gamma_u} \quad ; \quad S_u' = \frac{dr_b/dt}{1+\left(\frac{P_e}{P}-1\right)/\gamma_u}$$

| P Cm. Hg. | Time m.Sec. | $r_i$ Cm. | $\frac{dr_i}{dt}$ Cm./Sec. | $T_u$ K | $S_u$ Cm./Sec. | $r_b$ Calc. Cm. | $r_b$ Obs. Cm. | Difference % | $\frac{dr_b}{dt}$ Cm./Sec. | $S_u'$ Cm./Sec. |
|---|---|---|---|---|---|---|---|---|---|---|
| 60 | 3.2 | 1.695 | 513 | 320 | 123 | 3.26 | 3.50 | 6.85 | 830 | 123.5 |
| 76 | 4.42 | 2.365 | 610 | 341 | 144 | 4.23 | 4.55 | 7.03 | 755 | 141 |
| 86 | 4.92 | 2.645 | 670 | 350 | 153.2 | 4.59 | 4.90 | 6.34 | 732 | 150 |
| 100 | 5.41 | 2.96 | 784 | 370 | 179.0 | 4.87 | 5.25 | 7.24 | 732 | 180 |
| 150 | 6.35 | 3.74 | 1100 | 410 | 237 | 5.48 | 5.85 | 6.33 | 670 | 234 |

N.B. THE FIGURE GIVES ONLY THE QUALITATIVE PICTURE

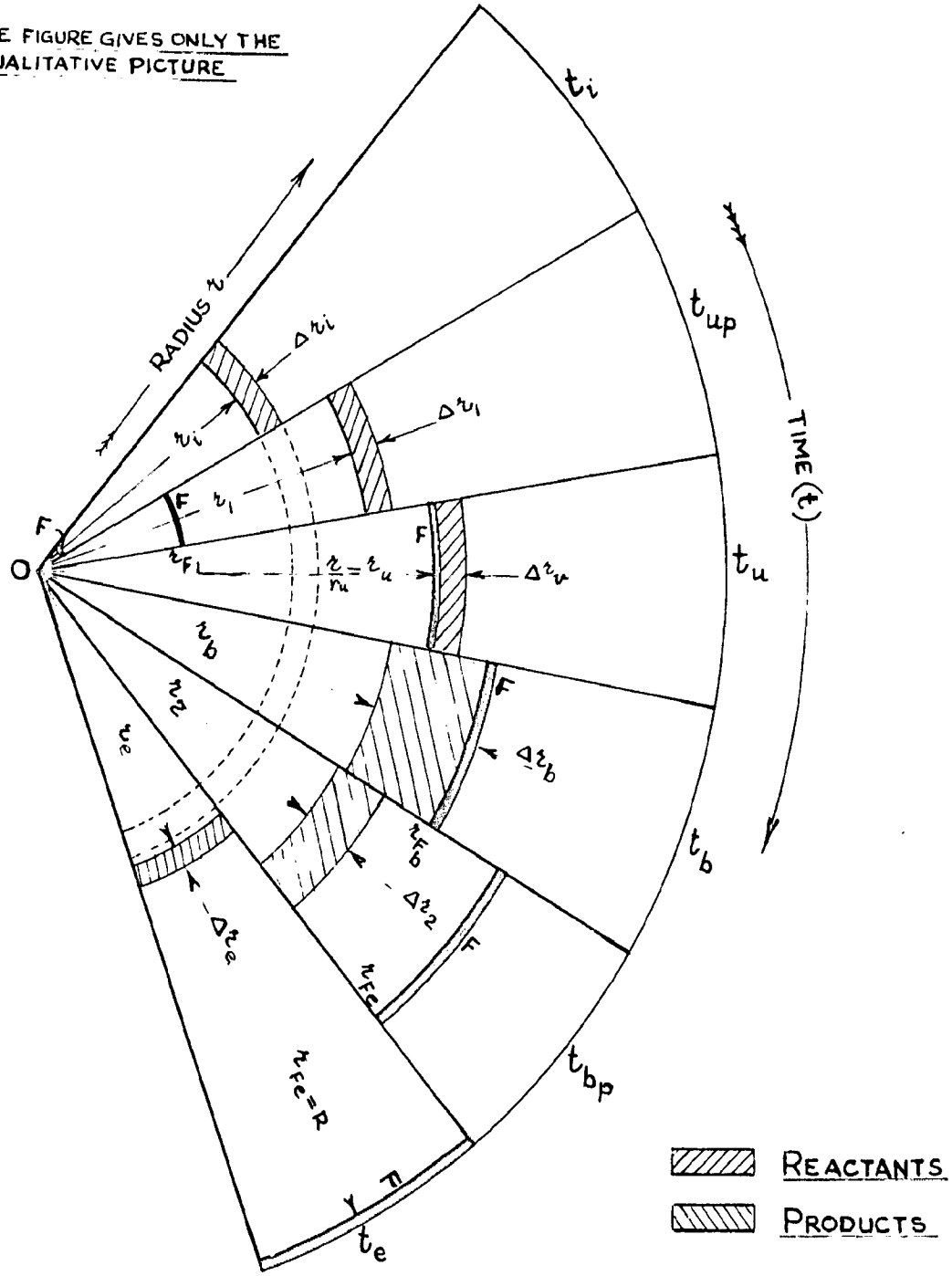


FIG. 1 POSITION OF AN ARBITRARY ELEMENTRY LAYER AT DIFFERENT TIMES.

INDICES i AND e REFER TO THE POSITION OF LAYER BEFORE CENTRAL IGNITION AND AFTER COMPLETE COMBUSTION.
INDICES u AND b REFER TO THE LAYER WHEN THE FLAME HAS JUST REACHED THE ADIABATICALLY COMPRESSED UNBURNED LAYER AND WHEN IT HAS JUST CROSSED THE LAYER.

INDICES 1 AND 2 REFER TO SOME INTERMEDIATE STAGE OF LAYER WHEN (1) THE FLAME IS PROGRESSING TOWARDS IT AND (2) AFTER IT HAS OVERTAKEN THAT LAYER.

$r$ = INNER RADIUS OF LAYER AT TIME INTERVAL $t$.
$\Delta r$ = THE THICKNESS OF LAYER.
$r_F$ = FLAME RADIUS.

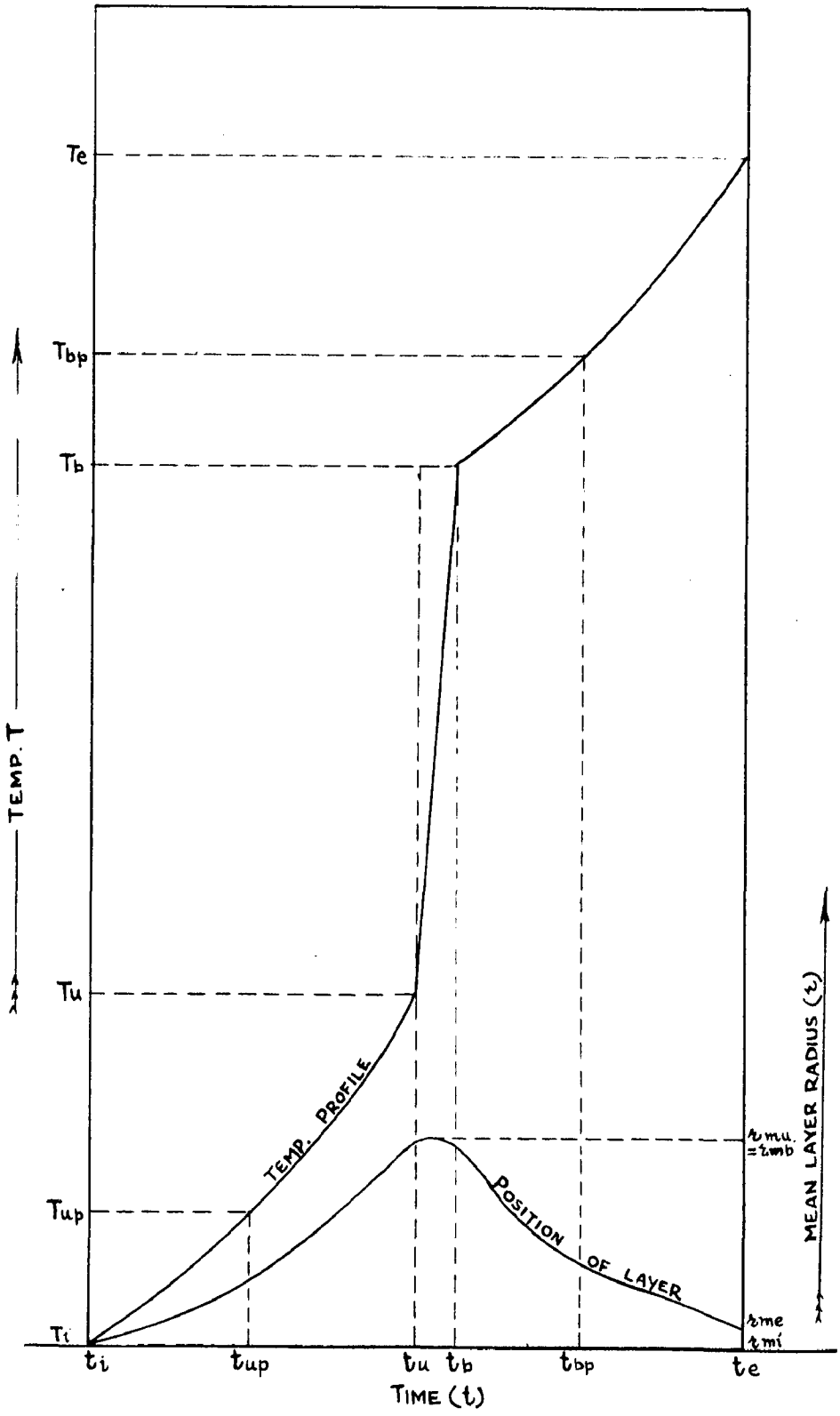


FIG. 2 TIME VARIATIONS IN TEMPERATURE AND RADIUS OF AN ELEMENTRY LAYER DURING EXPLOSION IN A SPHERICAL BOMB.

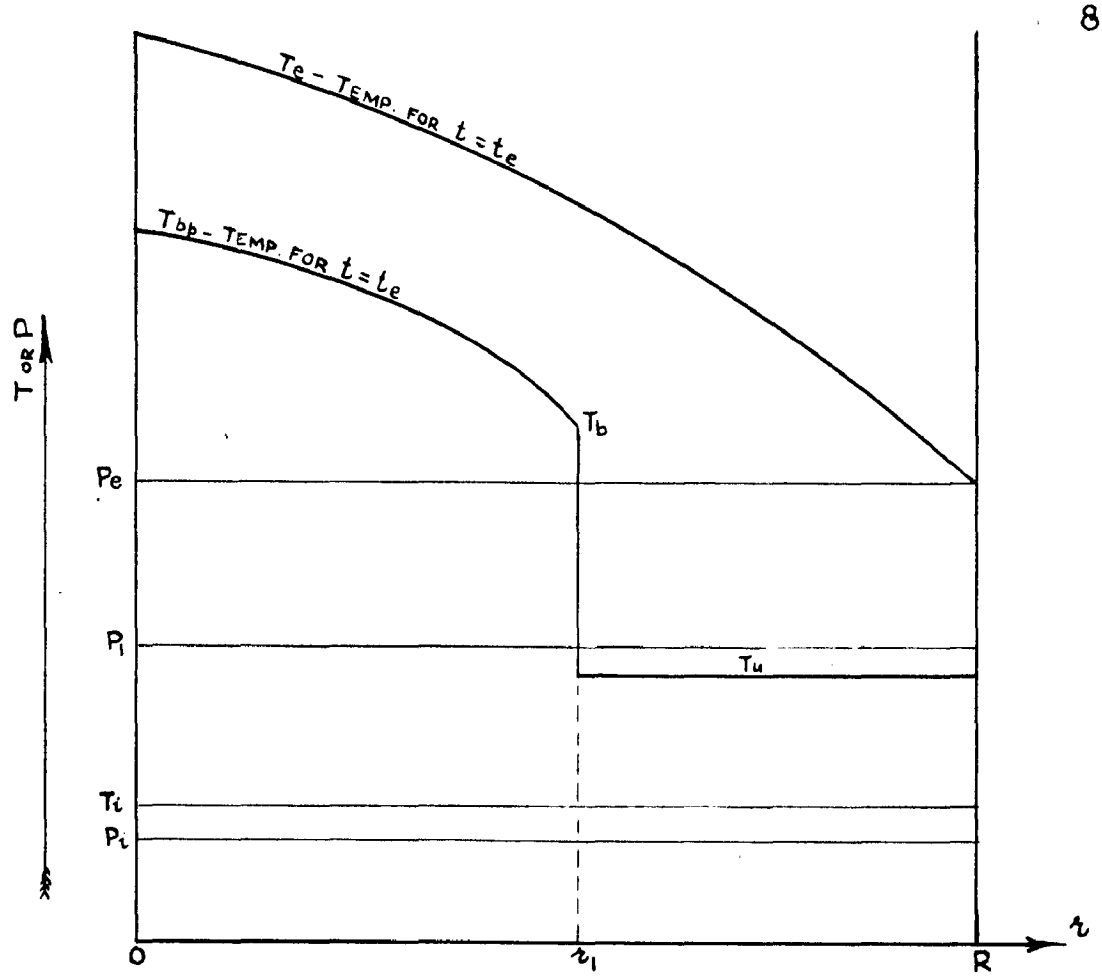


FIG. 3. INITIAL INTERMEDIATE AND FINAL SPATIAL VARIATIONS IN PRESSURE AND TEMPERATURE DURING EXPLOSION IN A SPHERICAL BOMB.

INDICES i, 1 AND e. REFER TO THE BEGINNING, INTERMEDIATE CONDITION AND THE FINAL PROFILES RESPECTIVELY

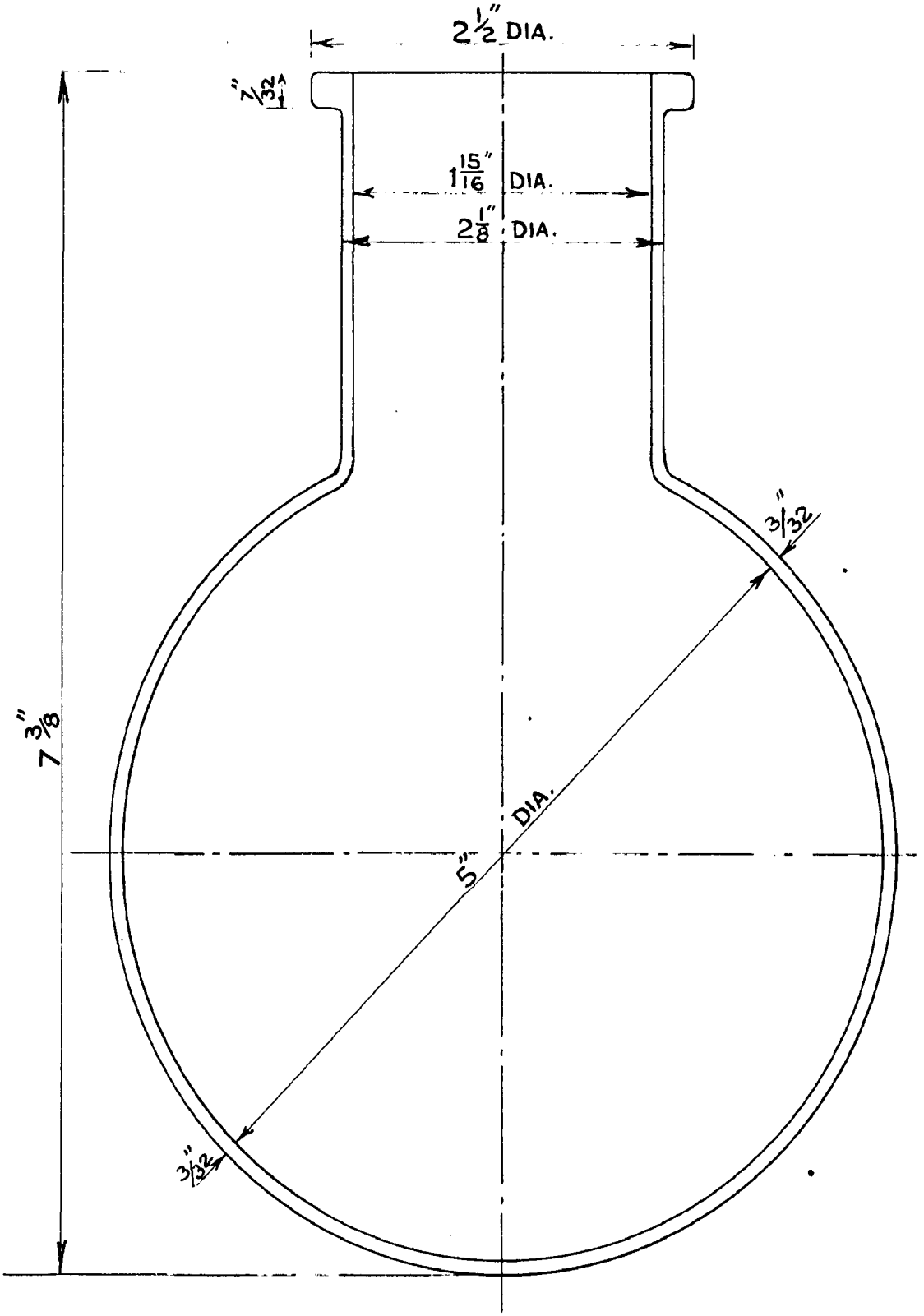


FIG. 4 SPHERICAL BOMB

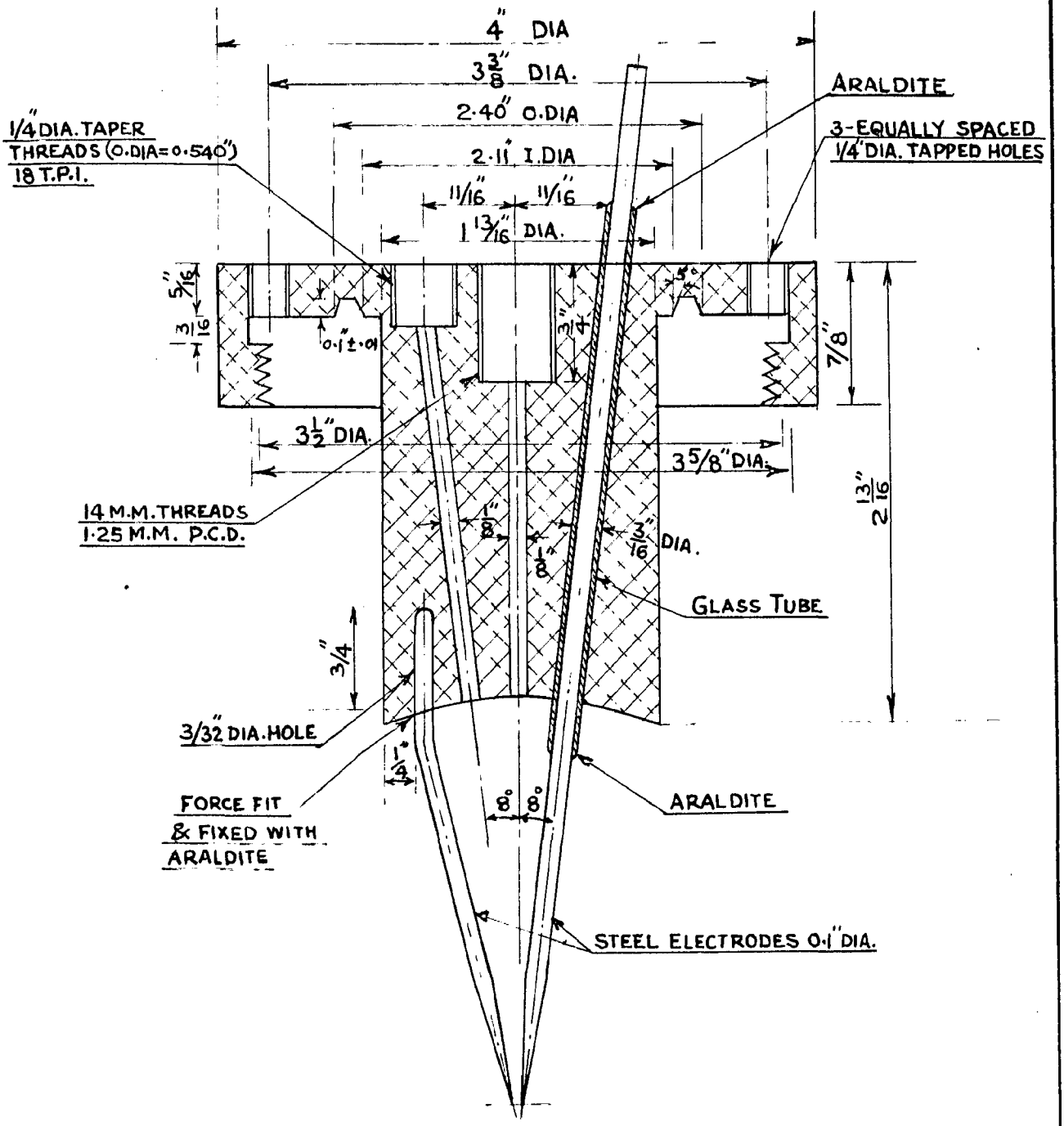


FIG. 5

| UNIVERSITY OF ROORKEE MECH. ENGG. DEPTT. | |
|---|---|
| BURNING VELOCITY SET UP | |
| PLUG | |
| SCALE FULL SIZE | MATERIAL ALUMINIUM |
| 5-10-63 | S.P. SHARMA, |

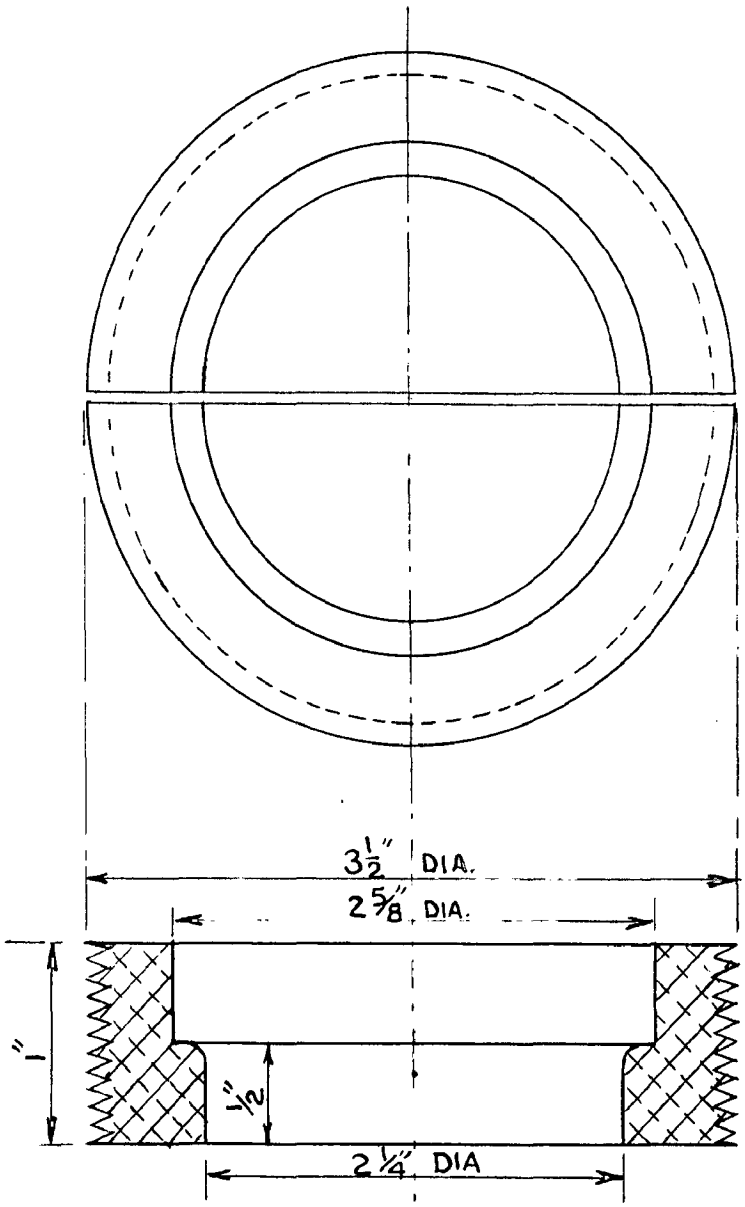


FIG. 6

| | |
|---|---|
| UNIVERSITY OF ROORKEE<br>MECH. ENGG. DEPTT. | |
| BURNING VELOCITY SETUP<br>SPLIT RING | |
| SCALE<br>FULL SIZE | MATERIAL<br>PRESPEX |
| 5.10.63 | S.P. SHARMA |

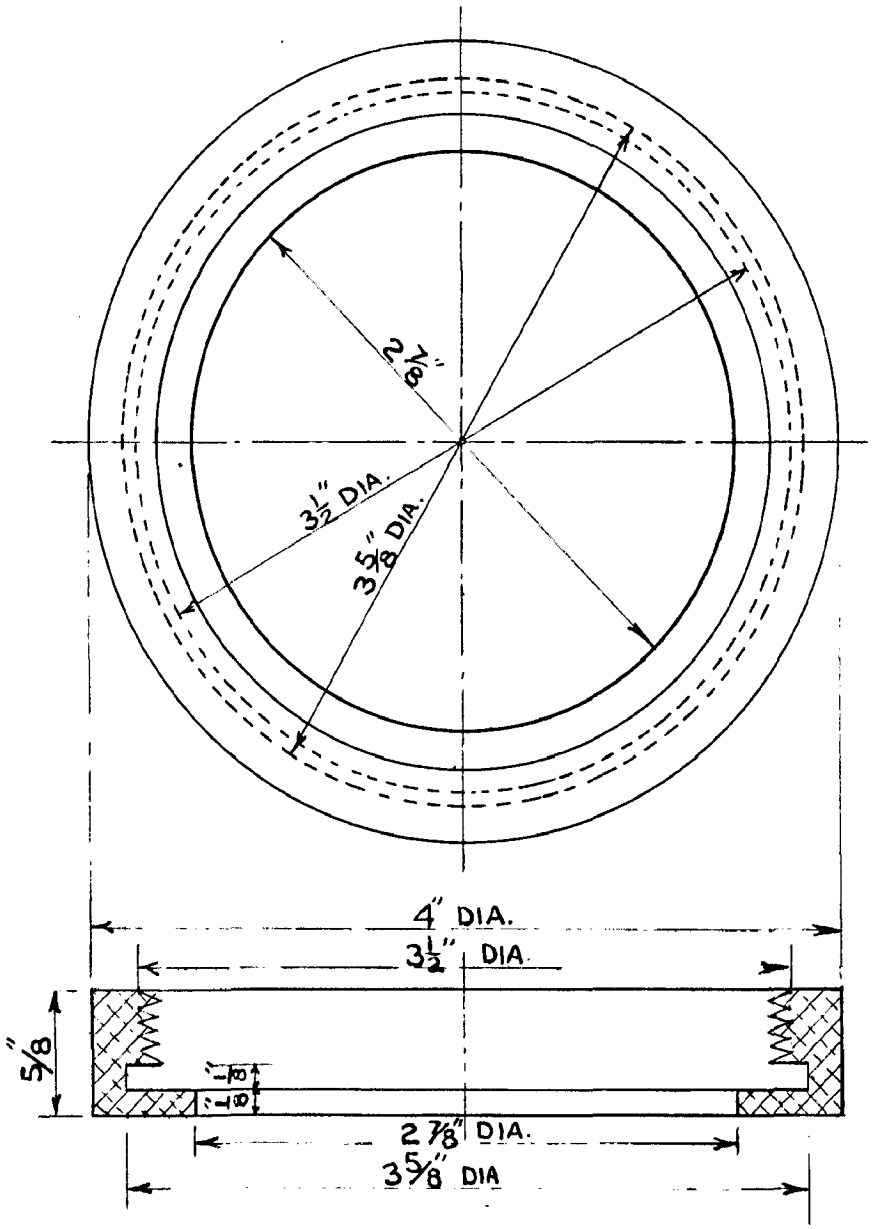


FIG. 7

| UNIVERSITY OF ROORKEE<br>MECH. ENGG. DEPTT. | |
|---|---|
| BURNING VELOCITY SET UP<br>RING | |
| SCALE<br>FULL SIZE | MATERIAL<br>ALUMINIUM |
| 5-10-63 | S.P. SHARMA |

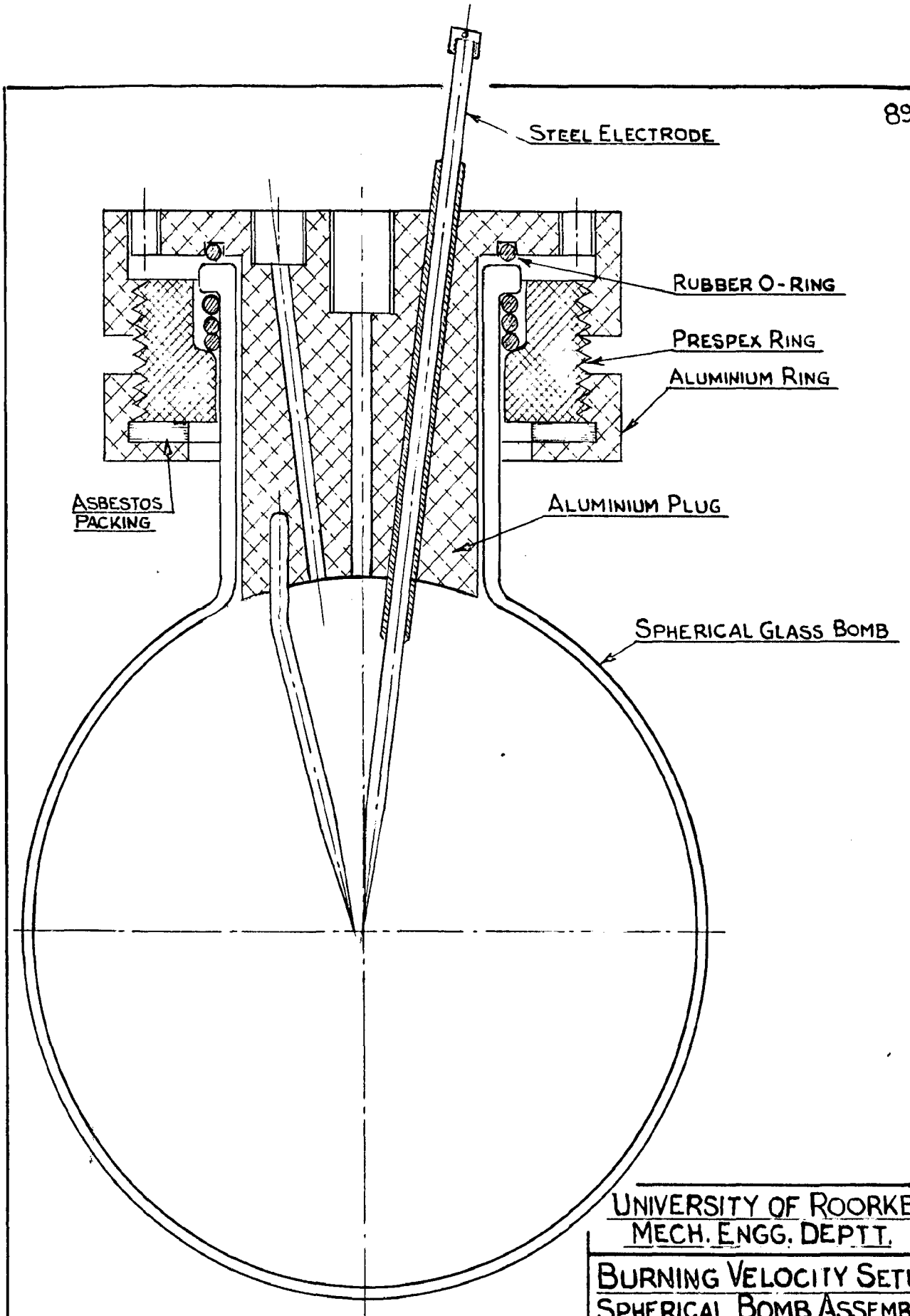


FIG. 8

UNIVERSITY OF ROORKEE
MECH. ENGG. DEPTT.

BURNING VELOCITY SETUP
SPHERICAL BOMB ASSEMBLY

| SCALE FULL SIZE | MATERIAL |
|---|---|
| 5.10.63 | S.P. SHARMA |

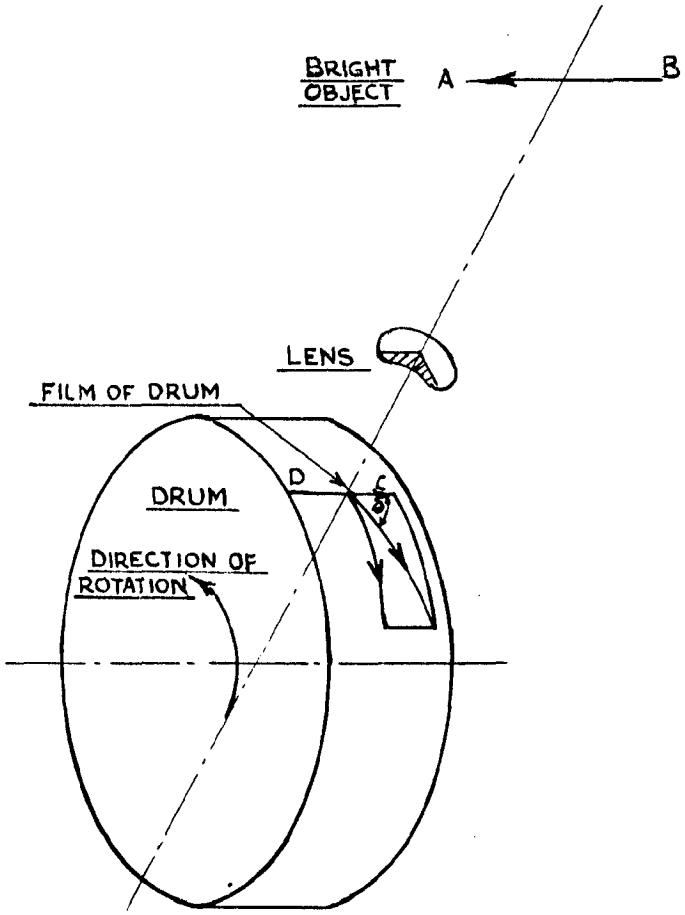


FIG. 9 DIAGRAM OF SIMPLE DRUM CAMERA

R ON SIDE
PRAXIS = 3¾"

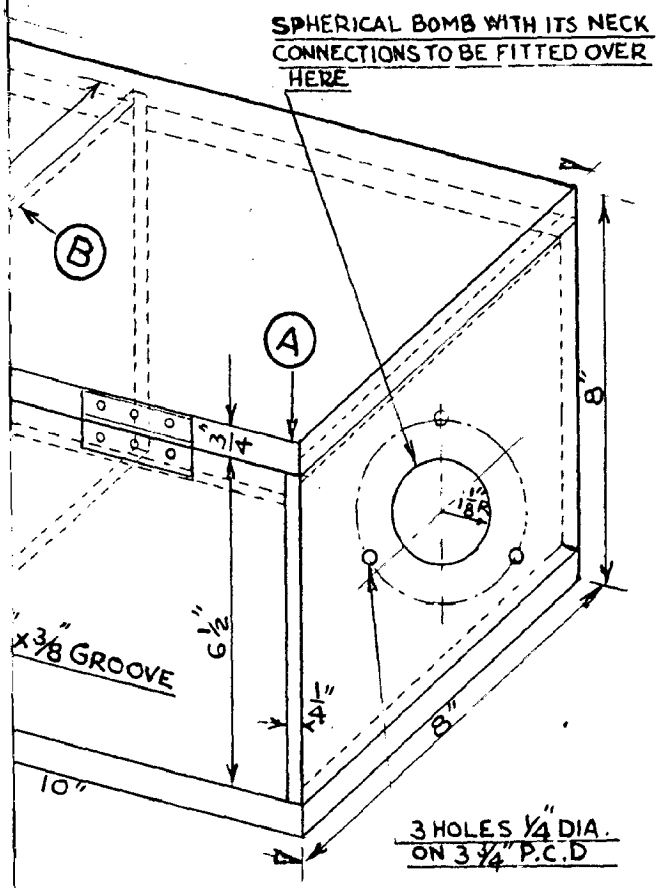


7¼" × 7¼" × 1/16" THICK ALUMINIUM PLATE WITH A CENTRAL HOLE TO HOLD THE CAMERA LENSES.

| | |
|---|---|
| UNIVERSITY OF ROORKEE<br>MECH. ENGG. DEPTT. | |
| BURNING VELOCITY SETUP<br>LIGHT-TIGHT-BOX | |
| SCALE<br>1/4 FULL SIZE | MATERIAL<br>TEAK WOOD |
| 9.12.63. | S.P. SHARMA |

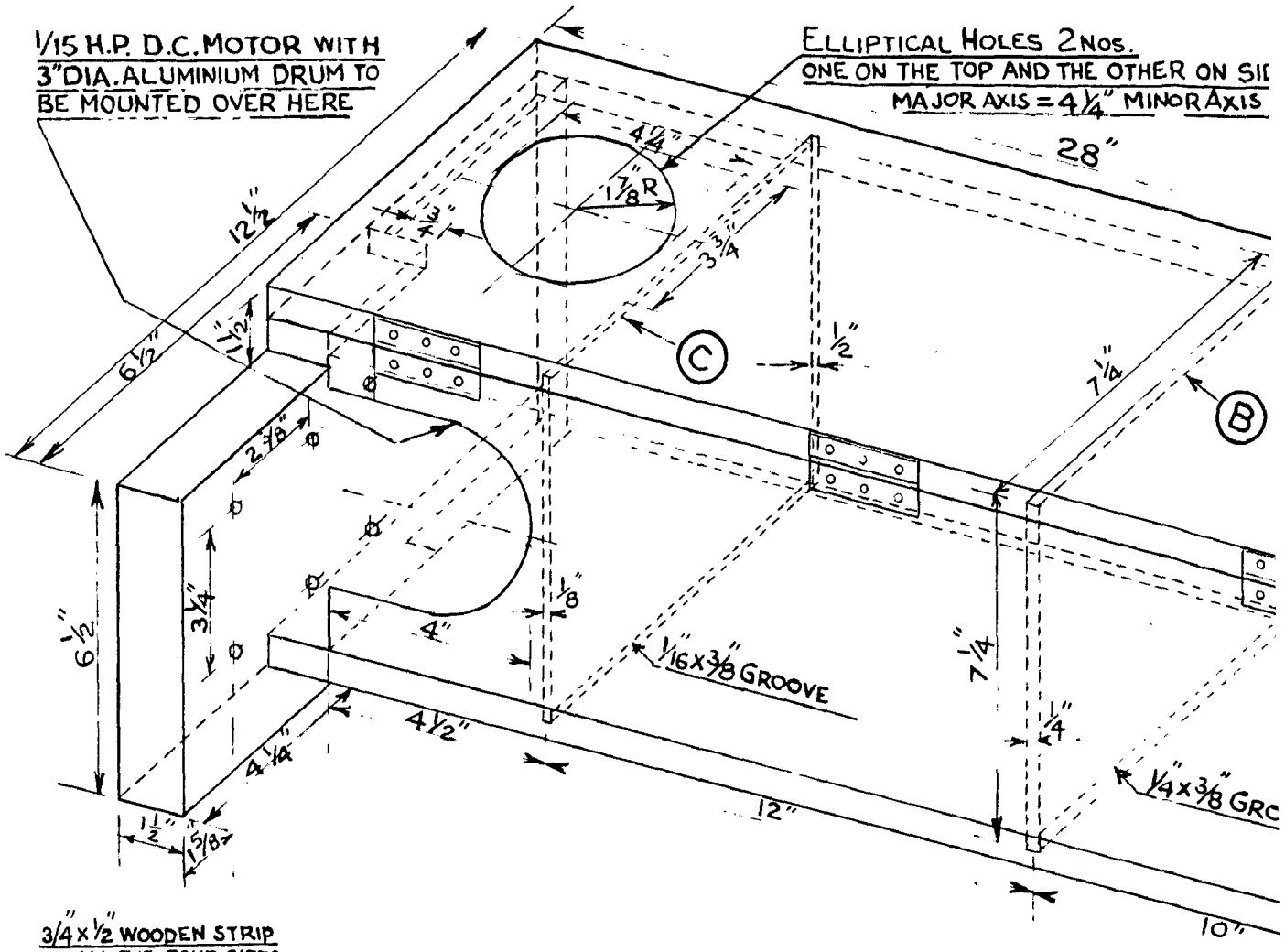


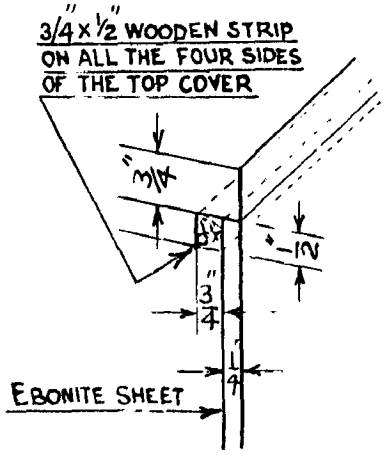


DETAIL AT A

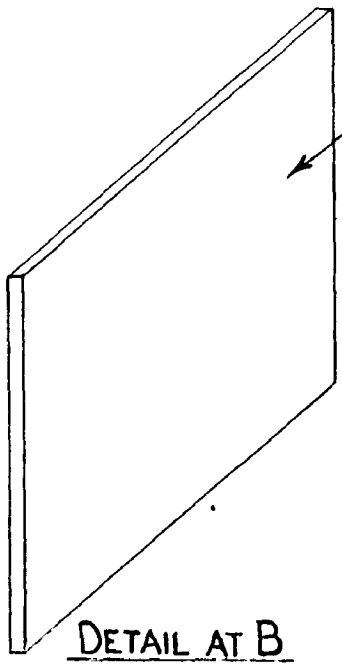

7 1/4 X 7 1/4 X 1/4 THICK GLASS PLATE TO PROTECT THE CAMERA LENSES

DETAIL AT B

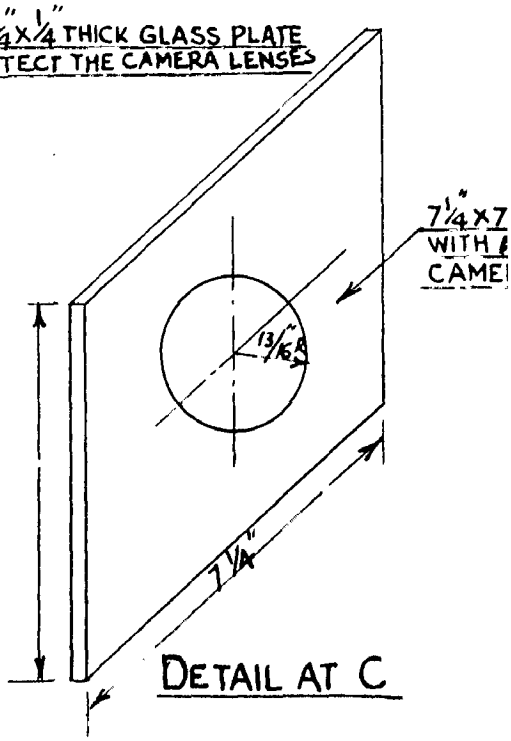


DETAIL AT C

FIG. 11

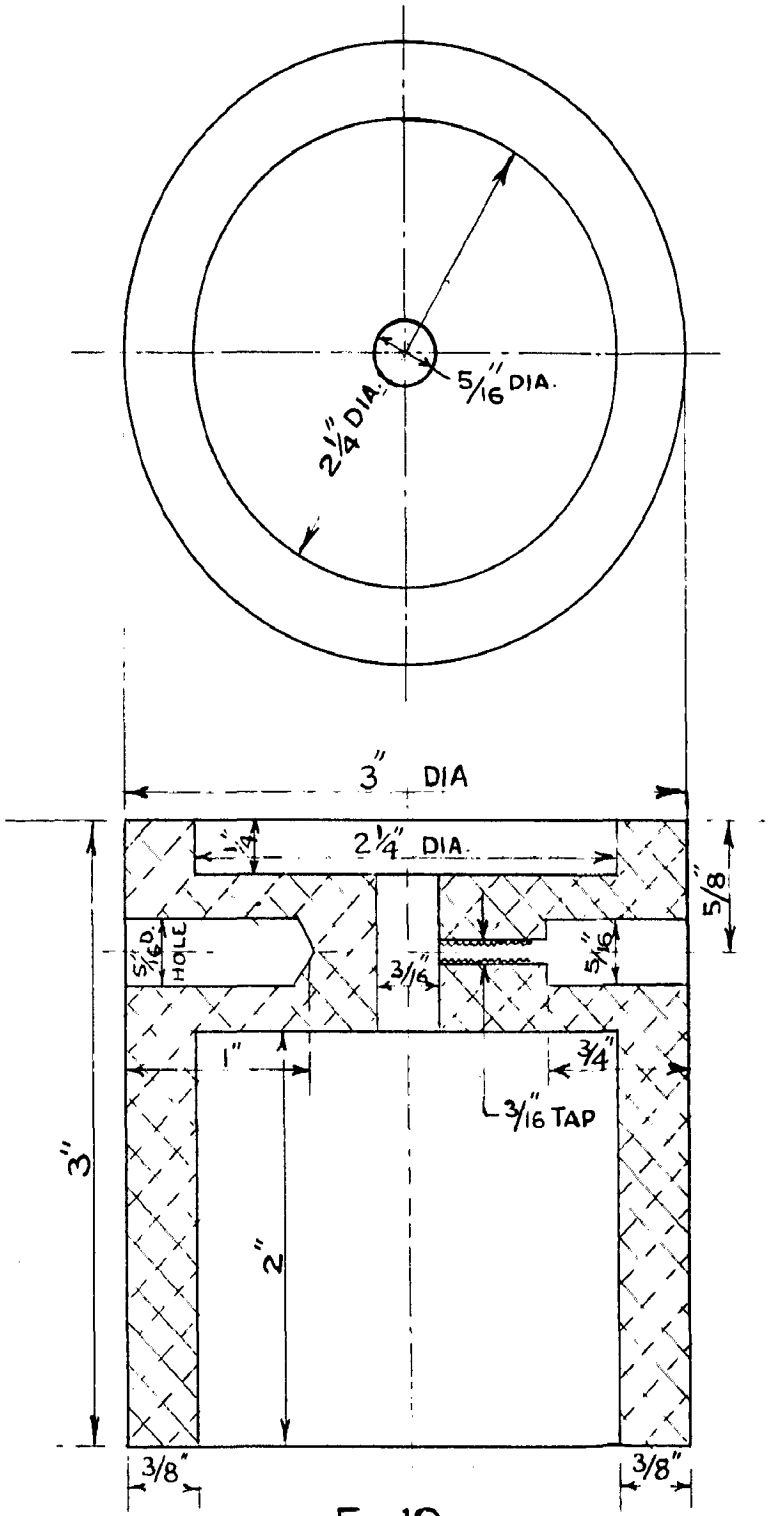


FIG. 10

| UNIVERSITY OF ROORKEE<br>MECH. ENGG. DEPTT. | |
|---|---|
| BURNING VELOCITY SET UP<br>ALUMINIUM DRUM | |
| SCALE<br>FULL SIZE | MATERIAL<br>ALUMINIUM |
| 5.10.63 | S.P. SHARMA |

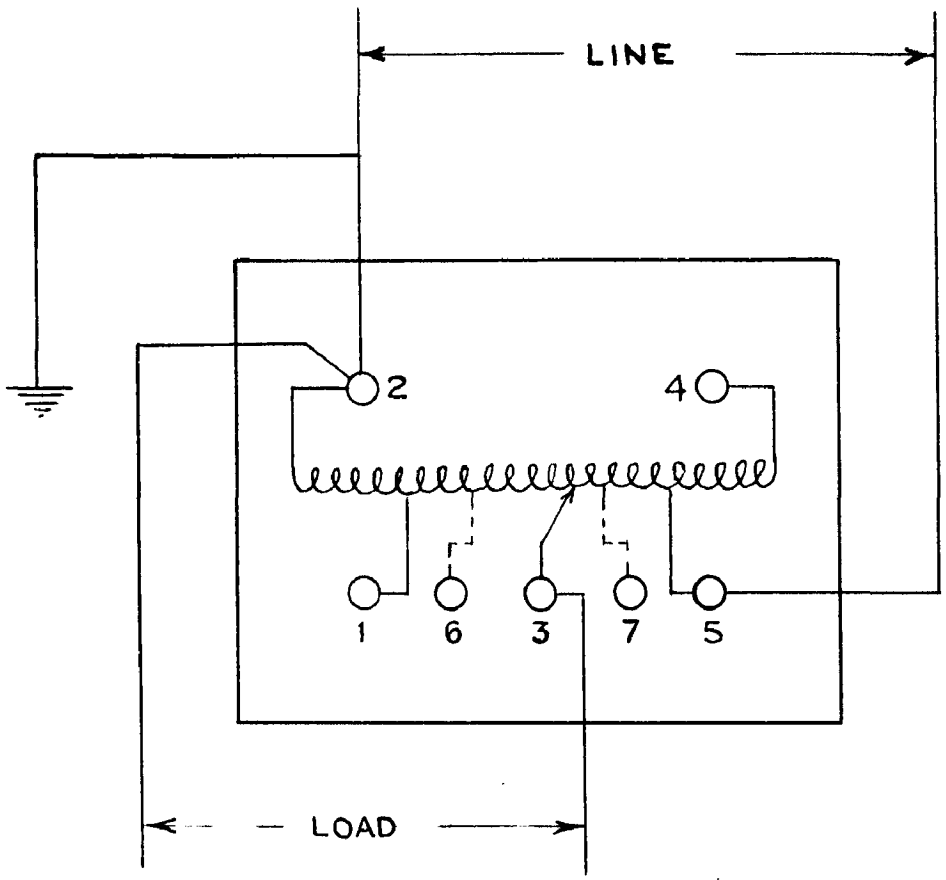


LINE : 230 V; 50 CPS
LOAD: 0-280 VOLTS

FIG. 12 LINE AND LOAD CONNECTIONS TO THE VARIAC AUTO TRANSFORMER (SURFACE MOUNTING)

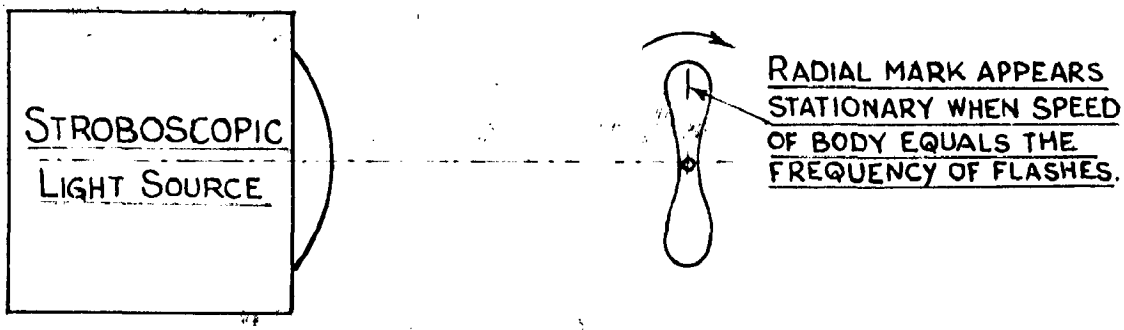


FIG. 13 STROBOSCOPIC PRINCIPLE

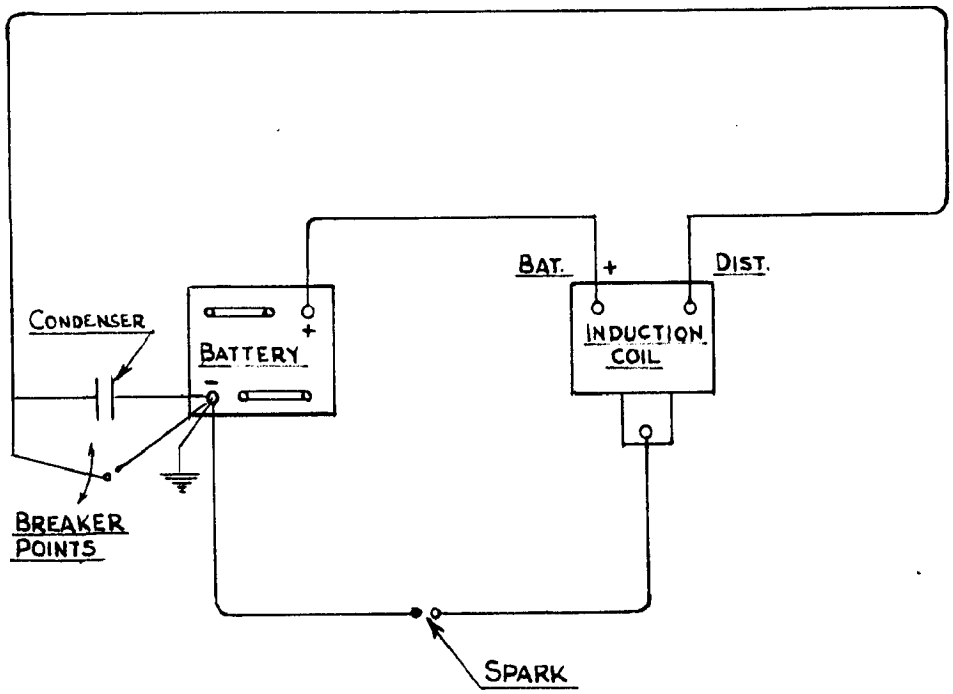


FIG.14 IGNITION SYSTEM

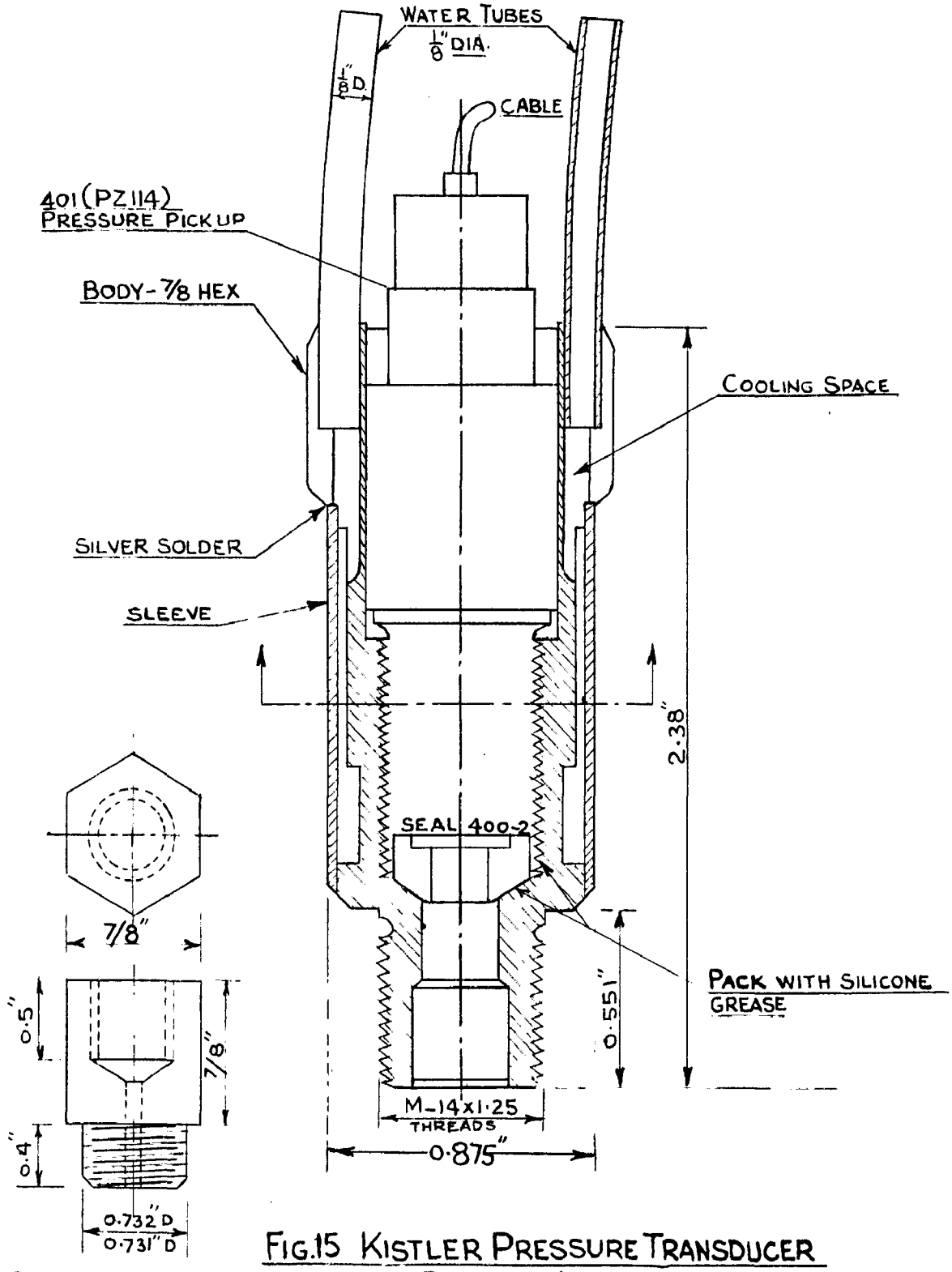


FIG.15 KISTLER PRESSURE TRANSDUCER AND COOLING ADOPTER

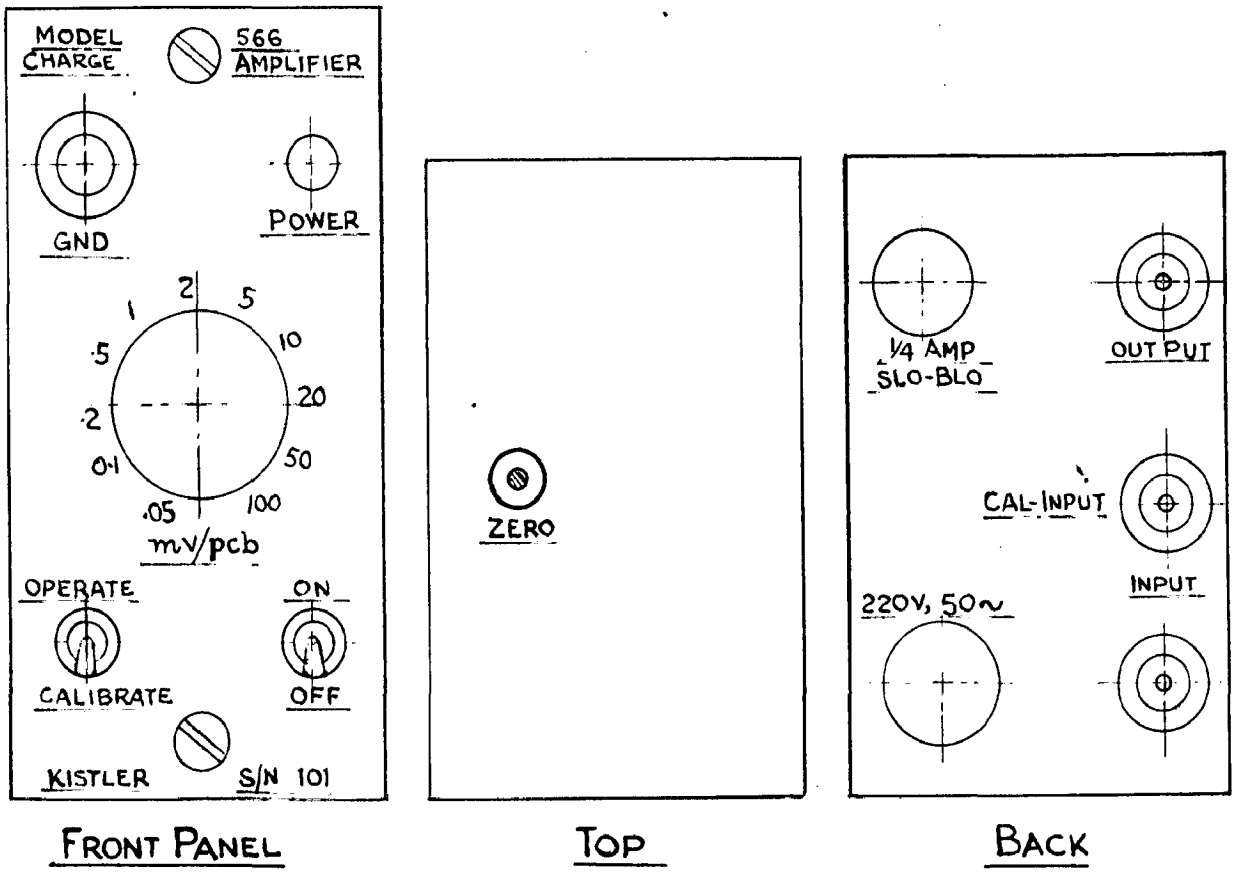


FIG. 16 PANEL LAYOUT

MODEL 566 CHARGE AMPLIFIER

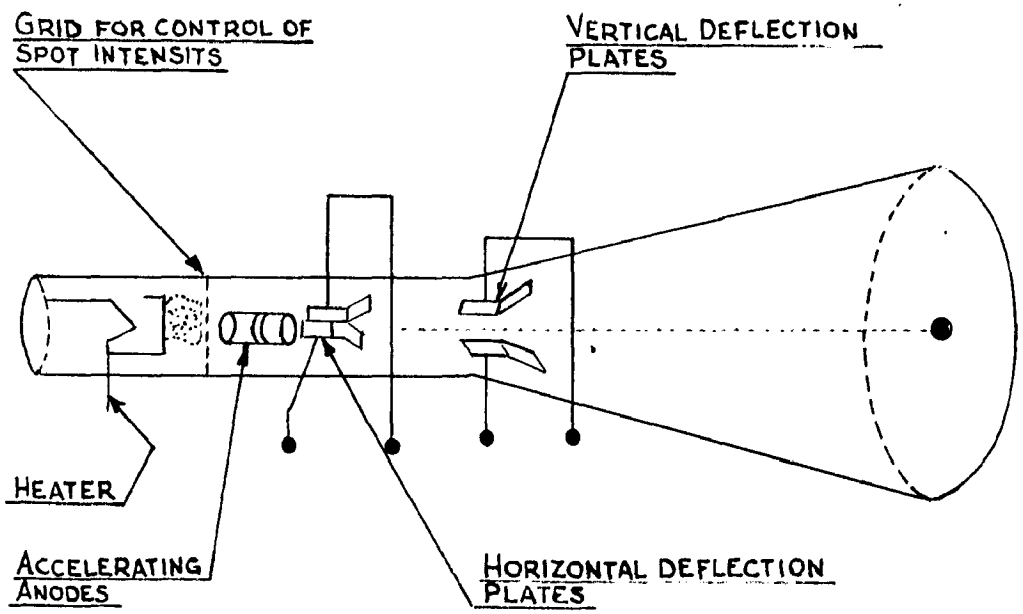


FIG.17 CATHODE RAY TUBE

**TRIGGER SELECTOR** – DETERMINES WHETER TRIGGERING OCCURS ON THE RISING PORTION (+ SLOPE) OR FAILING PORTION (- SLOPE) OF THE TRIGGERING WAVEFORM. ALSO SELECTS A.C. OR D.C.

**TRIGGERING LEVEL.** SELECTS THE VOLTAGE POINT ON THE TRIGGERING WAVEFORM WHERE THE SWEEP IS TRIGGERED ALSO SELECTS AUTOMATIC OR RECURRENT OPERATION

**TIME/CM:-** SELECTS DESIRED SWEEP RATE.

**SCALE ILLUMINATION:** CONTROLS THE ILLUMINATION OF THE GRATICULE

**FOCUS** – FOCUSES UPPER AND LOWER BEAM DISPLAY.

**INTENSITY** – CONTROLS THE INTENSITY OF UPPER AND LOWER BEAMS.

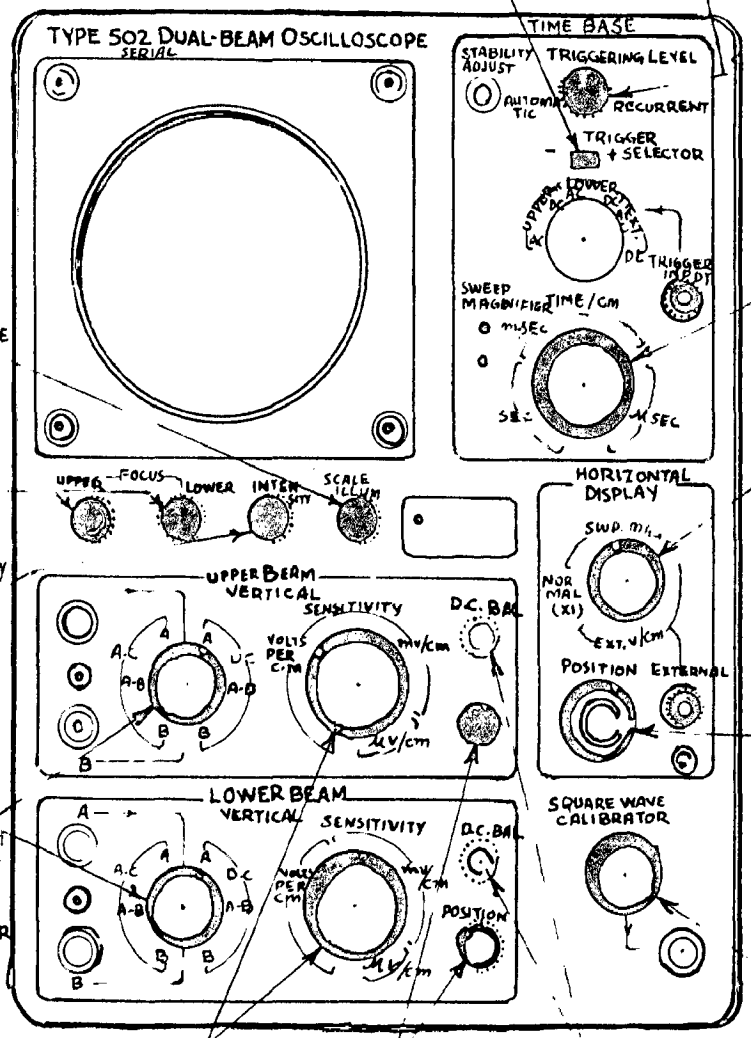


**HORIZONTAL DISPLAY** SELECTS 1, 2, 5, 10 AND 20 TIMES HORIZONTAL MAGNIFICATION OF THE DISPLAYED WAVE FORM. ALSO CONTROLS HORIZONTAL SENSITIVITY FOR EXTERNAL INPUTS APPLIED AT THE EXTERNAL CONNECTOR.

**POSITION** – POSITIONS BOTH UPPER AND LOWER BEAMS HORIZONTALLY.

**INPUT SELECTOR** CONNECTS INPUTS FROM SELECTED INPUT CONNECTOR(S) TO VERTICAL AMPLIFIER AND ALSO SELECTS EITHER A.C. OR D.C. COUPLING OF THE INPUT SIGNAL.

**SENSITIVITY:-** SELECTS THE SENSITIVITY OF THE VERTICAL AMPLIFIER.

**POSITION** – POSITIONS TRACE VERTICALLY.

**D.C. BALANCE** BALANCES VERTICAL AMPLIFIER ON HIGH RANGES OF SENSITIVITY CONTROL.

**SQUARE-WAVE CALIBRATOR** CONTROLS AMPLITUDE OF THE CALIBRATOR SQUARE WAVES AT THE CAL. OUT CONNECTOR.

FIG. 18 FUNCTIONS OF THE TYPE 502 FRONT PANEL CONTROLS

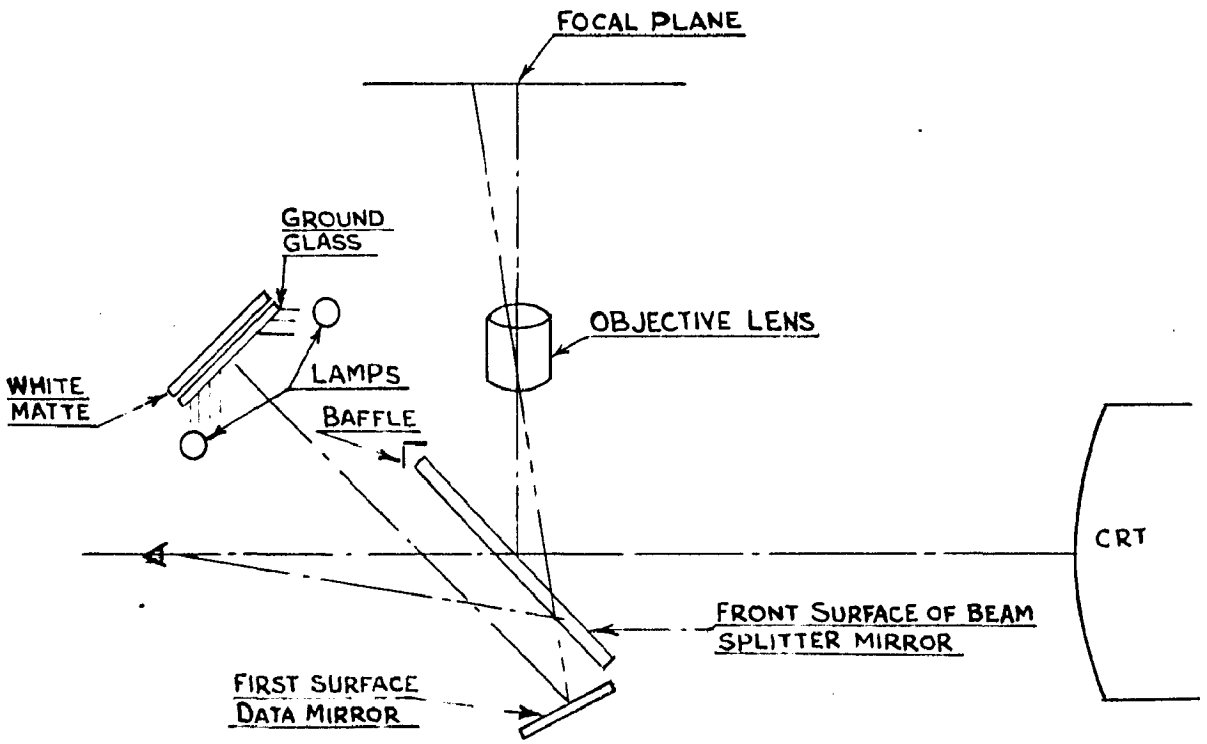


FIG. 19 OPTICAL SYSTEM OF TYPE 299 CAMERA

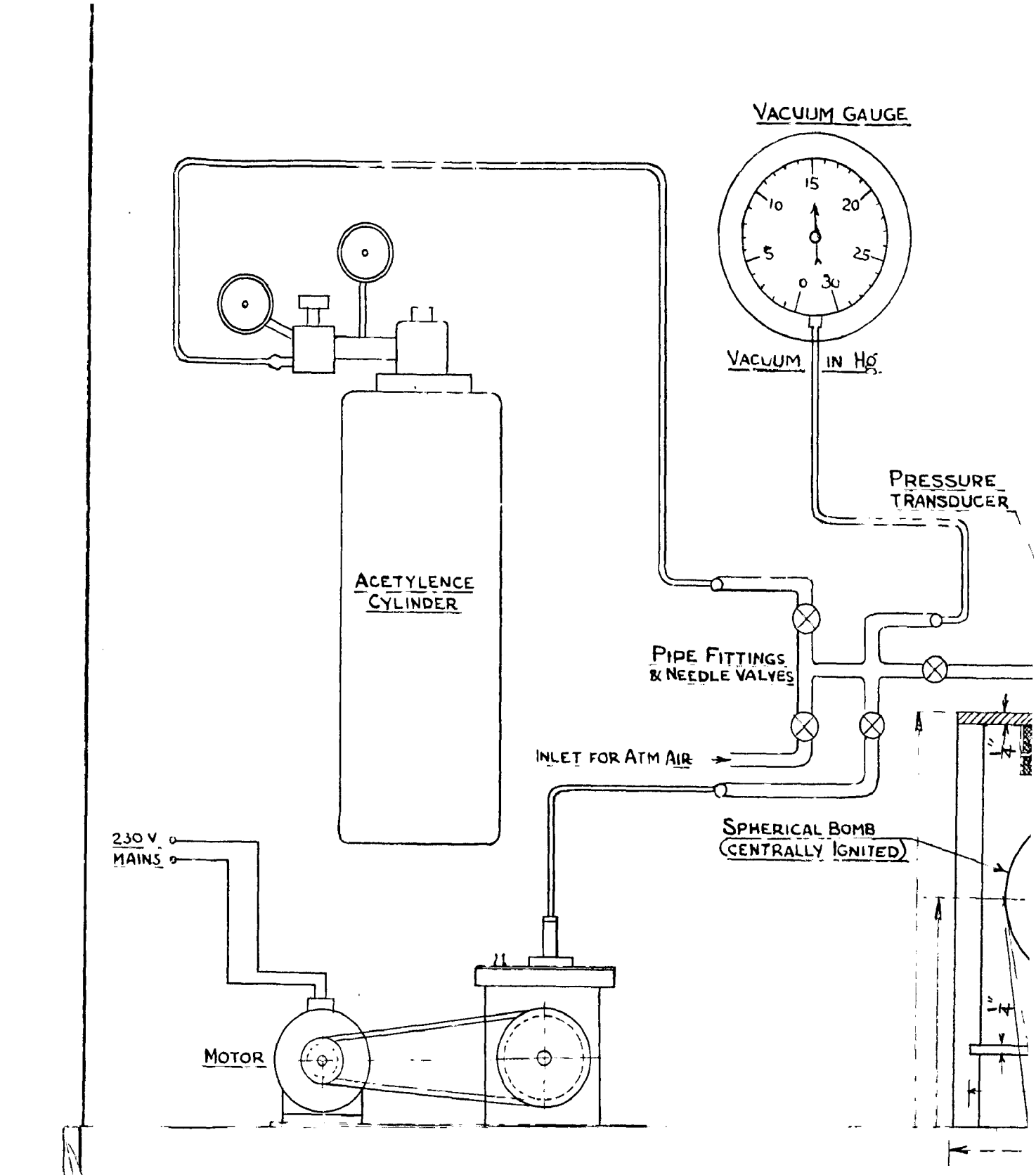


FIG. 20 GENERAL ARRANGEME

(SECTIONAL PLAN VIEW OF

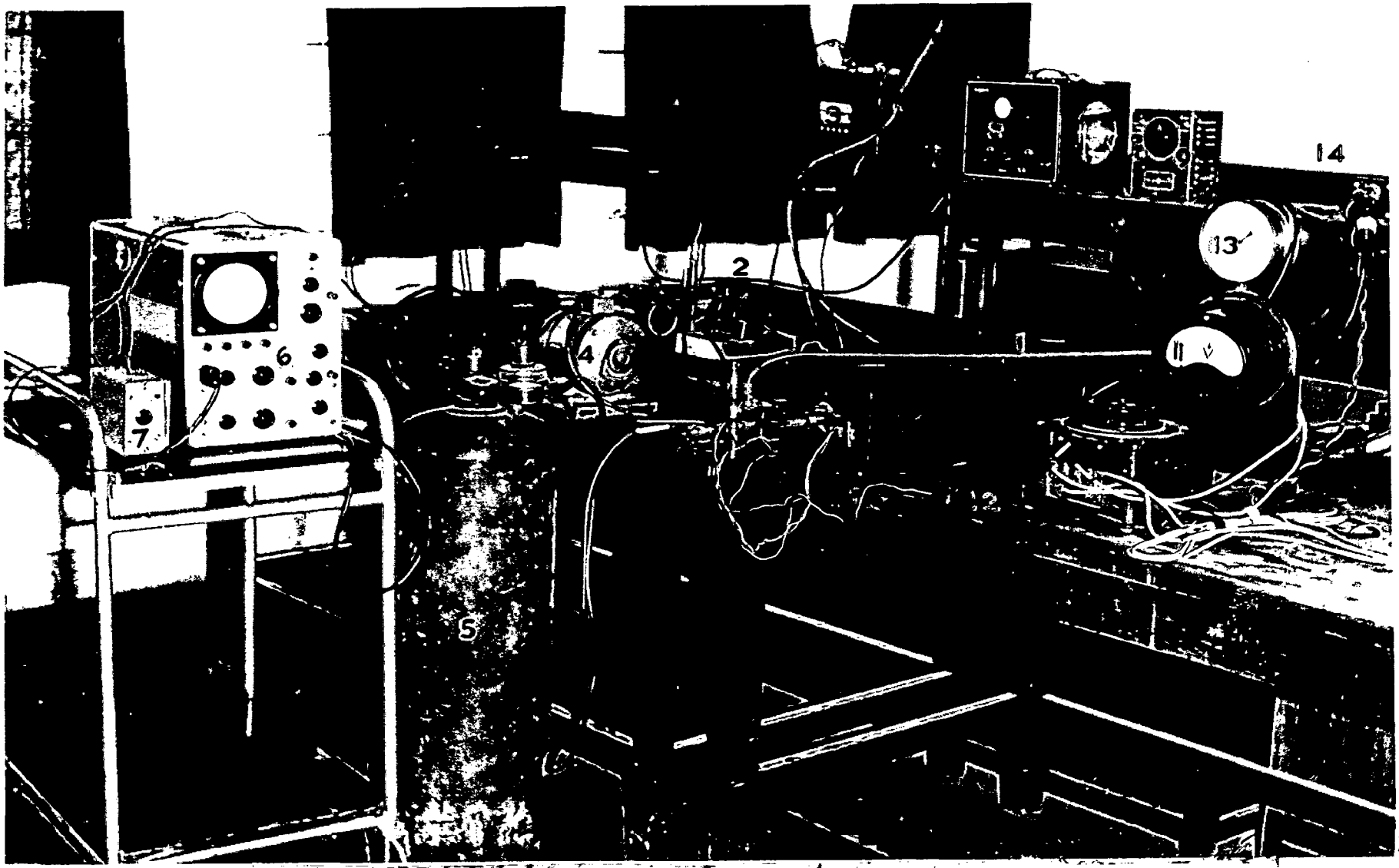


FIG. 21. A VIEW OF EXPERIMENTAL SET UP WITH IDENTIFICATION OF COMPONENTS.

1. Light tight box. 2. Induction Coil. 3. 6-V Battery. 4. Vaccum Pump 5. Acetylene cylinder. 6. Dual Beam Oscilloscope. 7. Charge amplifier. 8. Strobumeter 9. Variac Speed Control. 10. Variac Autotransformer. 11. Voltmeter. 12. Ignition Switch. 13. Vacuum Gauge. 14. 220/110V Transformer.

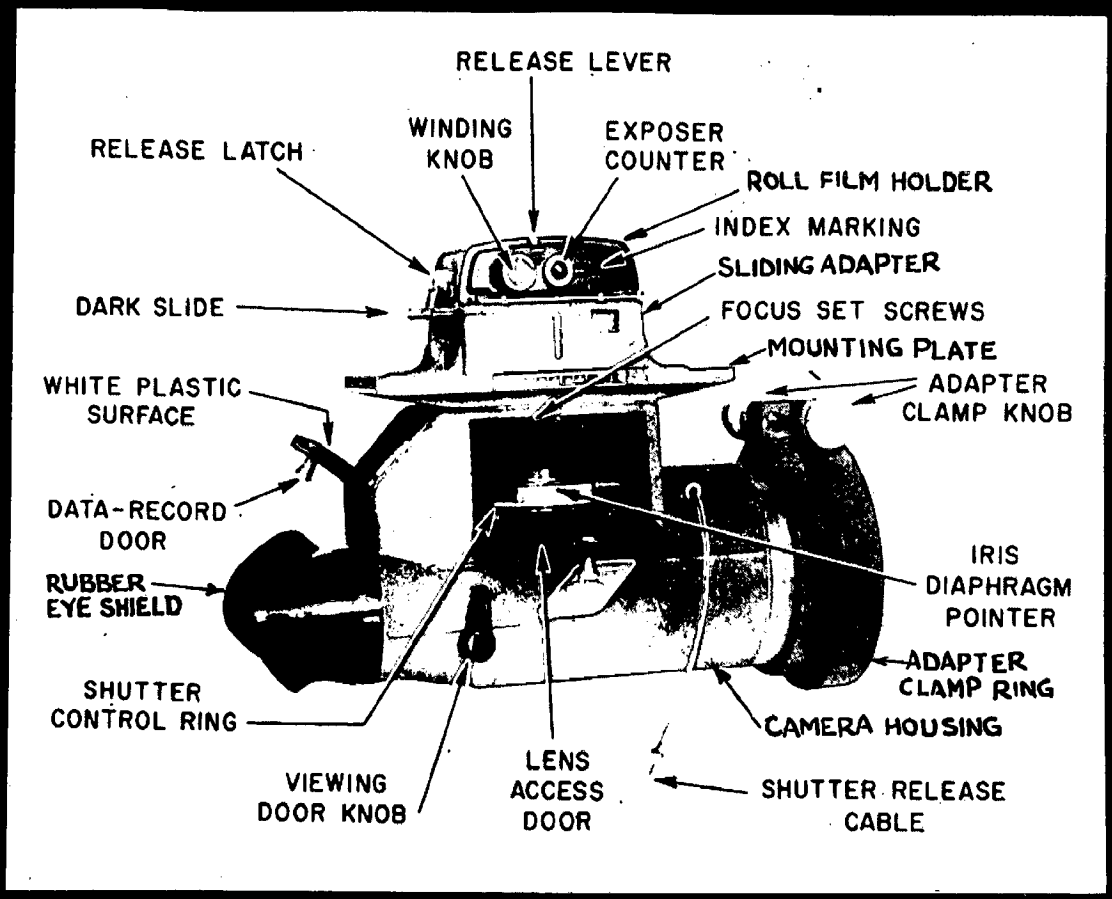


FIG. 22. OSCILLOGRAPH RECORD CAMERA:

(From Oscilloscope Cameras Instruction Manual Ref. 38)

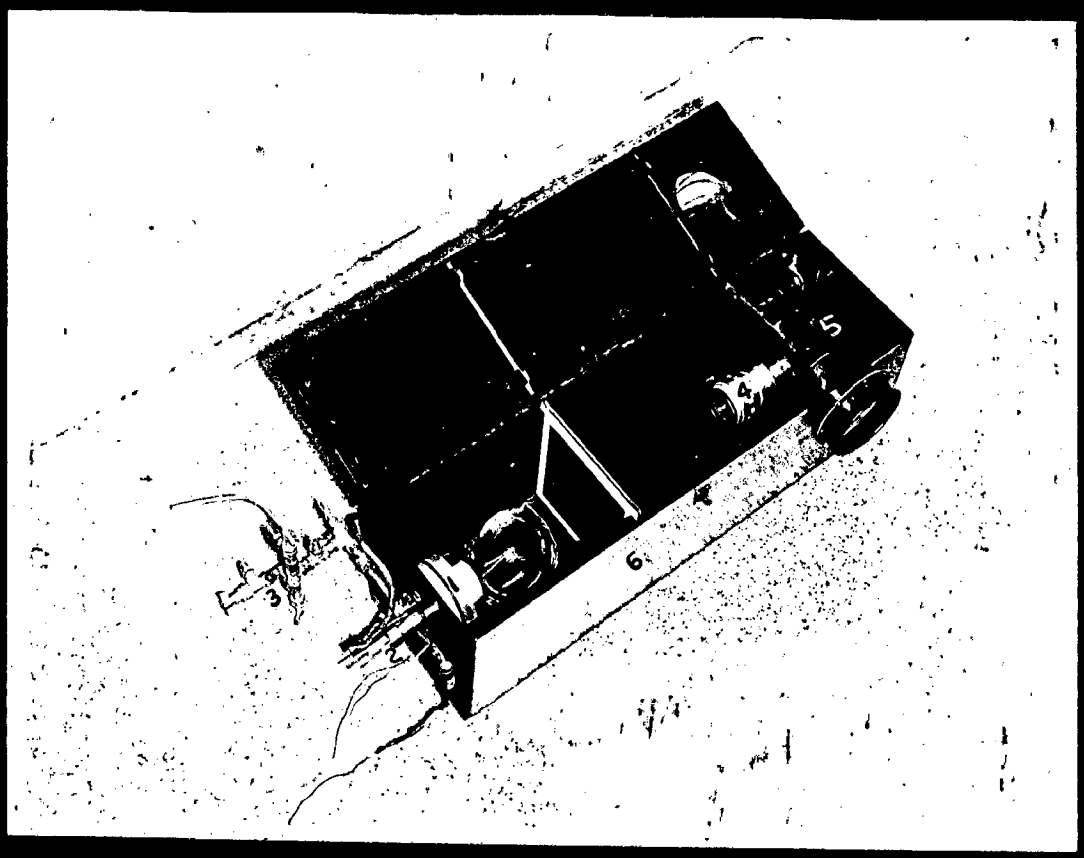


FIG. 23. SPHERICAL BOMB & DETAILS OF DRUM CAMERA:

1. Spherical Bomb. 2. Pressure Transducer with adapter.
3. Pipe fittings and valves. 4. Camera Lens.
5. Aluminium Drum. 6. Light tight Box.

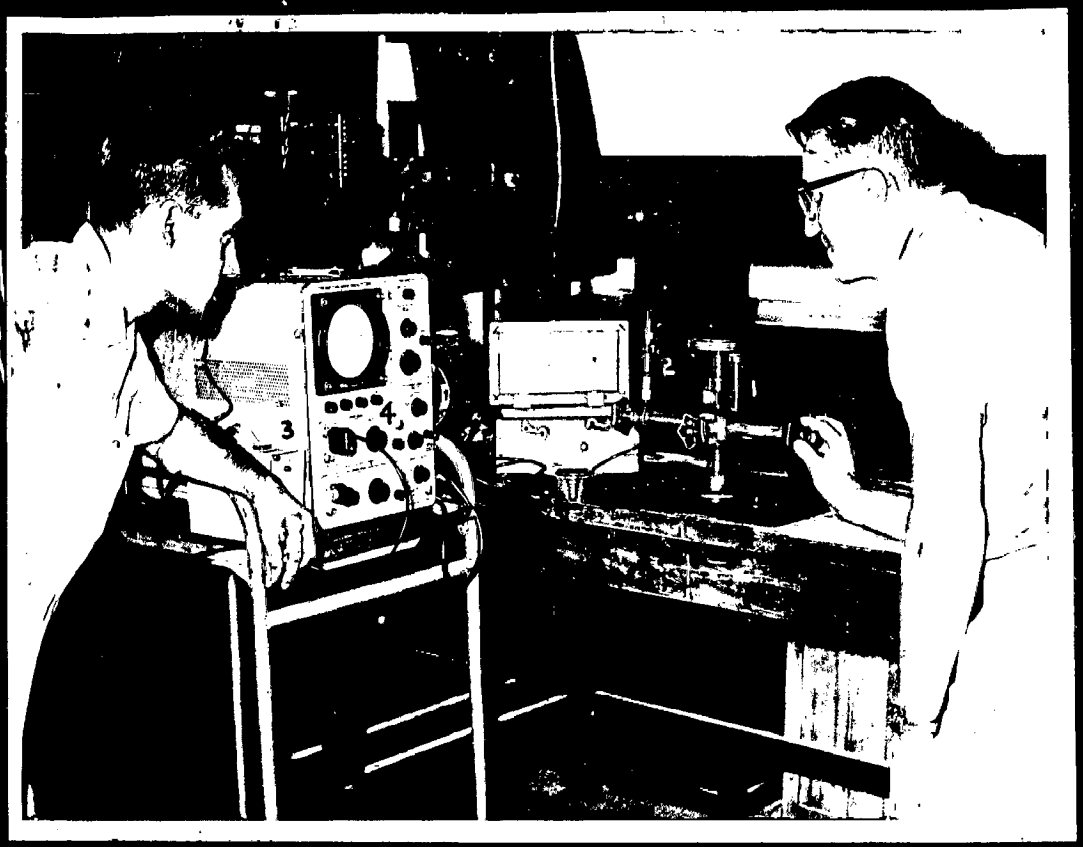


FIG. 24. CALIBRATION OF PRESSURE TRANSDUCER:

1. Dead Weight Tester. 2. Pressure Transducer with adapter. 3. Charge Amplifier. 4. Oscilloscope.

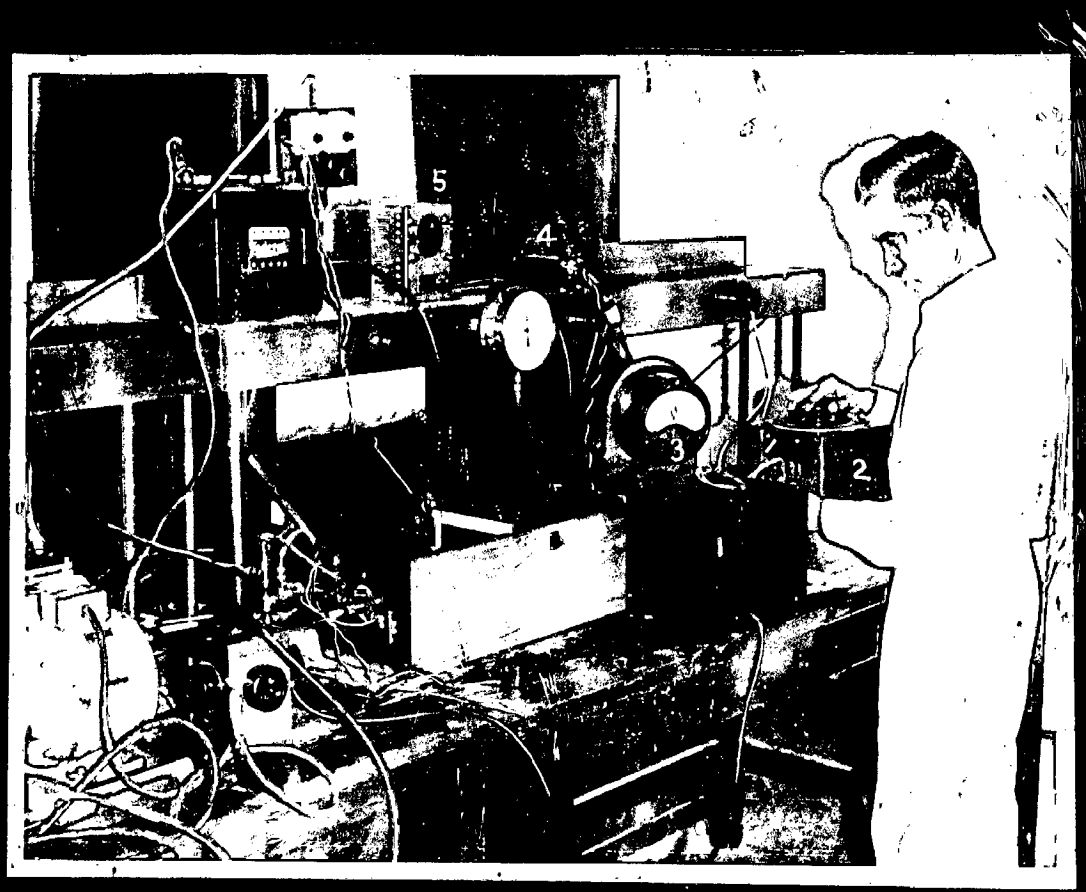


FIG. 25. CALIBRATION OF VARIAC MOTOR SPEED CONTROL:

1. Strobometer. 2. Variac autotransformer. 3. Voltmeter 4. Single phase 220/110V transformer. 5. Variac motor speed control.

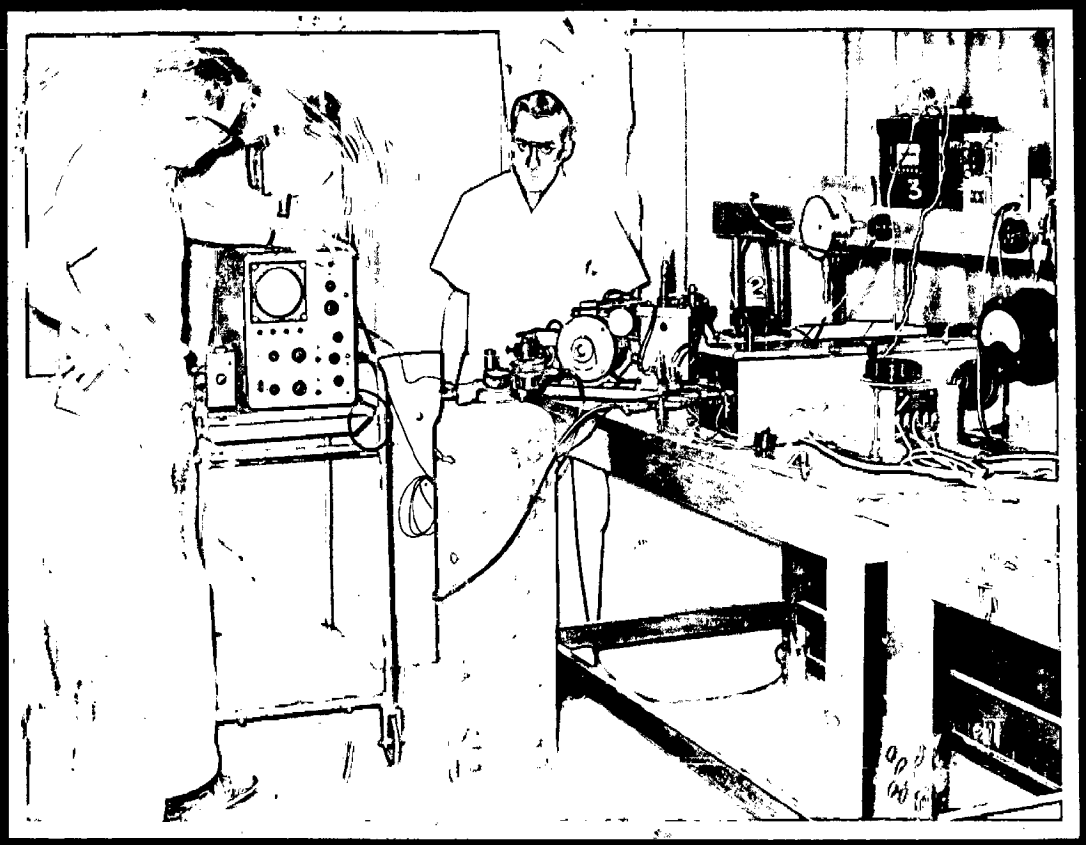

FIG. 26. EXTERNAL TRIGGERING OF SWEEP:

1. Trigger Level knob. 2. Induction coil. 3. Battery. 4. Ignition Switch.

Note: When the trigger level knob(1) is turned counter-clockwise, the beam disappears. On closing the ignition switch(4) and breaking the circuit again, the spark jumps across the electrodes to ignite the mixture and simultaneously the sweep is triggered.

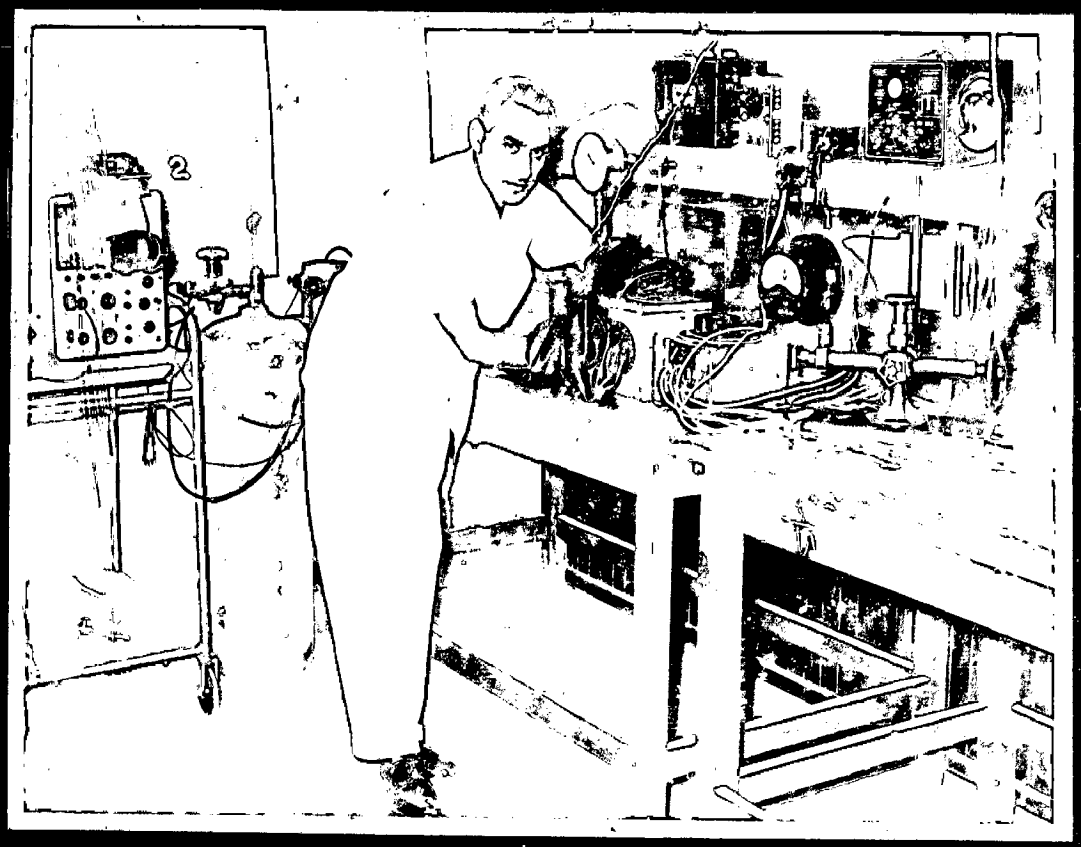


FIG. 27. LOADING THE FILM ON DRUM CAMERA.

Notes: The black sleeves(1) with rubber bands contain the film storage can. The operator puts the sleeves on his hands and loads the film on camera drum by feel. The film is attached to the drum by a transparent "Scotch tape". On the left is shown the oscillograph record camera (2) attached to the oscilloscope screen.

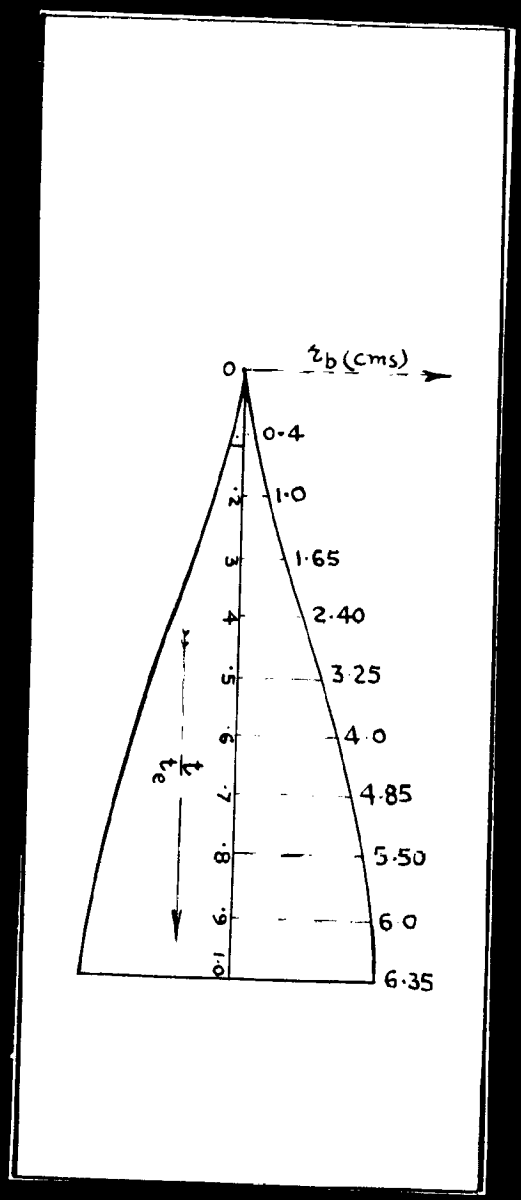


FIG. 28. ROTATING DRUM CAMERA RECORD:

$P_1$ 15·2 cm.Hg., $T_1$ 303°K , Drum Speed 850 RPM, 'f' number of Drum Camera Lens 2·0

Note: The vertical axis measures dimensionless time, and the horizontal axis measures flame radius in cms.

Higher ignition Lag at lower initial pressure may be observed. Re-illumination at the centre appears after about 6.8 m. Sec.

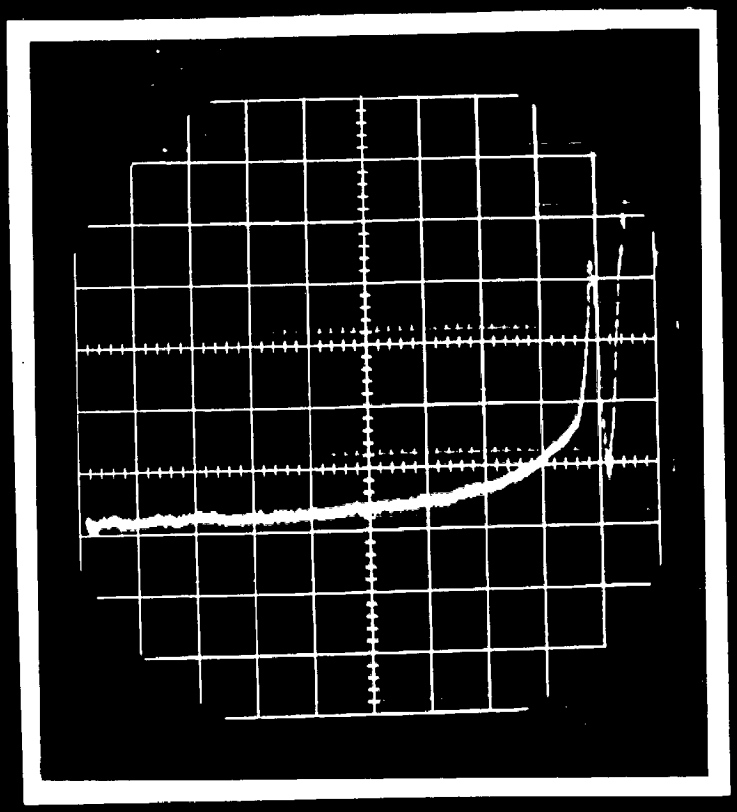

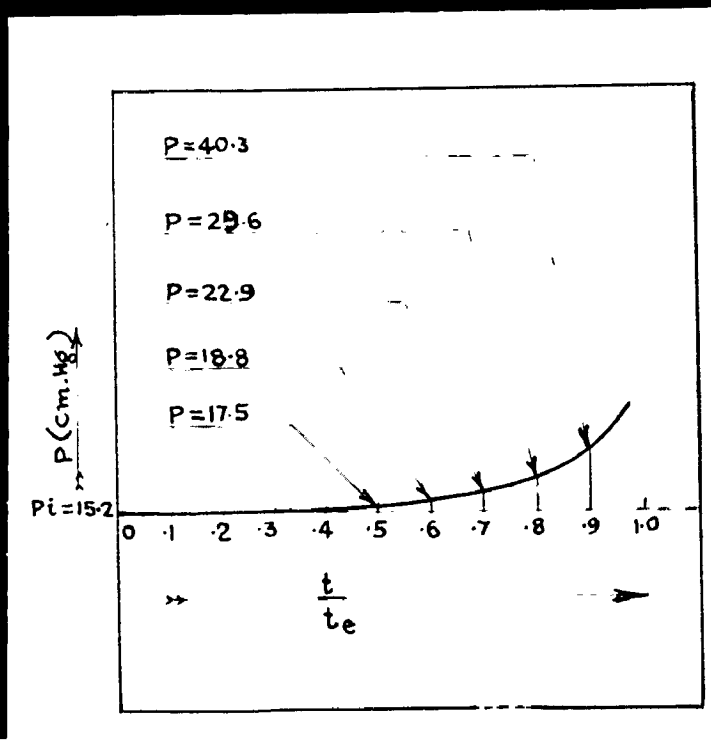


FIG. 29. PRESSURE RECORD IN BOMB EXPLOSION:

$P_1$ 15.2 cm.Hg, $T_1$ 303°K, Scope Sensitivity 5mV/cm, Time 1 m Sec./cm., Amplifier Sensitivity 20mV/pCb, Oscilloscope Camera Lens 'f' number 8.0 Shutter Speed set at B.

Note: The horizontal axis measures dimension less time, & the vertical axis measures absolute pressure in cm.Hg.

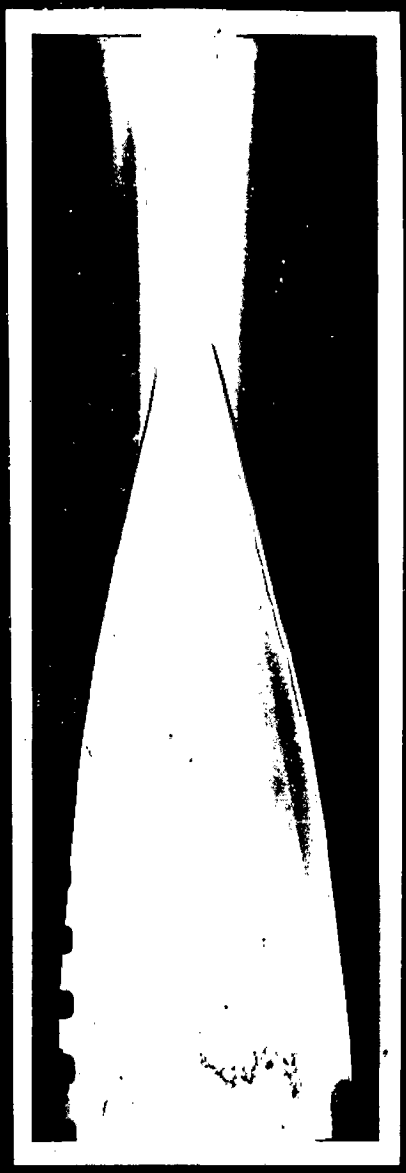

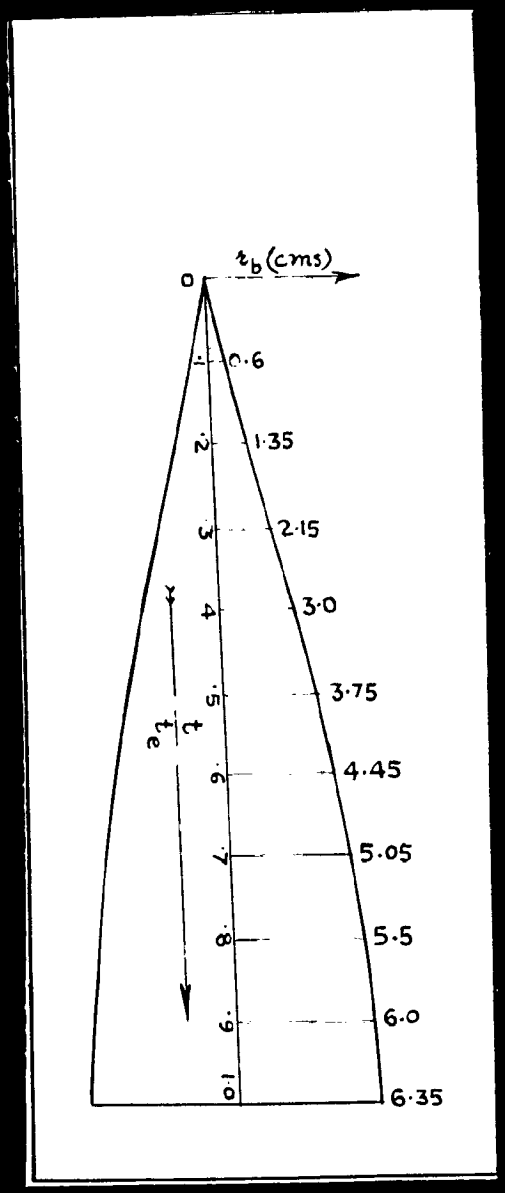


FIG. 30. FLAME RECORD IN SPHERICAL GLASS BOMB:

$P_i$ 10" Hg. Abs; $T_i$ 306°K; Drum Speed 1540 RPM; 'f' number 2.0,

Note: The re-illumination at the centre appears after about 6.5 m.sec. and persists during the cooling period.

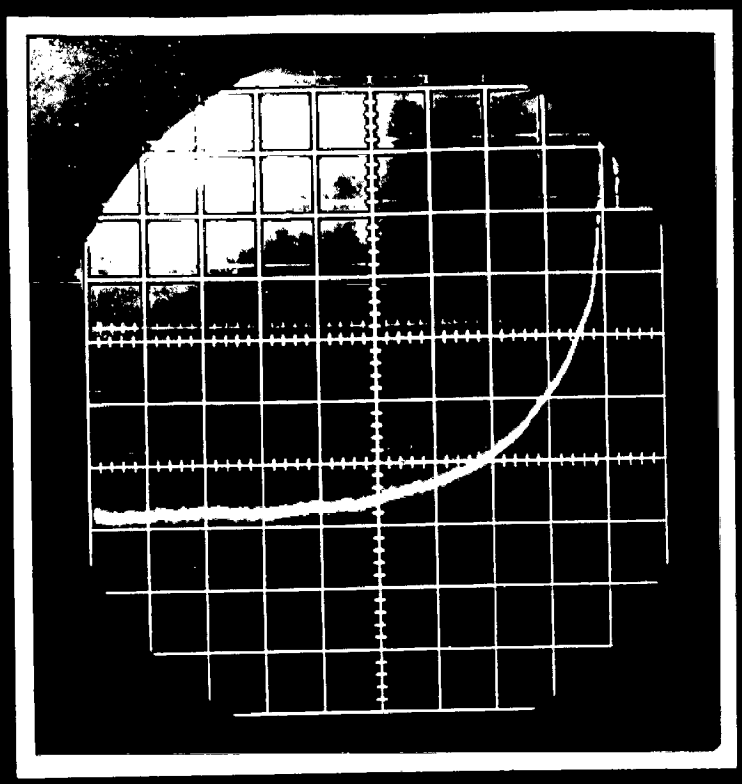

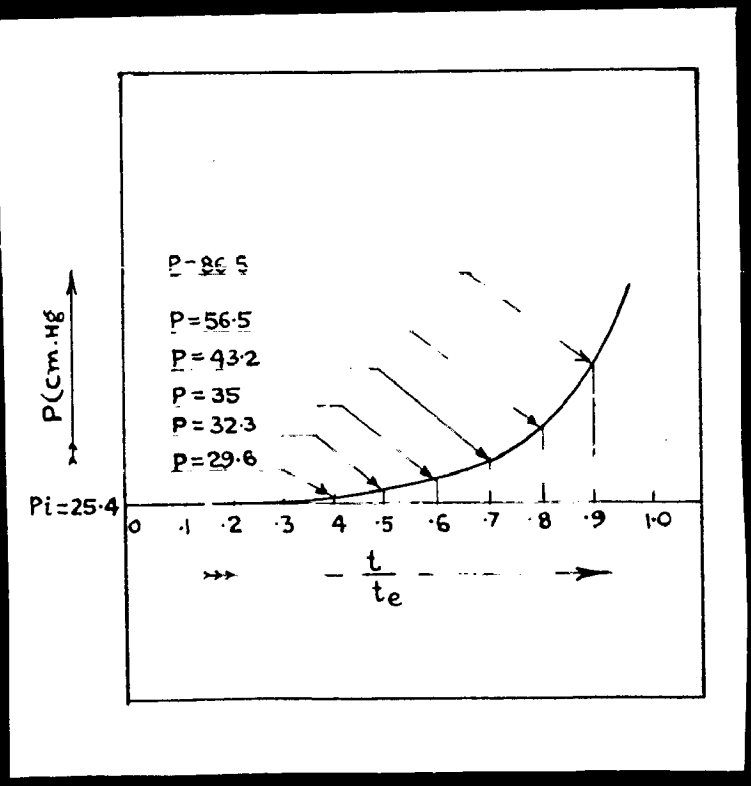


FIG. 31. PHOTOGRAPHIC RECORD OF PRESSURE- TIME TRACE:

$P_i$ 25.4 cm.Hg; $T_i$ 306°K., Scope Sensitivity 5 mV/cm.
Time 1 m.sec./cm., Amplifier Sensitivity 10 mV/pCb
Shutter speed set at B; 'f' number 8.0

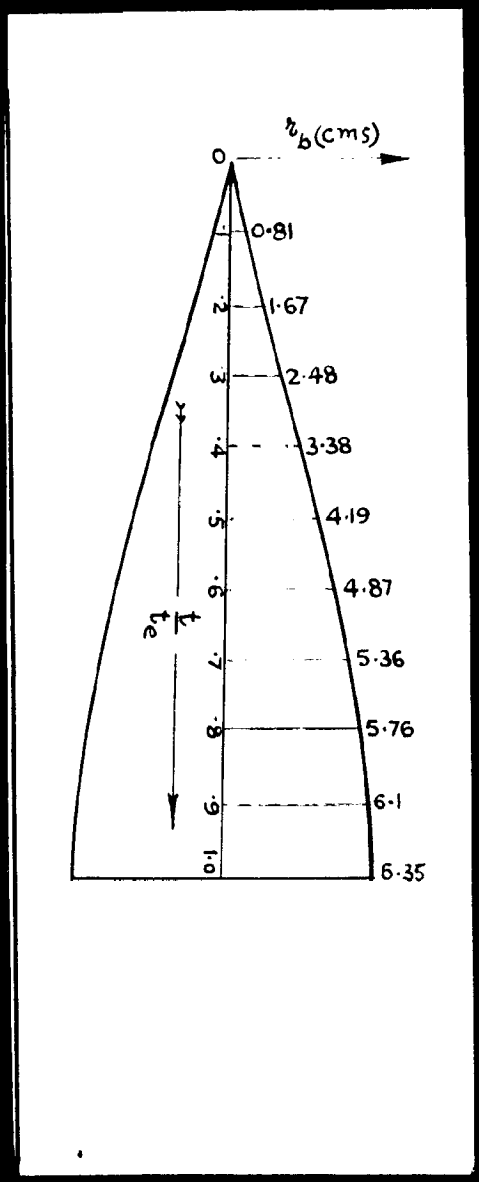


FIG. 32. RECORD OF FLAME SPREAD IN BOMB EXPLOSION ON A ROTATING DRUM:

$P_1$ 38 cm.Hg; $T_1$ 306°K; Drum Speed 1540 RPM, 'f' number 2,

Note: Re-illumination occurs after about 6.0 m.sec. The vertical black line at the centre of the flame record is probably due to flame quenching near the electrodes.

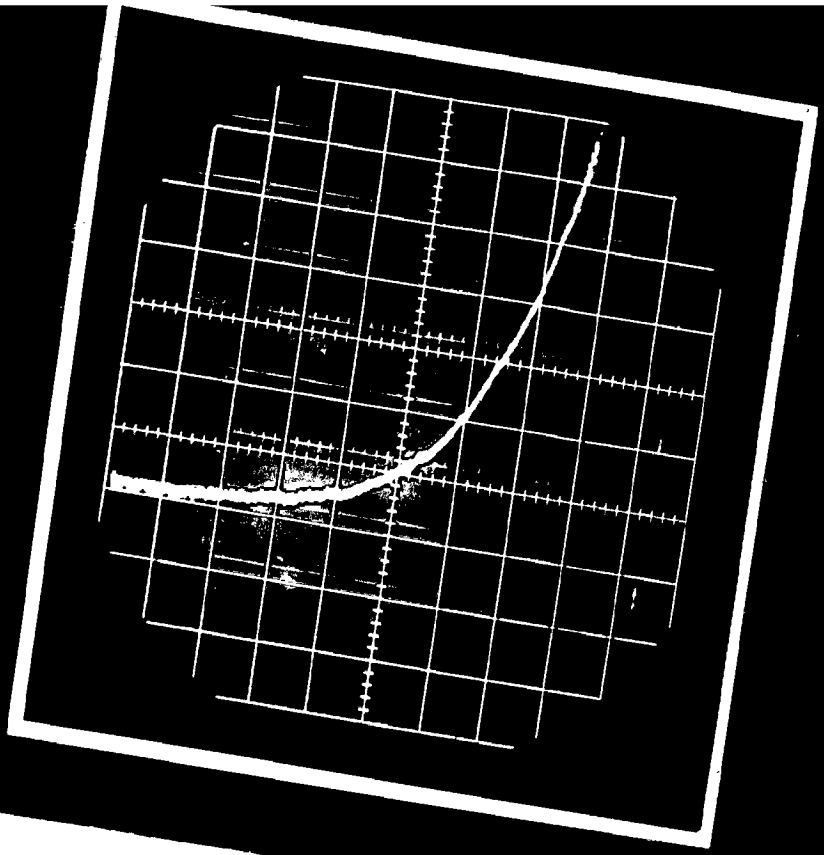

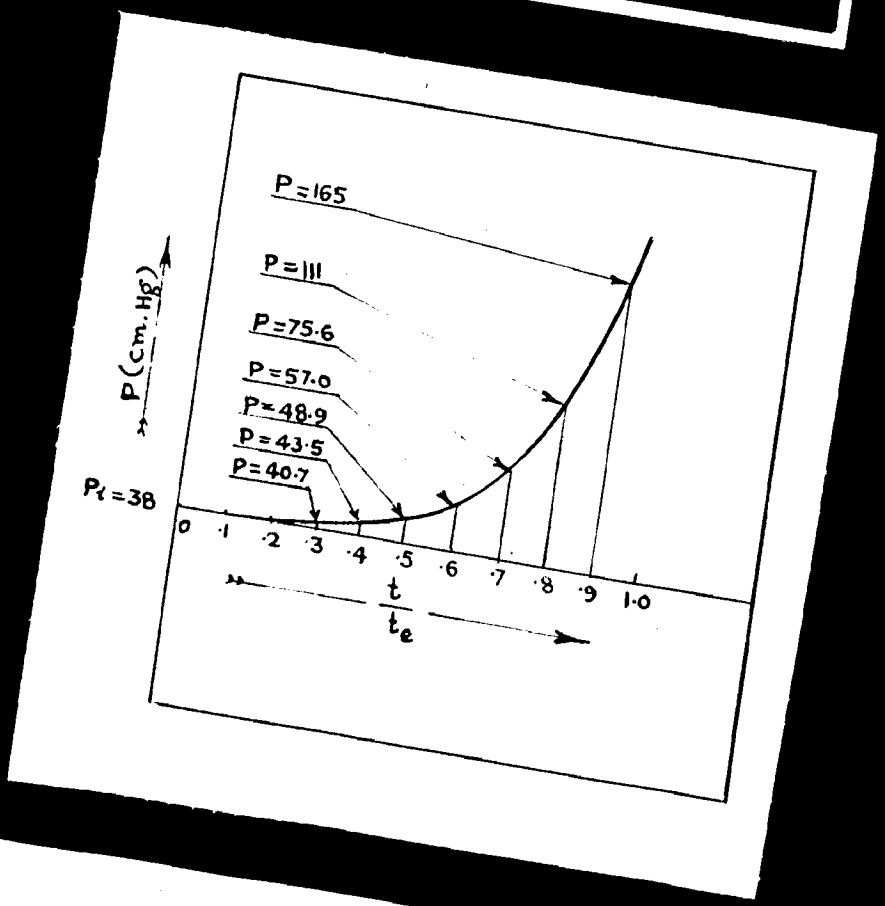


**G. 33. PRESSURE -TIME RECORD IN BOMB EXPLOSION:**

P1 38 cm.Hg; T1 306°K; Scope Sensitivity 5mV/cm;
Time 1 m.sec./cm; Amplifier sensitivity 10mV/pCb,
Shutter speed set at B; f: number 8.0

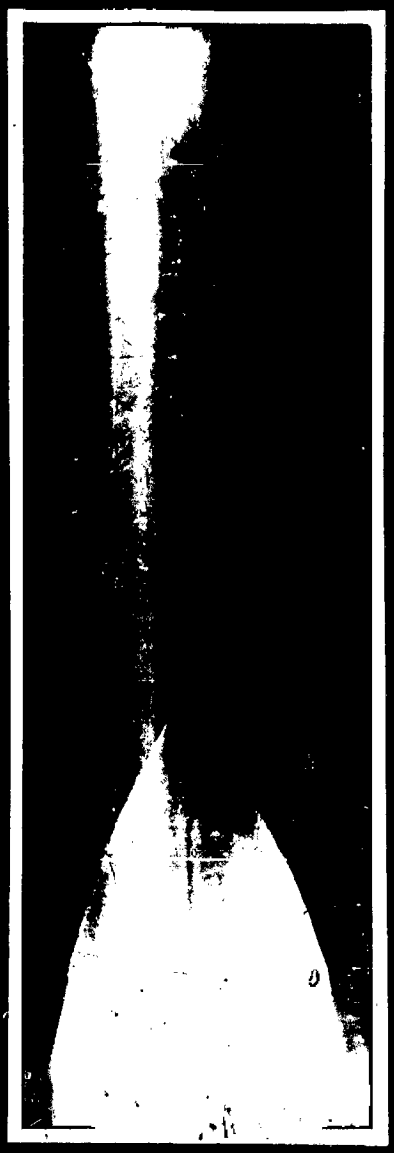

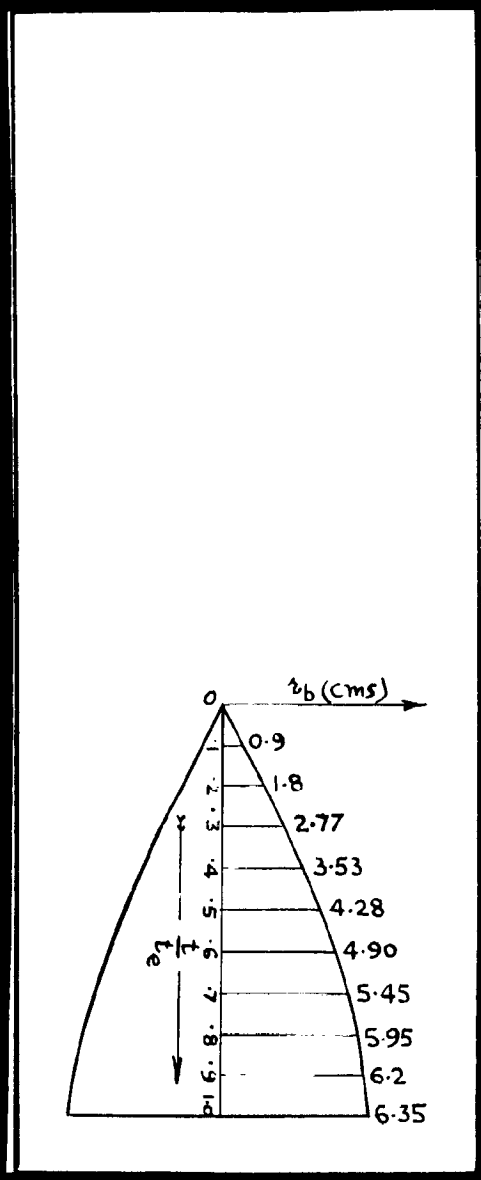


FIG.34. FLAME RECORD ON A ROTATING DRUM:

$P_i$ 50.8 cm.Hg; $T_i$ 308°K; Drumspeed 1050 RPM, 'f' number 2.0

Note: Re-illumination occurs after about 5.7 m.sec. & persists during the cooling period.
The slight departure from symmetrical flame growth might be due to oscillation of the flame sphere itself during progress of the flame.

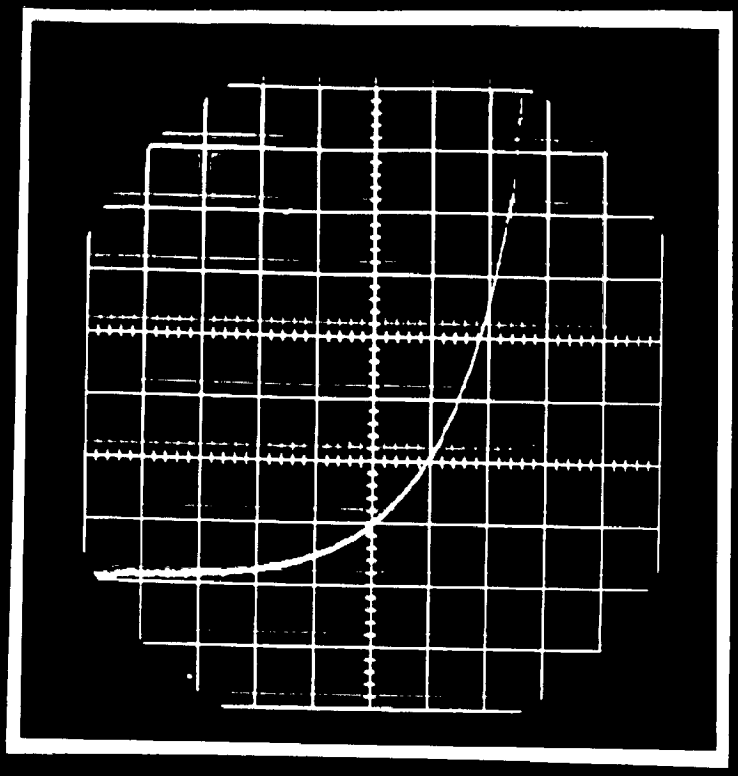

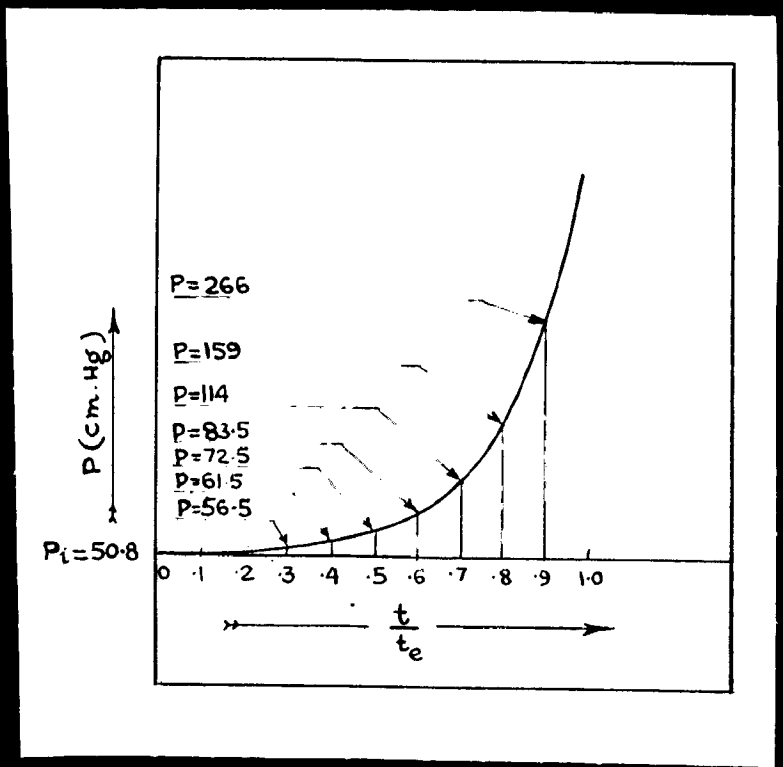


FIG.35. PRESSURE RECORD OF EXPLOSION IN A SPHERICAL BOMB:

$P_i$ 50.8 cm.Hg; $T_i$ 308°K; Scope Sensitivity 10 mV/cm., Time 1m.sec./cm., Amplifier Sensitivity 10mV/pCb, Shutter speed set at B; 'f' number 8.0

FIG.36 PRESSURE AND TEMPERATURE RELATIONSHIP FOR ADIABATIC COMPRESSION FOR UNBURN MIXTURES

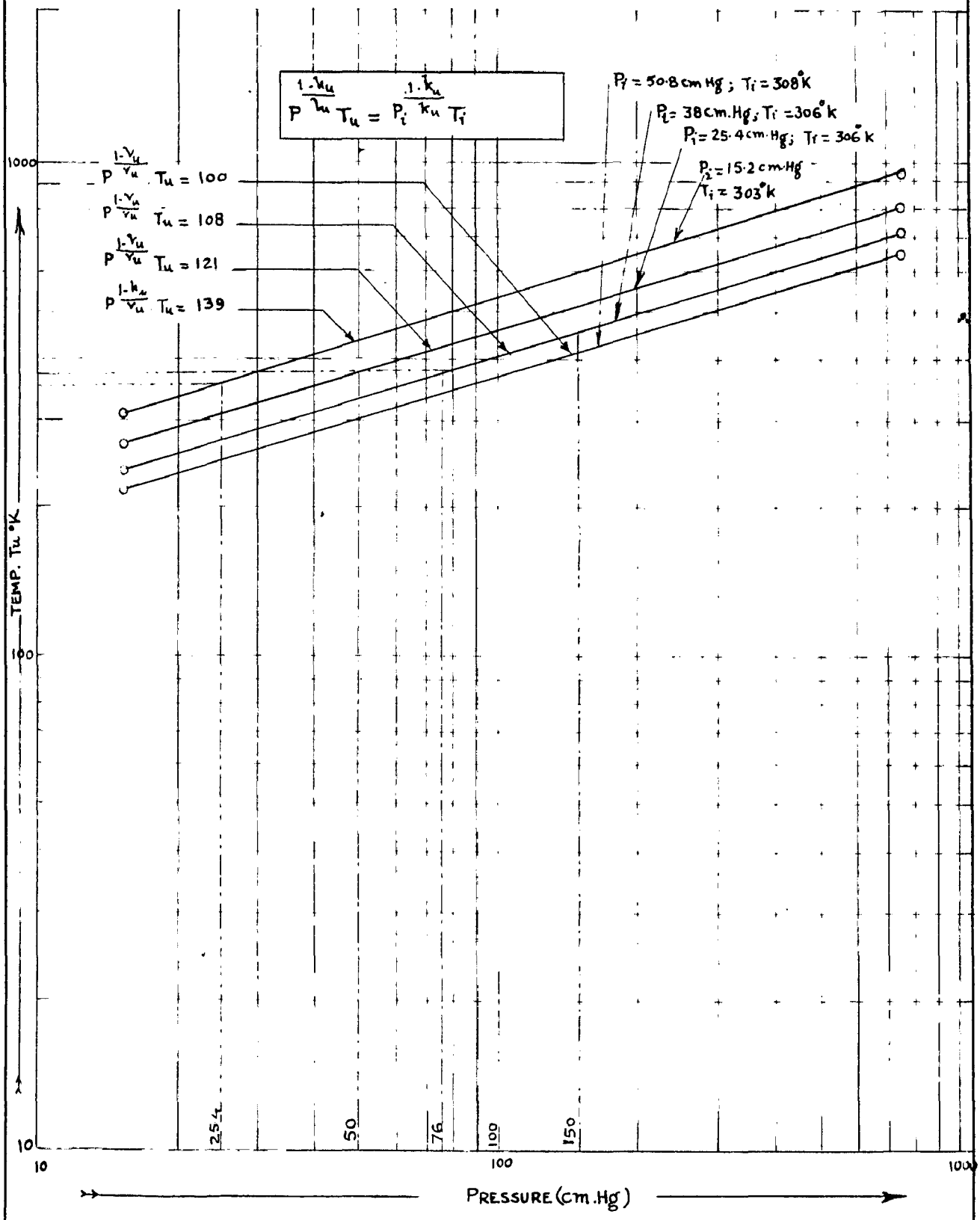

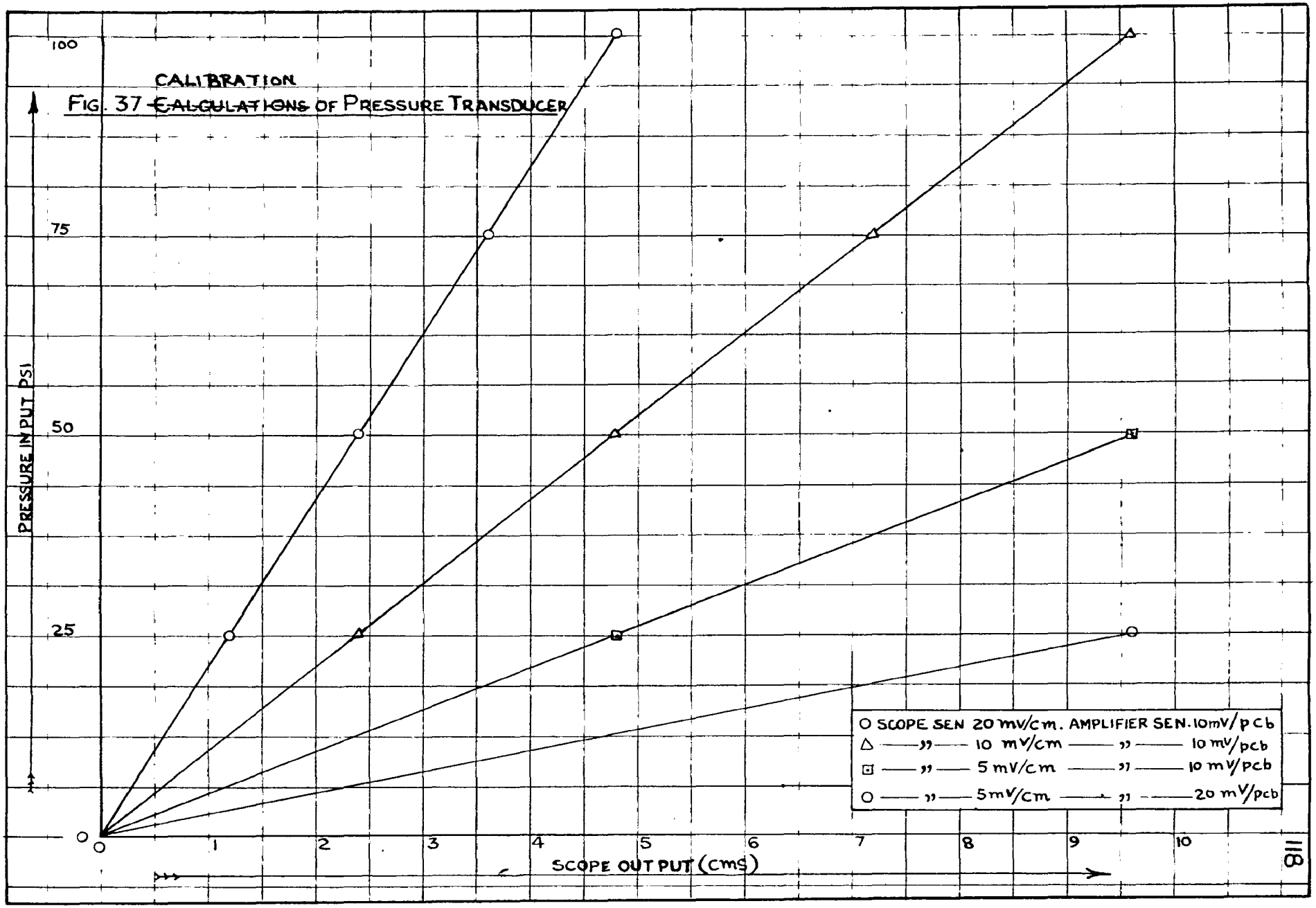
CALIBRATION
FIG. 37 ~~CALCULATIONS~~ OF PRESSURE TRANSDUCER
PRESSURE INPUT PSI
100
75
50
25
0
0
1
2
3
4
5
6
7
8
9
10
SCOPE OUT PUT (CMS)
O SCOPE SEN 20 mV/cm. AMPLIFIER SEN. 10mV/pcb
△ —"— 10 mV/cm —"— 10 mV/pcb
⊡ —"— 5 mV/cm —"— 10 mV/pcb
O —"— 5mV/cm —"— 20 mV/pcb

FIG. 38 CALIBRATION OF VARIAC MOTOR SPEED CONTROL

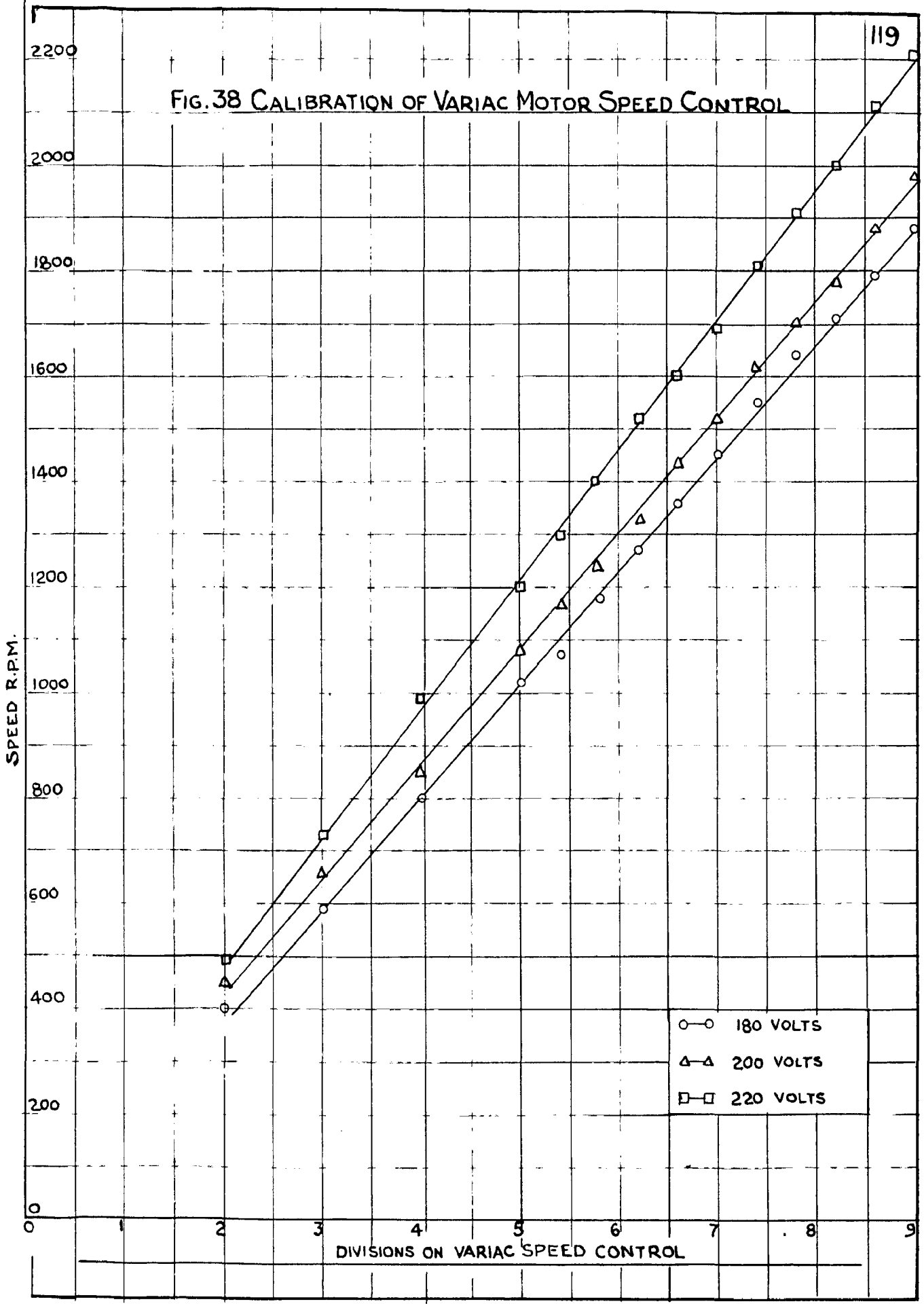

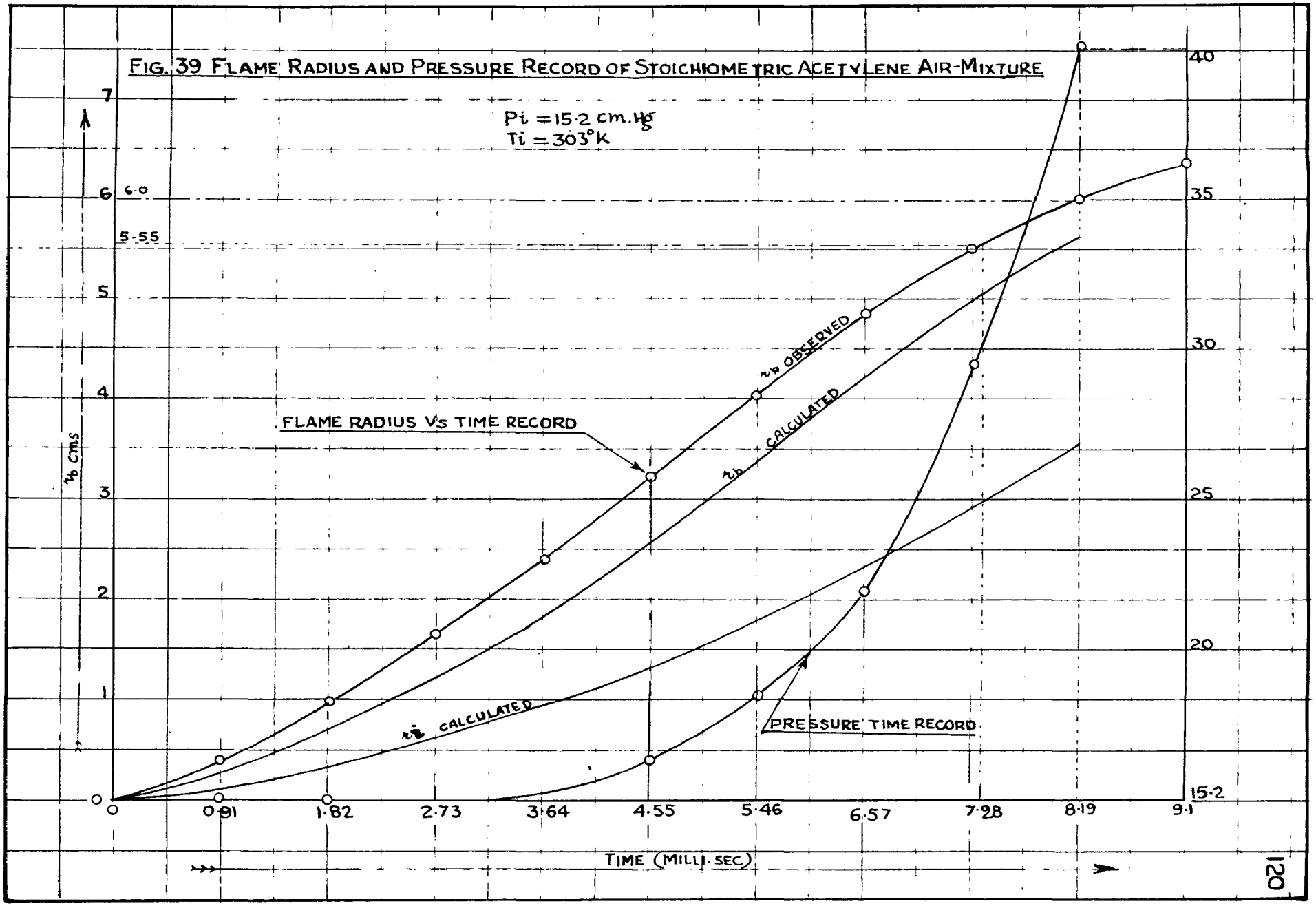
FIG. 39 FLAME RADIUS AND PRESSURE RECORD OF STOICHIOMETRIC ACETYLENE AIR-MIXTURE
Pi = 15·2 cm. Hg
Ti = 303°K
FLAME RADIUS Vs TIME RECORD
$r_b$ OBSERVED
$r_b$ CALCULATED
$r_b$ CALCULATED
PRESSURE TIME RECORD
$r_b$ CMS
TIME (MILLI SEC)
6·0
5·55
15·2
0
0·91
1·82
2·73
3·64
4·55
5·46
6·57
7·28
8·19
9·1
121

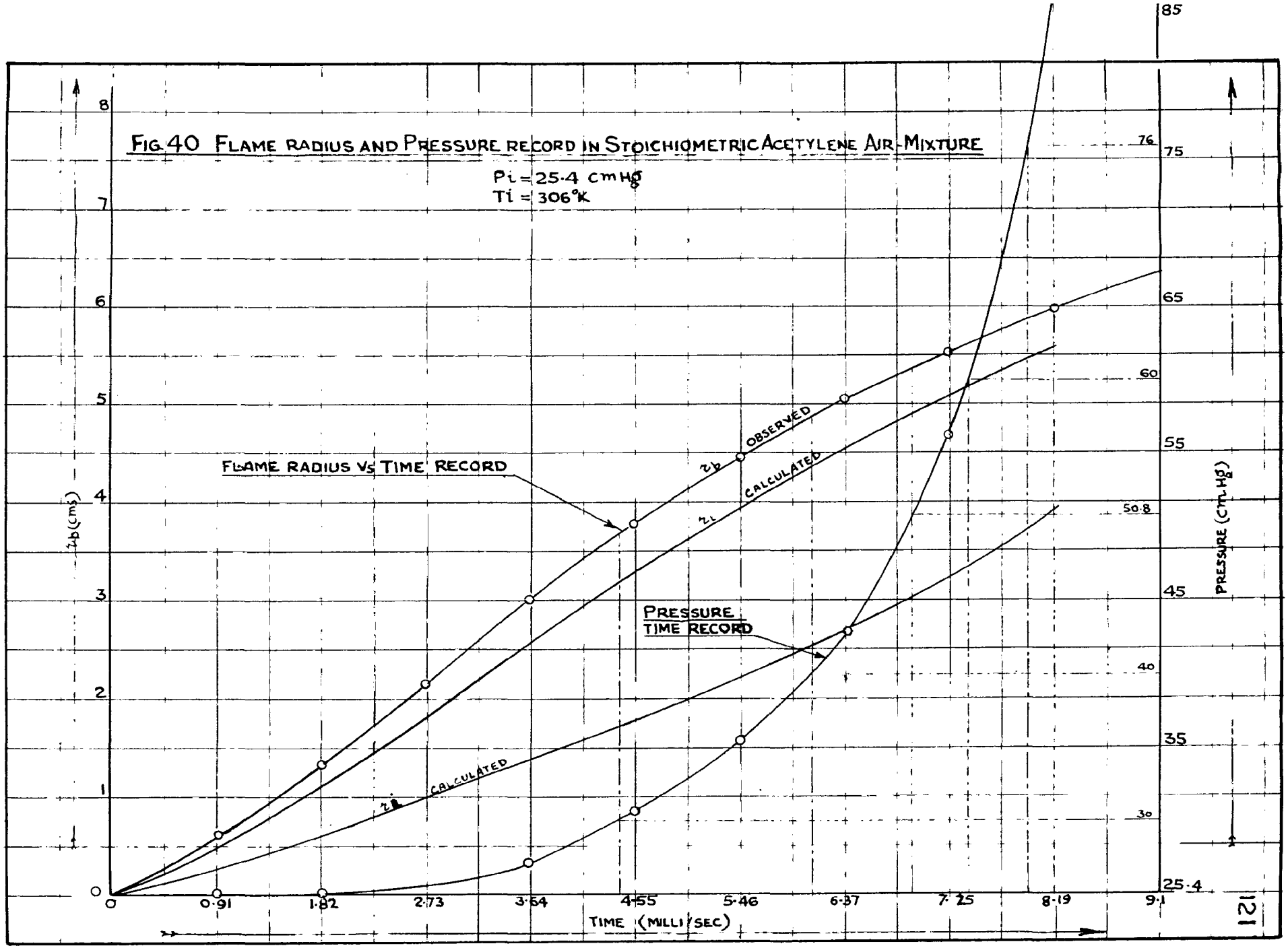
FIG 40 FLAME RADIUS AND PRESSURE RECORD IN STOICHIOMETRIC ACETYLENE AIR-MIXTURE
Pi = 25·4 cm Hg
Ti = 306°K
FLAME RADIUS Vs TIME RECORD
PRESSURE TIME RECORD
$r_b$ OBSERVED
$r_b$ CALCULATED
$r_i$ CALCULATED
$r_b$ (cms)
PRESSURE (CM. Hg)
TIME (MILLI/SEC)
0
0·91
1·82
2·73
3·64
4·55
5·46
6·37
7·25
8·19
9·1
8
7
6
5
4
3
2
1
85
76
75
65
60
55
50·8
45
40
35
30
25·4

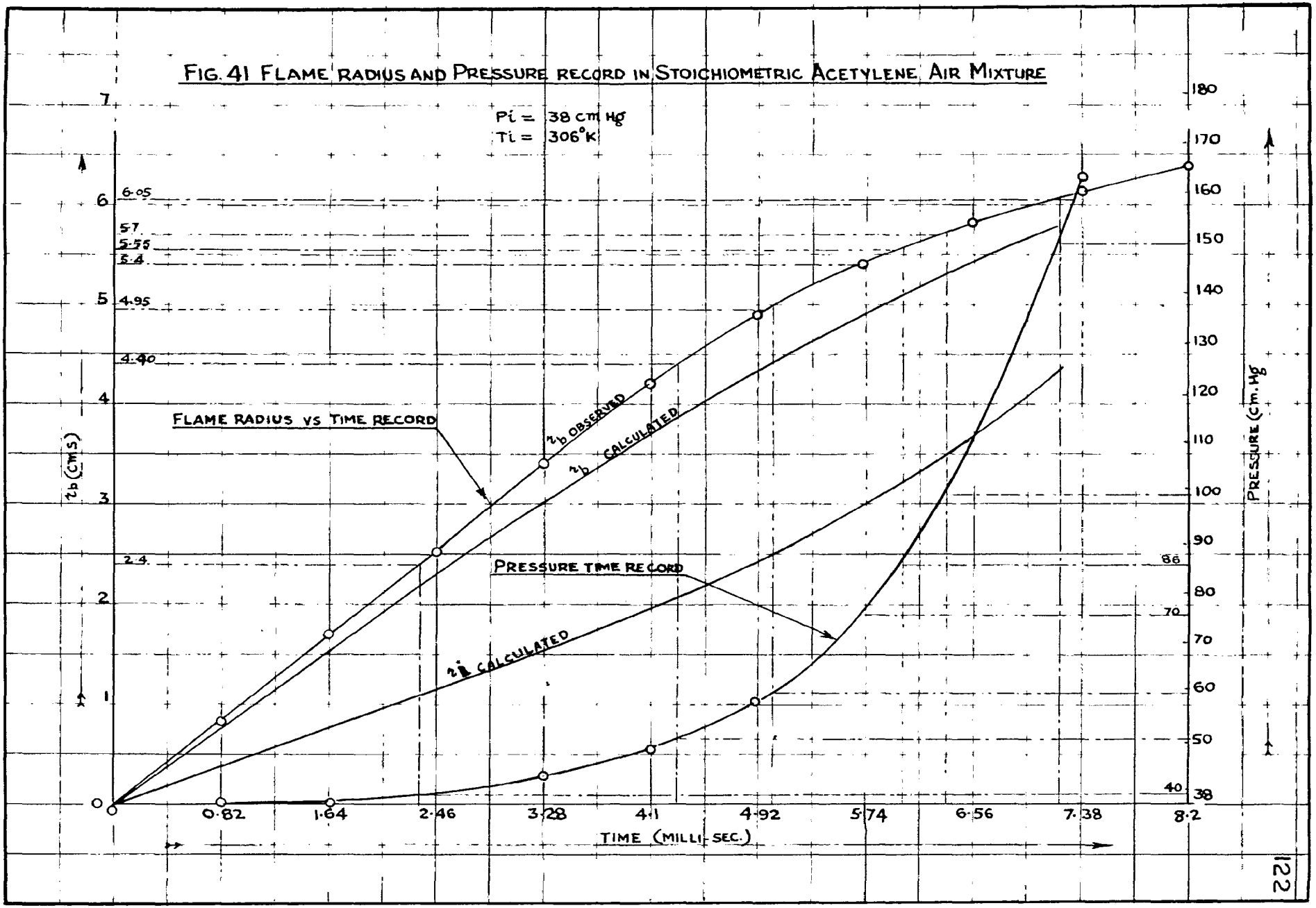
FIG. 41 FLAME RADIUS AND PRESSURE RECORD IN STOICHIOMETRIC ACETYLENE AIR MIXTURE
Pi = 38 cm Hg
Ti = 306°K
FLAME RADIUS VS TIME RECORD
PRESSURE TIME RECORD
$r_b$ OBSERVED
$r_b$ CALCULATED
$r_i$ CALCULATED
$r_b$ (CMS)
PRESSURE (cm. Hg)
TIME (MILLI-SEC.)
0
1
2
3
4
5
6
7
6.05
5.7
5.55
5.4
4.95
4.40
2.4
180
170
160
150
140
130
120
110
100
90
86
80
70
60
50
40
38
0.82
1.64
2.46
3.28
4.1
4.92
5.74
6.56
7.38
8.2

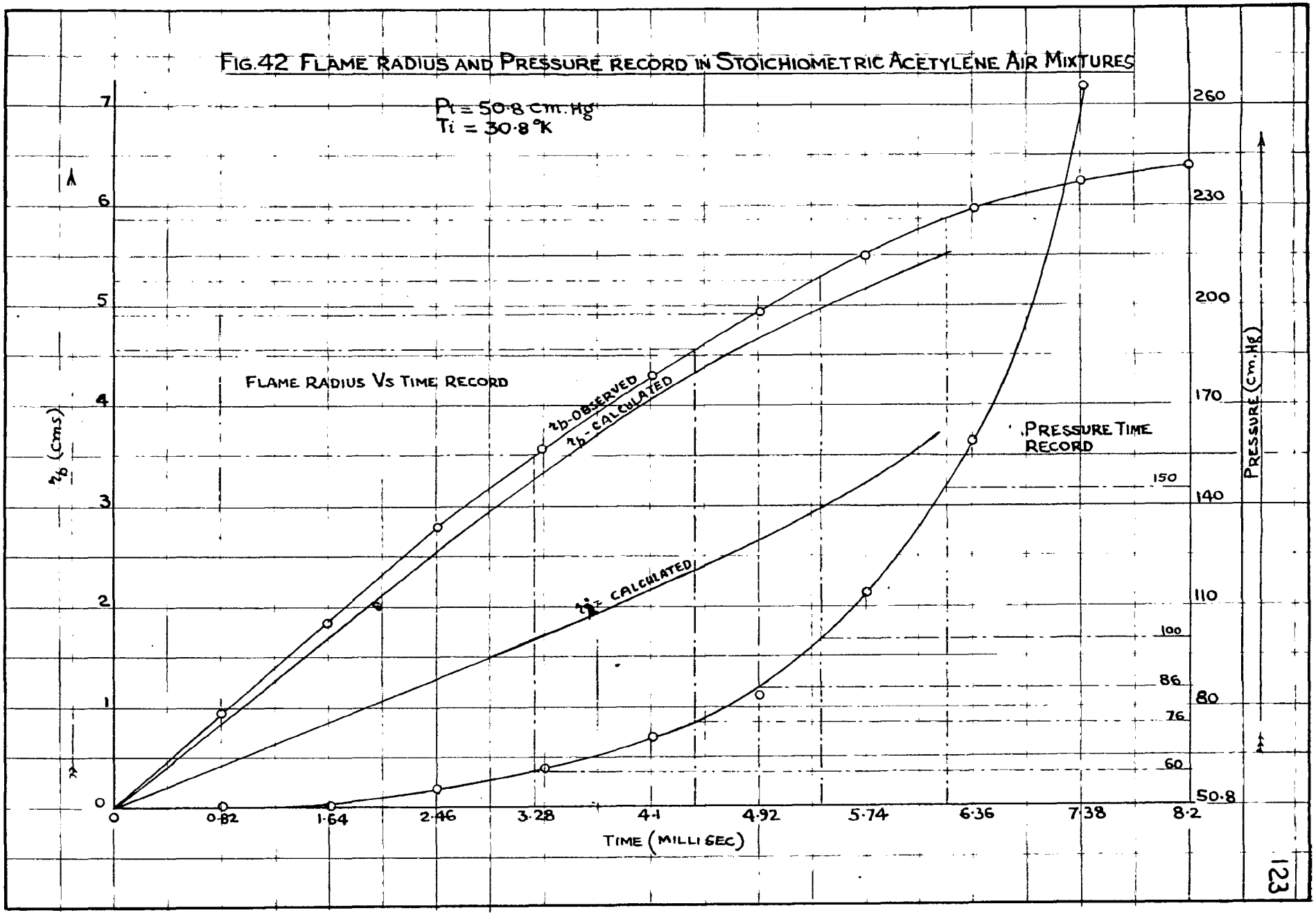
FIG.42 FLAME RADIUS AND PRESSURE RECORD IN STOICHIOMETRIC ACETYLENE AIR MIXTURES
Pi = 50·8 cm. Hg
Ti = 30·8 °K
FLAME RADIUS VS TIME RECORD
rb-OBSERVED
rb-CALCULATED
PRESSURE TIME RECORD
rb (cms)
PRESSURE (cm. Hg)
TIME (MILLI SEC)
0
0·82
1·64
2·46
3·28
4·1
4·92
5·74
6·36
7·38
8·2
1
2
3
4
5
6
7
260
230
200
170
150
140
110
100
86
80
76
60
50·8

# FIG. 43 BURNING VELOCITIES IN STOICHIOMETRIC ACETYLENE AIR MIXTURES

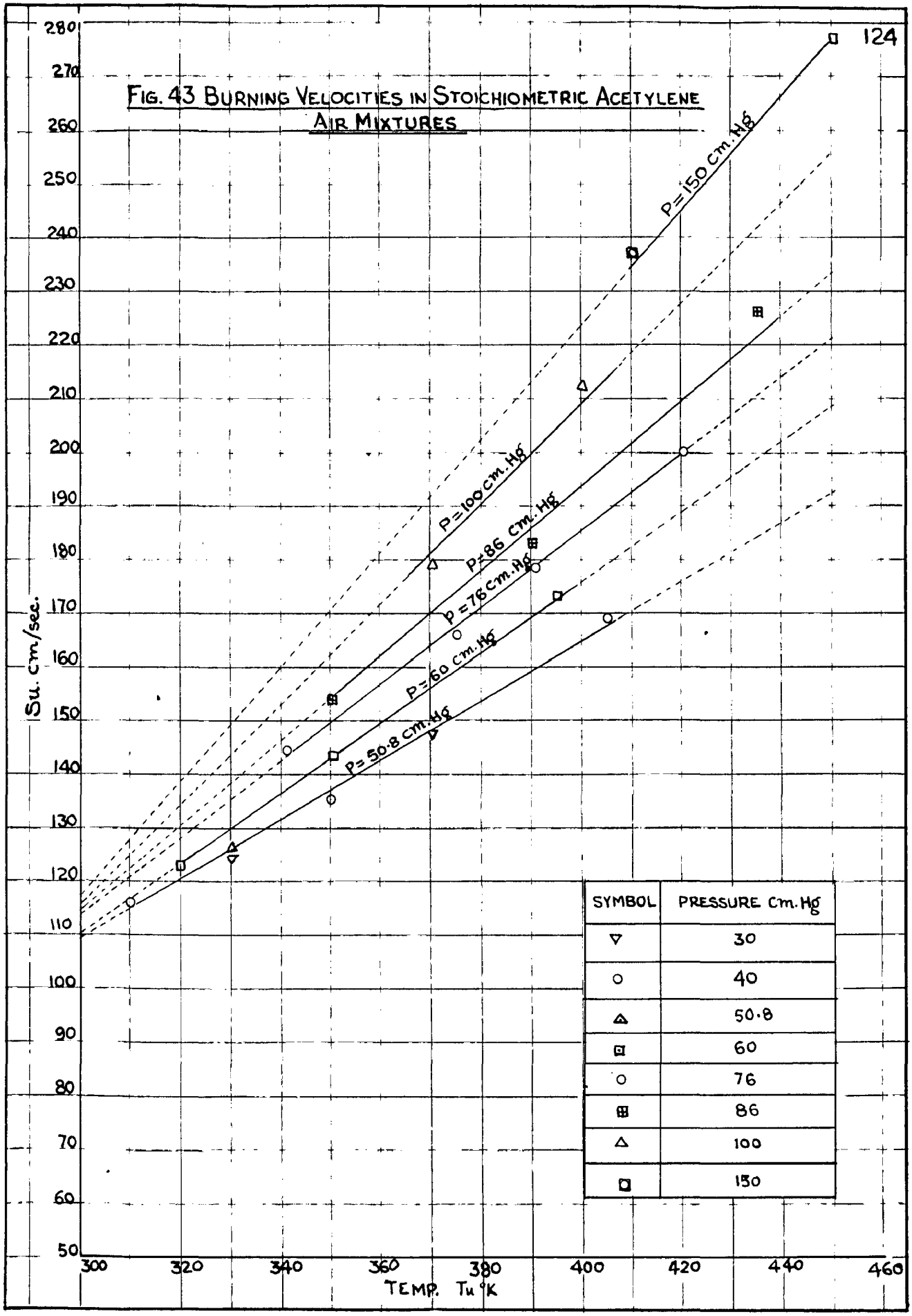

FIG. 44 BURNING VELOCITIES IN STOICHIOMETRIC ACETYLENE

AIR+MIXTURES

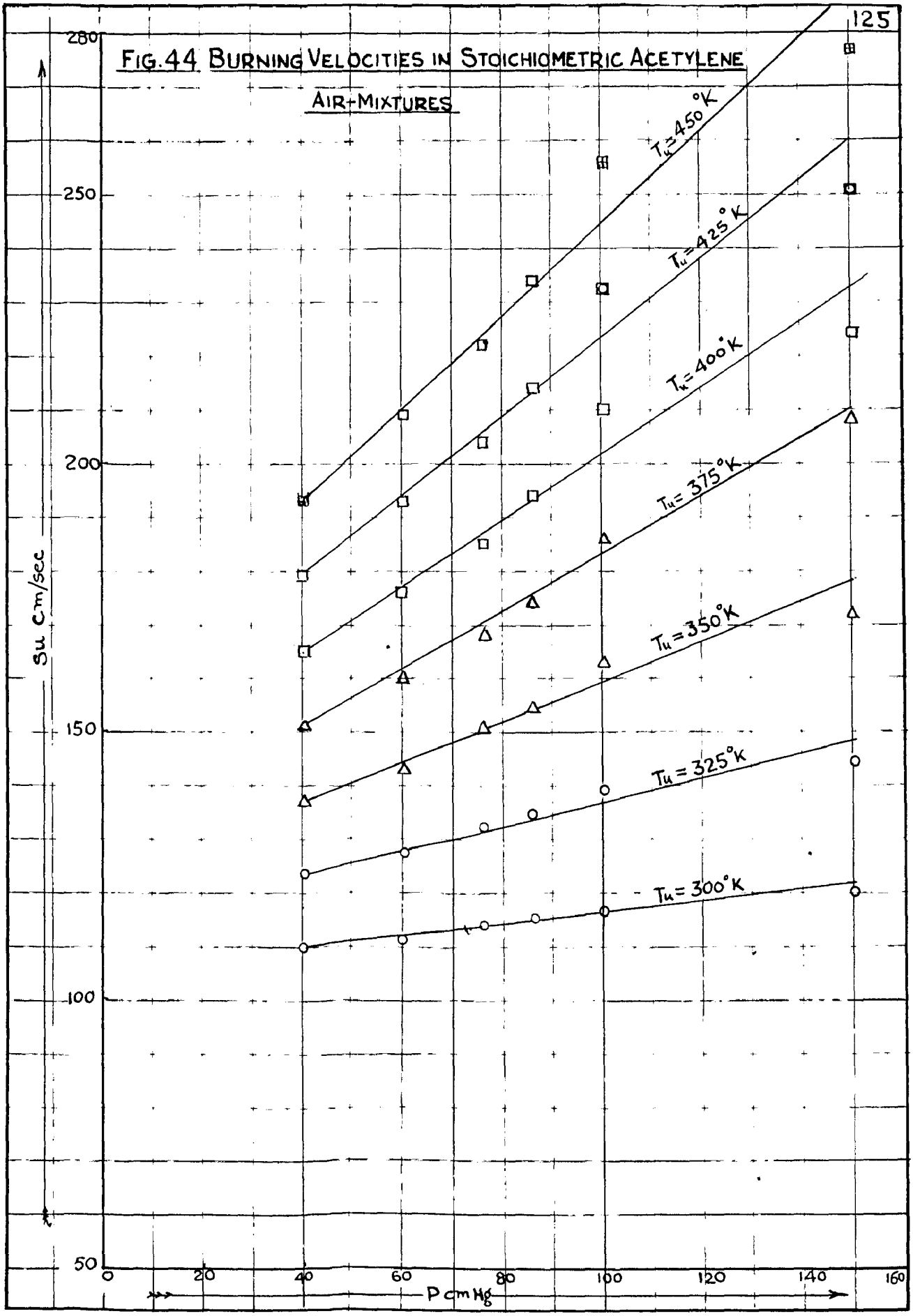

# APPENDIX A

## SAMPLE CALCULATIONS - SET NO. 3

(1) Initial conditions of mixture before Ignition

$P_i$ = 38 Cm.Hg. (= 15" Hg.Abs.)

$T_i$ = 306° K

(ii) Drum Camera Motor Speed: 1540 R.P.M. (from calibration curve)

(iii) Record of Flame Growth (Figure 32)

(iv) Pressure Record (Figure 33)

(v) Radius of Spherical Bomb, R = 6.35 Cms.

The analysis of data follows:

### (1) CALCULATIONS FOR PARTIAL PRESSURES OF $C_2H_2$ & AIR

The partial pressures of Acetylene and Air in Stoichiometric Acetylene-Air mixtures were calculated from the following combustion equation:

$$C_2H_2 + 2.5\ (O_2 + 3.76\ N_2) \rightarrow 2\ CO_2 + H_2O + 9.425\ N_2$$

$m_i$ = 12.925

$m_e$ = 12.425

F:A Ratio = 1 : 11.925

Making the assumption that partial pressures of component gases are proportional to their respective mole fractions, we have

$$P_{C_2H_2} = \frac{m_{C_2H_2}}{m_i} \cdot P_i = 2.94 \text{ Cm.Hg.} = \frac{1}{12.925} \cdot (38)$$

$$P_{Air} = \frac{m_{Air}}{m_i} \cdot P_i = \frac{11.925}{12.925} \cdot (38) = 35.06 \text{ cm.Hg.}$$

Acetylene by Volume $= \frac{1}{12.925} \times 100 = 7.75\%$

$\therefore$ Air by Volume $= 92.25\%$

(2) PRESSURE & TEMPERATURE RELATIONSHIP FOR ADIABATIC COMPRESSION OF UNBURNED MIXTURE

From Equation (2.8)

$$P^{\frac{1-\gamma_u}{\gamma_u}} T_u = P_i^{\frac{1-\gamma_u}{\gamma_u}} T_i = F$$

Since Acetylene to Air Ratio by volume is 1:11.925; the Stoichiometric Acetylene-Air mixture is almost pure air. Hence $\gamma_u$ for the mixture may be assumed as 1.4.

Now different values of P were chosen and the corresponding values of $T_u$ were calculated from the above equation. A plot of P Vs. $T_u$ is shown in Figure 36 on a Log-Log paper.

(3) CALCULATIONS FOR TIME OF COMBUSTION

The effective length of the film on Drum = 9.43" $\simeq$ 9.5"

The length Flame Trace on negative = 2.0"

The R.P.M. of Drum = 1540

$\therefore$ R.P.S. of Drum = 1540/60 = 25.6

Time for one revolution of Drum = 1/25.6 = 0.039 Sec.

The fraction of revolution which the drum makes when the flame travels from the centre of the bomb to the vessel-wall = 2/9.5 = 0.21

Hence total time required for travel of flame =

$0.039 \times 0.21 = 8.2 \times 10^{-3}$ Sec. = 8.2 m.Sec.

The pressure-time record also confirms that the above calculations are correct.

# APPENDIX B

## THERMODYNAMIC CALCULATIONS FOR $P_e'$

### (1) Calculations for Adiabatic Flame Temperature

**Reactions :** $CO + \frac{1}{2}O_2 \rightleftharpoons CO_2$

$OH + \frac{1}{2}H_2 \rightleftharpoons H_2O$

**Process:** $C_2H_2 + 2.5\,(O_2 + 3.77\,N_2) \rightarrow 2yCO + 2(1-y)CO_2 + yO_2$

$+ z\,OH + (1-z)H_2O +$

$+ \frac{z}{2}H_2 + 9.425\,N_2$

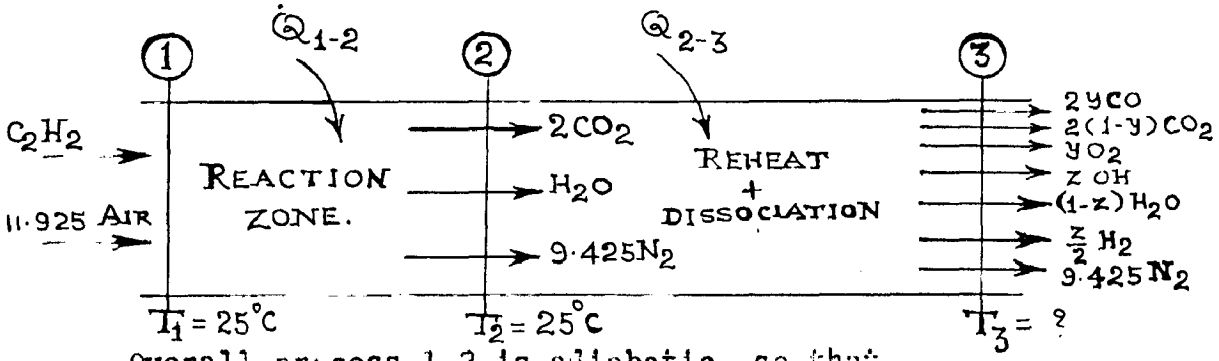


Overall process 1-3 is adiabatic, so that

$$Q_{1-3} = Q_{1-2} + Q_{2-3} = 0 \qquad \ldots (1)$$

$$Q_{1-2} = (h_{RP})_{C_2H_2,\ 25^\circ C.} = -300,086 \text{ Cal./g-mole } C_2H_2$$

Thus equation (1) yields: $Q_{2-3} = 300,086$ Cal./g-mole $C_2H_2$

... (2)

Applying energy equation to system 2-3

$$Q_{2\,3} = \sum_3 n_j h_j - \sum_2 n_i h_i \qquad \ldots (3)$$

where

$$\sum_2 n_i h_i = 2(2239) + (2364) + 9.425\,(2086) = 26,542 \text{ Cal/g-mol}$$

Equations (2) and (3) yield:

$$300,086 = \sum_3 n_j h_j - 26,542$$

or $326,628 = \sum_3 n_j h_j$

$$= \left(2y h_{CO} + 2(1-y) h_{CO_2} + y h_{O_2} + z h_{OH} + (1-z) h_{H_2O} + \frac{z}{2} h_{H_2} + 9.425\, h_{N_2}\right)_{T_3} \quad \ldots (4)$$

The unknowns in this equation are $T_3$, y and z. Two more independent equations are required:

The equilibrium contents $K_7$ and $K_3$ are required:

$$K_7 = \frac{x_{CO_2}}{x_{CO} \cdot x_{O_2}^{1/2}} \cdot P_i^{-\frac{1}{2}} \quad \ldots (5)$$

$$K_3 = \frac{x_{H_2O}}{x_{OH} \cdot x_{H_2}^{1/2}} \cdot P_i^{-\frac{1}{2}} \quad \ldots (6)$$

Substituting values of mole fractions (x) at state (3); equations (5) and (6) become:

$$K_7 = \frac{(1-y)\left(y + \frac{z}{2} + 12.425\right)^{1/2}}{y^{3/2}} \cdot P_i^{-\frac{1}{2}} \quad \ldots (5a)$$

$$K_3 = \frac{1.414(1-z)\left(y + \frac{z}{2} + 12.425\right)}{z^{3/2}} \cdot P_i^{-\frac{1}{2}} \quad \ldots (6a)$$

As a first approximation, assuming z = 0; Equations (5a) & (6a) become:

$$K_7 = \frac{(1-y)(y+12.425)^{1/2}}{y^{3/2}} \cdot P_i^{-\frac{1}{2}} \quad \ldots (5b)$$

$$K_3 \cong \infty \quad \ldots (6b)$$

Thus we have now two equations (4) & (5b) and two unknowns y & $T_3$. Few trials for value of $T_3$ were made and by trial and error values of 'y' from equation (5b) and that of 'z' from (6a) for the value of y found from equation (5b) were obtained. These values of y and z for the trial temperature $T_3$ should simultaneously satisfy equation (4). The final trial is given here:

Assume a trial temperature $T_3 = 2600^\circ$ K.

This yields values of $K_7 = 16$ and $y = 0.35$

Substituting $K_3 = 100$ in (6a), we get $z = 0.022$

Substitute y = 0.35 and z = 0.029 in equation (4) (Right-side) we get:

$\sum_j n_j h_j$ = 0.70 x 37,662 + 1.30 x 32986 + 0.35 x 21734 + 0.029 x 57860 + 0.971 x 27412 + 0.0145 x 76820 + 3.425 x 20643 = 3,35,692.

This is nearly equal to 326,620.

Hence these values of $T_3$, y and z are fairly satisfactory for our calculation purposes:

(8) Calculations for $C_{p(b)}$, $T'_e$ & $P'_e$

From graph the value of molalspecific heat at constant pressure Cp for the products CO, $CO_2$, $O_2$, $H_2O$, $H_2$ and $N_2$ are 13, 8, 8.5, 10.5, 7.7 and 8.0 Cal./g-mole, °K respectively at 2600° K. and the mole fractions of these constituents work out to be $x_{co}$ = 0.0547, $x_{co_2}$ = 0.1013, $x_{o_2}$ = 0.0274, $x_{H_2O}$ = 0.0750, $x_{H_2}$ = 0.00113 and $x_{N_2}$ = 0.737

Thus, for the burned products, the value of $C_{p(b)}$ is found out by multiplying the molal specific heats of the constituents with their respective mole fractions and summing up, we get:

$C_{P(b)} = \Sigma f c_p = 8.46$ cal/g-mole, °K

$C_{v(b)} = C_{P(b)} - R = 8.46 - 1.99 = 6.47$ cal/g-mole, °K

Now from Equation: (2.29) Viz:

$C_{v(b)} T'_e + \frac{m_i}{m_b} \cdot RT_i = C_{P(b)} \cdot T_b$ ; Here $T_b = T_3$, $m_b = m_e$,

We get: 6.47 $T'_e$ + 12.925/12.789 x 1.99 x 306 = 8.46 x 2600

$\therefore$ $T'_e$ = 3300° K

From equation 2.31, we have:

$$P_e' = P_i \frac{m_b}{m_i} \cdot \frac{T_e'}{T_i} = \left(\frac{1}{2} \text{ atm.}\right) \cdot \frac{12.789}{12.925} \cdot \frac{3300}{306}$$

$\therefore$ $P_e'$ = 5.33 Atm.

The following table gives the value of $P_e'$ and $\frac{P_e'}{P_i}$ for various initial pressures of the combustible mixture. It has been assumed that composition of the products of the reaction does not change in the range of pressures used in the present work:

| $P_i$ Atm. | $T_i$ °K | $P_e'$ Atm. | $\frac{P_e'}{P_i}$ |
|---|---|---|---|
| 1/3 Atm. | 303 | 3.55 | 10.65 |
| 1/2 " | 306 | 5.33 | 10.66 |
| 2/3 " | 308 | 7.07 | 10.60 |

# APPENDIX C

## CALCULATIONS FOR BURNING VELOCITY, $S_u$

### (1) Calculations for '$r_i$' and '$r_b$' for Set No. 3

When P = 76 Cm.Hg.

$T_u = 375^\circ$ K

$\frac{P_e}{P_i}$ = 10.65 as found in Appendix B.

Applying Equation (2.33)

$$\frac{r_i}{R} = \left(\frac{P-P_i}{P_e-P_i}\right)^{1/3}$$

$$\frac{r_i}{6.35} = \left(\frac{76-38}{405-38}\right)^{1/3} = \frac{3.36}{7.16}$$

$\therefore$ $r_i$ = 2.96 Cms.

Applying Equation (2.35)

$$\frac{r_b}{R} = \left(1 - \frac{P_i}{P}\cdot\frac{T_u}{T_i}\cdot\frac{P_e-P}{P_e-P_i}\right)^{1/3}$$

$$\frac{r_b}{6.35} = \left(1 - \frac{38}{76}\cdot\frac{375}{306}\cdot\frac{405-76}{405-38}\right)^{1/3}$$

$\therefore$ $r_b$ = 4.87 Cms.

From the Drum Camera Record, the value of '$r_b$' observed was found to be 5.40 Cms.

$\therefore$ The difference = 5.40 - 4.87 = +0.53 Cms.

and % Difference = $\frac{0.53}{5.40} \times 100$ = 9.81%

### (2) Calculations for $S_u$

#### (A) From Pressure Record Alone

From Equation (2.30), we have:

$$S_u = \frac{dr_i}{dt}\cdot\left(\frac{r_i}{r_b}\right)^2\left(\frac{P_i}{P}\right)^{1/\gamma_u}$$

A plot was obtained for values of $r_i$ corresponding to any given

pressure on the pressure time record as a function of time and the slopes $\frac{dr_i}{dt}$ were determined.

For P = 76 Cm.Hg., $r_i$ = 2.96 Cms. at time, t = 5.74 m.sec.

$$\frac{dr_i}{dt} = 732 \text{ cm./sec.}$$

Substituting the values in the last equation, we get:

$$S_u = 732 \left(\frac{2.96}{4.87}\right)^2 \left(\frac{38}{76}\right)^{1/1.4} = 165.5 \text{ cm./sec.}$$

(B) From Flame Record

Also applying equation 2.45, we get:

$$S_u = \frac{dr_b/dt}{1+\left(\frac{P_e}{P}-1\right)/\gamma_u}$$

From observed Flame record, we get at P = 76 Cm.Hg;

$r_b$ = 5.40 Cm. at time 5.74 m.sec.

$$\frac{dr_b}{dt} = 690 \text{ cm./sec.} \quad \text{and} \quad \frac{P_e}{P} = \frac{405}{76}$$

Substituting the values we get:

$$S_u = \frac{690}{1+\left(\frac{405}{76}-1\right)/1.4} = 168 \text{ cm./sec.}$$

The values of $S_u$ obtained from pressure record alone and from experimentally observed flame record in conjunction with the thermodynamically calculated value of $P_e$ are comparable and hence the self consistency of the method is confirmed.

## APPENDIX D

## DERIVATION OF EMPIRICAL CORRELATION FROM BURNING VELOCITY DATA

The curves of Figure (44) are extrapolated and it is found that all of them nearly converge in a single point at which the abscissa and ordinate read P = -70 Cm.Hg. and $S_u$ = 98 Cm./Sec. That is, if the abscissa of Figure (44) is changed to (P + 70) instead of P, then the various curves would diverge from a point on the ordinate where $S_u$ = 98 Cm./Sec. Since burning velocity varies Linearly with pressure, an empirical equation may be set up as follows:-

$$S_u = m(P + 70) + 98 \qquad \ldots (1)$$

Where $S_u$ = Burning velocity, Cm./Sec.

P = Pressure, Cm.Hg.;

m = coefficient which varies with temperature.

The coefficient 'm' is determined for one particular temperature by selecting two points on P Vs. $S_u$ curve for that temperature and applying the equation (1)

$$S_{u_1} = m(P_1 + 70) + 98$$

$$S_{u_2} = m(P_2 + 70) + 98$$

Hence $$= \frac{S_{u_2} - S_{u_1}}{P_2 - P_1} \qquad \ldots (2)$$

In order to determine the nature of variation of 'm' with '$T_u$' the following data are extracted from Figure (44).

The last column in the Table on the next page suggests that the increase in the value of slope at equal temperature intervals is nearly constant. That is to say, 'm' is also a Linear Function of '$T_u$'. (See also Fig.43)

| $T_u$ (°K) | $S_u$ (Cms /Sec) $P_1$ = 40 | $P_2$ = 140 | m | Difference of two consecutive 'm' values. |
|---|---|---|---|---|
| 300 | 110 | 121 | 0.11 | |
| | | | | 0.26 |
| 350 | 137 | 174 | 0.37 | |
| | | | | 0.25 |
| 400 | 165 | 227 | 0.62 | |
| | | | | 0.25 |
| 450 | 193 | 280 | 0.87 | |

Therefore we may write $m = aT_u + b$ ... (3)

Where 'a' and 'b' are constants which may be evaluated from equation (3):

$$m_1 = a T_{u_1} + b$$

$$m_2 = a T_{u_2} + b$$

$$\text{Hence } a = \frac{m_2 - m_1}{T_{u_2} - T_{u_1}} \quad \ldots (4)$$

$$\text{and } b = m_1 - \frac{m_2 - m_1}{T_{u_2} - T_{u_1}} T_{u_1} \quad \ldots (5)$$

Making use of the tabulated data and equations (4) and (5) we obtain:

$$a = 5.06 \times 10^{-3}$$

$$b = -1.41$$

Combining equations (1) and (3) we get, finally

$$S_u = (5.06 \times 10^{-3} T_u - 1.41)(P + 70) + 98 \quad \ldots (6)$$

For Example At $T_u = 300^\circ$ K and P = 76 Cm. Hg. from formula (6) $S_u$ = 114 Cm./Sec. and from Figure (44), at P = 76 Cm. Hg. & $T_u$ = 300° K, $S_u$ = 114 Cm./Sec. Similarly at $T_u = 350^\circ$ K & P = 76 Cm. Hg. From Empirical correlation $S_u$ = 152 Cm./Sec. and from Figure (44) $S_u$ = 150 Cm./Sec.